IPP-Report

Max-Planck-Institut für Plasmaphysik

Wolfrang Eckstein

Penetration (Range)

IPP 17/20
June 2010

Penetration (Range)

W.Eckstein
Max-Planck-Institut für Plasmaphysik
Boltzmannstr.2, D-85748 Garching
wolfgang.eckstein@ipp.mpg.de

June 8, 2010

1 Abstract

This report gives an overview of available calculated mean penetration depths (ranges) of energetic ions in elemental targets. The energy and angular dependences of the mean depth are fitted by simple formulae for a large number of elemental targets and light (hydrogen and helium) and heavy (mainly noble gases and selfbombardment) bombarding atoms. The incident energies cover a range from 10 to 10^5 eV, in some cases up to MeV energies.

2 Introduction

In recent years surveys on sputtering [1] and reflection [2] have been published, comparing experimental and calculated data as well as fitting available calculated values. Based on the same calculations this report provides values for the energy and angular dependence of the mean penetration depths of energetic ions into solids. Here only calculted values are given due to the lack of experimental data.

Bombarding a solid (or liquid) with energetic ions (or neutrals) leeds to backscattering, sputtering and implantation. The energetic ions are slowed down in the solid until some of them come to rest in the target. These implanted atoms show a distribution in depth. The mean value of this depth distribution is the mean penetration depth or range. This report shows the energy and the incidence angle dependence of the mean penetration depth and corresponding fits for a large number of incident ions and elemental targets.

At low energies the mean penetration depth is at larger energies than the maximum of the depth distribution, at high energies the opposite is true. The distributions can be reconstructed from the moments of the distributions [3]. The damage distribution has its maximum at a lower energy than the range and its width is smaller than that of the depth distribution of implanted species.

For helium, a fitting formula for the mean depth exists for all elements in the energy range from 10 keV to high energies [4]. This report extends the energy range down to 10 eV and to other incident elemental ions as hydrogen, noble gases and targetions.

3 Calculational Methods

The calculated results reported in this review are determined with a Monte Carlo program based on the binary collision model [5]. The programs used are TRIM (Transport of Ions in Matter) [6], TRIM.SP [5, 7] and the newest version SDTrimSP [8]. The most important input for the program is the interaction potential. In the programs mentioned, mostly the WHB (KrC) potential [9] is applied; but other potentials such as the ZBL [10] and Moliere [11] potentials are also used sometimes. All these potentials are purely repulsive and only dependent on the interatomic distance. For Si a special potential with an attractive part has been used in a few cases [12]. Reflection coefficients determined with different potentials agree usually better than a factor of two. Another important input is the electronic (inelastic) energy loss. Here, an equipartition of the local Oen-Robinson model [13] and the nonlocal velocity proportional loss [14, 15] is applied at low energies for hydrogen, helium, and for heavy ions in the whole energy range (1 to 10^5 eV) investigated. At high energies the formulae of Ziegler [4] for helium and the formulae of Andersen and Ziegler [16] for hydrogen are used. Other input parameters for the calculations [5] are the surface binding energy of target atoms, E_{sb}, which is only important in reflection for selfbombardment, the binding energy of projectiles, E_{sp}, to the target surface (about 1

eV), which is only of importance for hydrogen and nitrogen (for most elements but not for Cu, Ag, Au), and finally a cutoff energy of projectiles of 0.5 eV. For other calculational approaches see [5].

Mean penetration depth values calculated with TRIM, TRIM.SP and SDTrimSP are documented in [18, 19, 20], which implies that all calculated values are only valid for zero fluence (static case) or in other words, the influence of implanted species are not taken into account. The absolute error depends on the applied interaction potential and on the inelastic energy loss model; it should be smaller than a factor ot two, in most cases better than 30%. The calculational error is usually better than a few percent, in many cases better than 1%. References [19, 20] contain more but not enough calculated values to make a good fit; these values do not appear in this report.

The implantation of bombarding species in the target and the resulting change of the target composition with fluence can be treated by a dynamical program like TRIDYN [17] or in the dynamic mode of SDTrimSP [8].

4 Fitting

The following empirical formula for the mean penetration depth at normal incidence, md, is taken from [4].

$$md(E) = \exp(a_1 + a_2 E + a_3 E^2 + a_4 E^3) \tag{1}$$

The formula in [4] is applied only to helium for energies larger than 10 keV and it uses six fitting parameters.

The fitting is performed in the energy range from 10 to 10^5 eV in most cases, but the same formula also applies to higher energies up tp 10 MeV as shown for a few cases, namely several ions on Be, C, Cu, Nb, Ag, W, Au, Hg. The fitting parameters are provided in tables 1 to 9. It should be mentioned, that the fitting parameters are only valid in energy range given in the plots.

For the angular dependence of the mean penetration depth another fit formula which has been used also in [2]:

$$md(\alpha) = c_1 + c_2 \tanh(c_3 \alpha \pi / 180 + c_4) \tag{2}$$

where α is the angle of incidence (counted from the surface normal in degree). The fit is sensitive to the values at large angles, which explains the different fit parameters for small differences in incident energies.

The fits for md, using the parameters in the tables, are given in Å, whereas in the figures md is shown in nm.

5 Energy Dependence of the Mean Depths

Generally, for each elemental target and several incident ions a plot is provided. The fits using formula (1) describe the energy dependence quite well.

Impurities in a target can change the mean penetration depth depending on the mass ratio of target mass to ion mass. Also diffusion of the implanted species may change the depth distribution and the range (temperature dependent).

The fits are shown in figures 1 to 10. The fitting parameters of formula (1) are provided in tables 1 to 9.

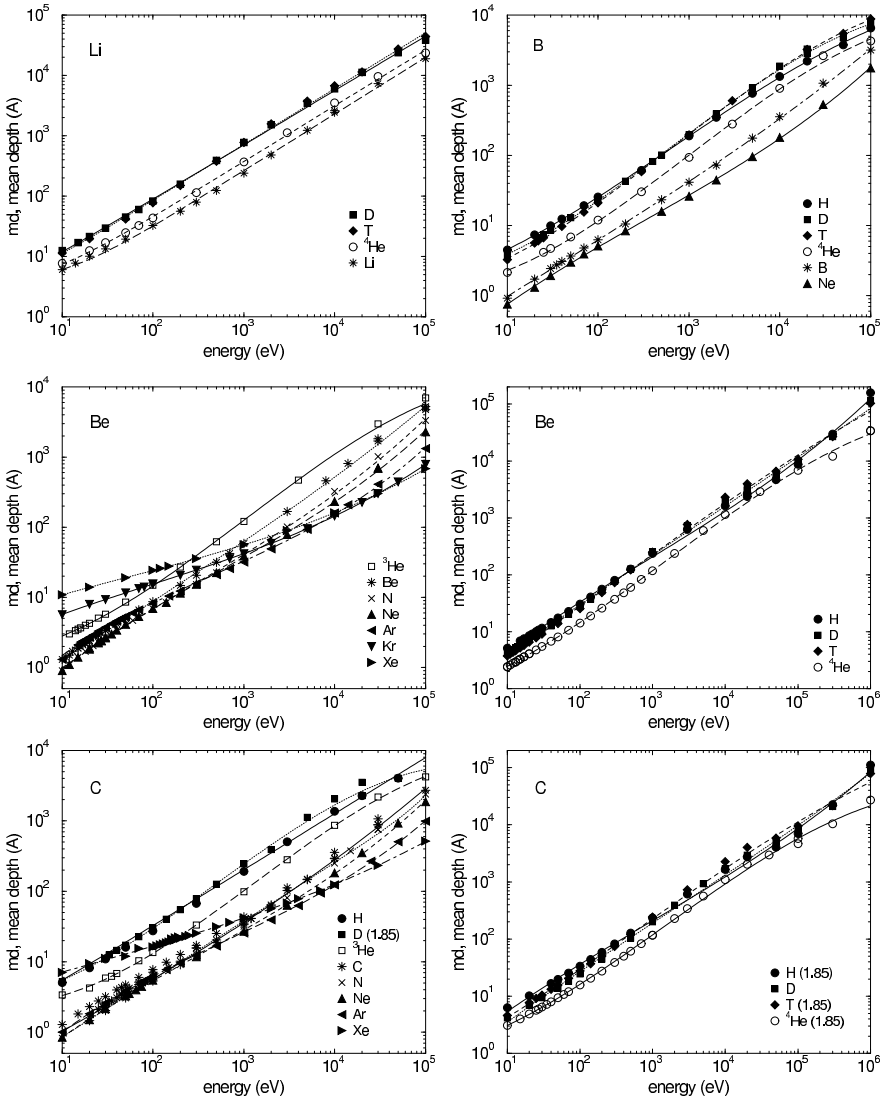

Figure 1: Calculated values for the energy dependence of the average depth of implanted projectiles at normal incidence for the bombardment of Li, B, Be and C with several incident ions [18, 19, 20]. Lines are fits to the calculated values (parameters see table 1). Numbers in brackets give the carbon density in g/cm^3 different from 2.26 g/cm^3.

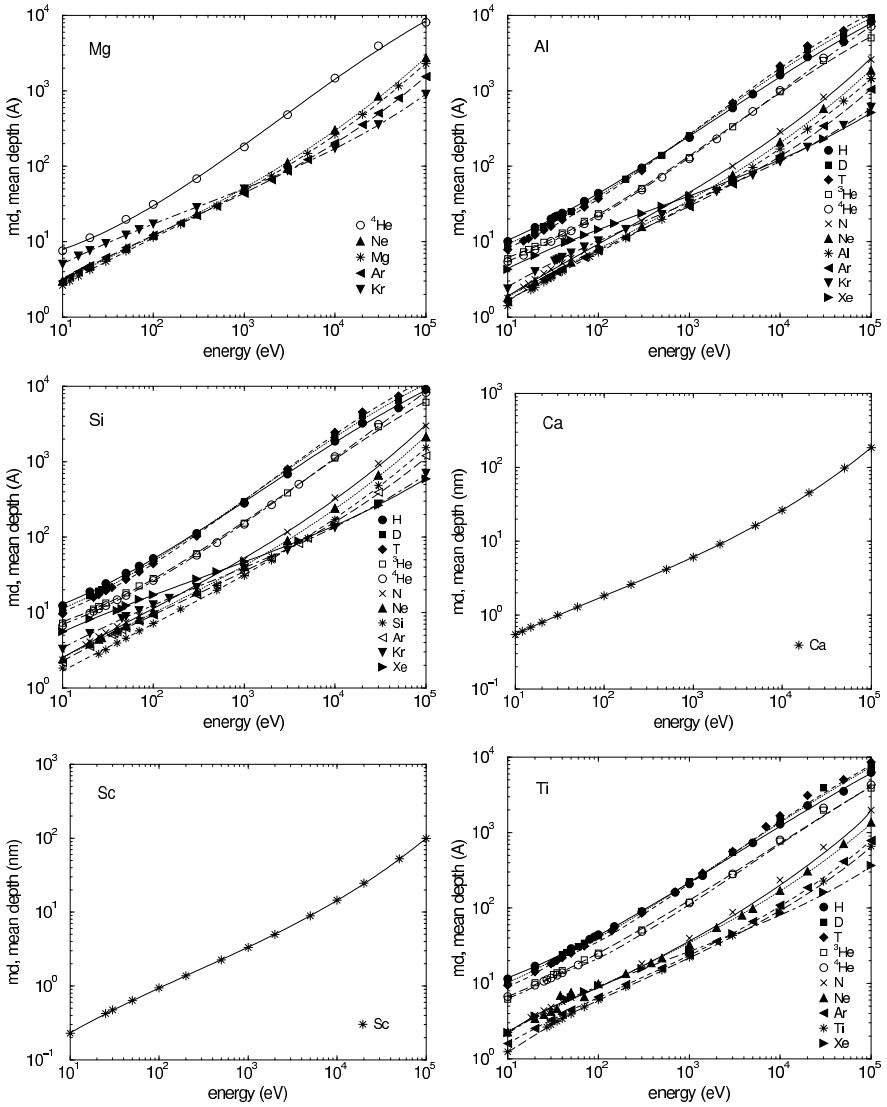

Figure 2: Calculated values for the energy dependence of the average depth of implanted projectiles at normal incidence for the bombardment of Mg, Al, Si, Ca, Sc and Ti with several incident ions [19, 20]. Lines are fits to the calculated values (parameters see tables 1 and 2).

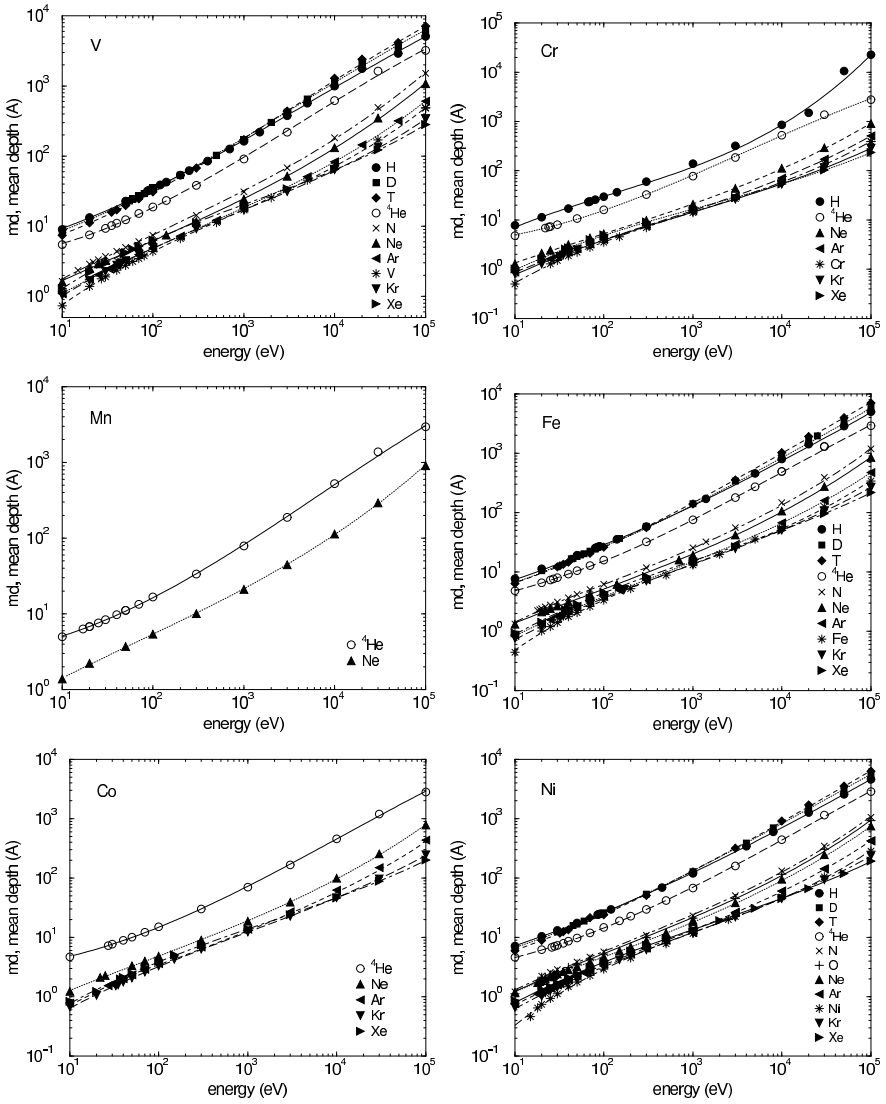

Figure 3: Calculated values for the energy dependence of the average depth of implanted projectiles at normal incidence for the bombardment of V, Cr, Mn, Fe, Co and Ni with several incident ions [19, 20]. Lines are fits to the calculated values (parameters see table 3).

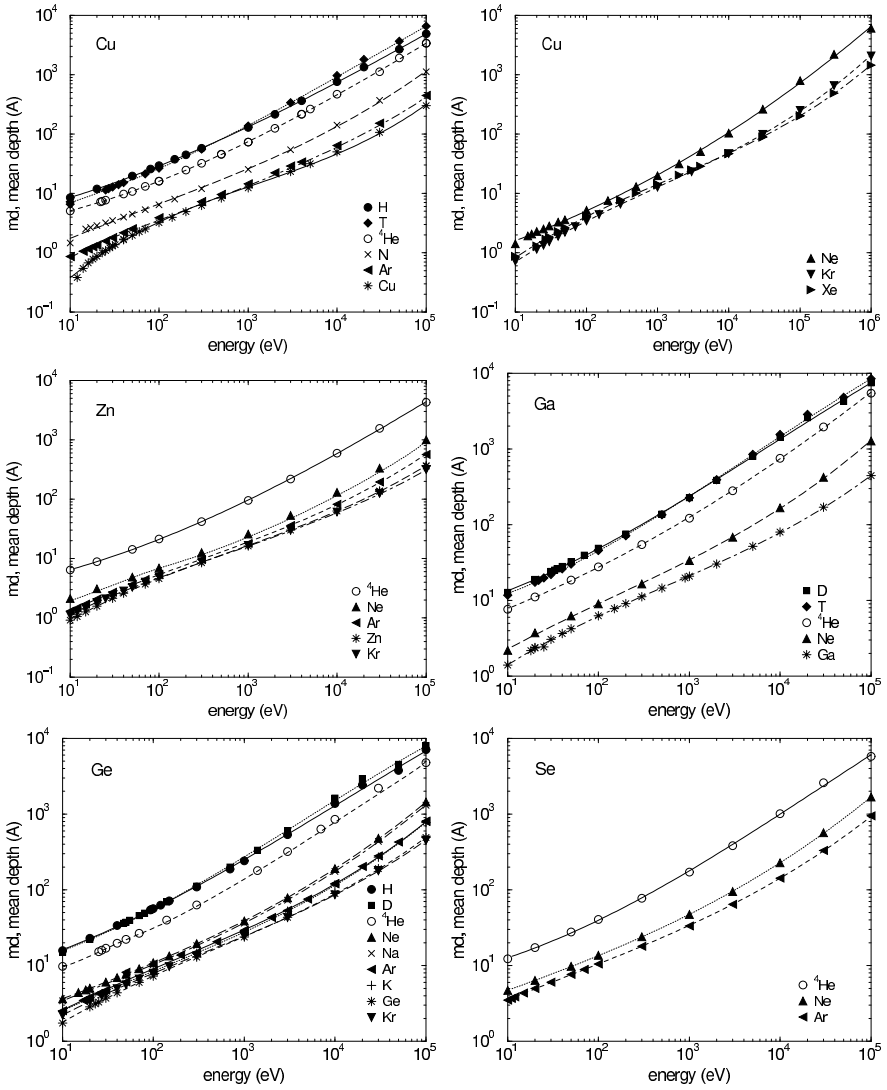

Figure 4: Calculated values for the energy dependence of the average depth of implanted projectiles at normal incidence for the bombardment of Cu, Zn, Ga, Ge and Se with several incident ions [19, 20]. Lines are fits to the calculated values (parameters see table 4).

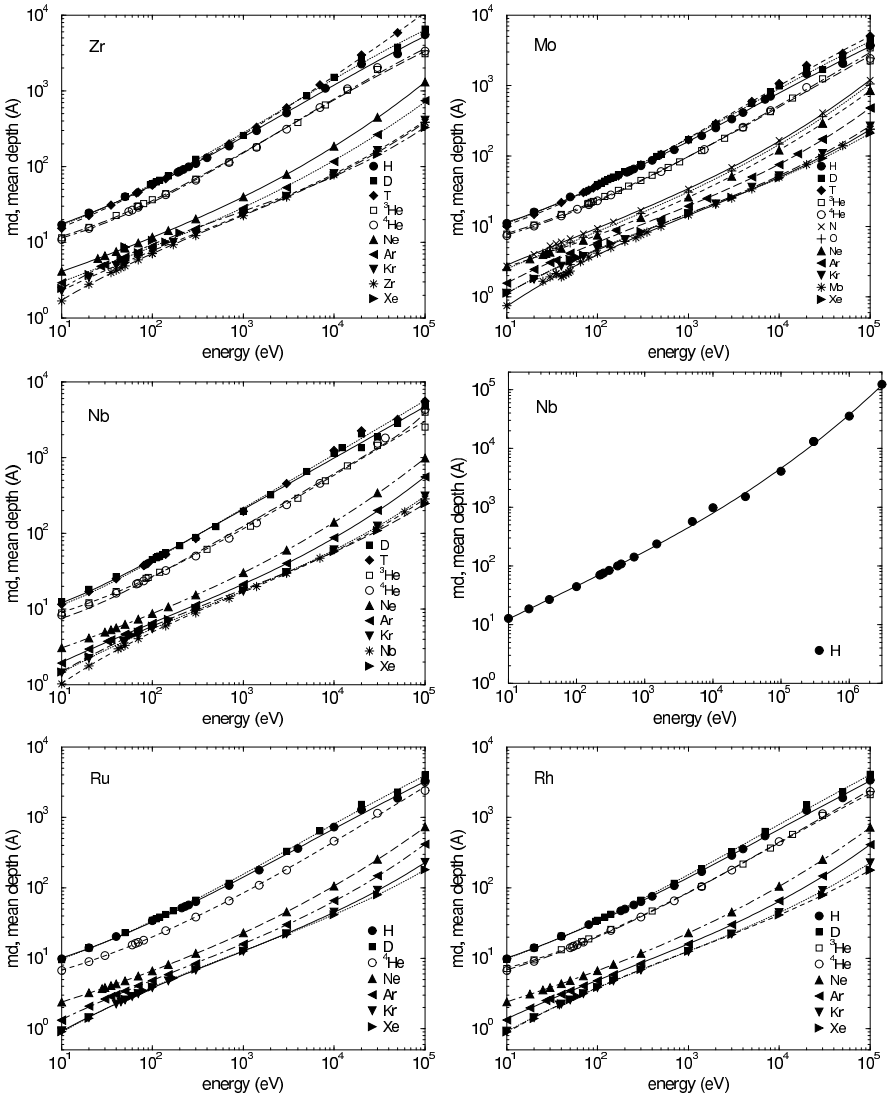

Figure 5: Calculated values for the energy dependence of the average depth of implanted projectiles at normal incidence for the bombardment of Zr, Mo, Nb, Ru and Rh with several incident ions [19, 20]. Lines are fits to the calculated values (parameters see tables 4 and 5).

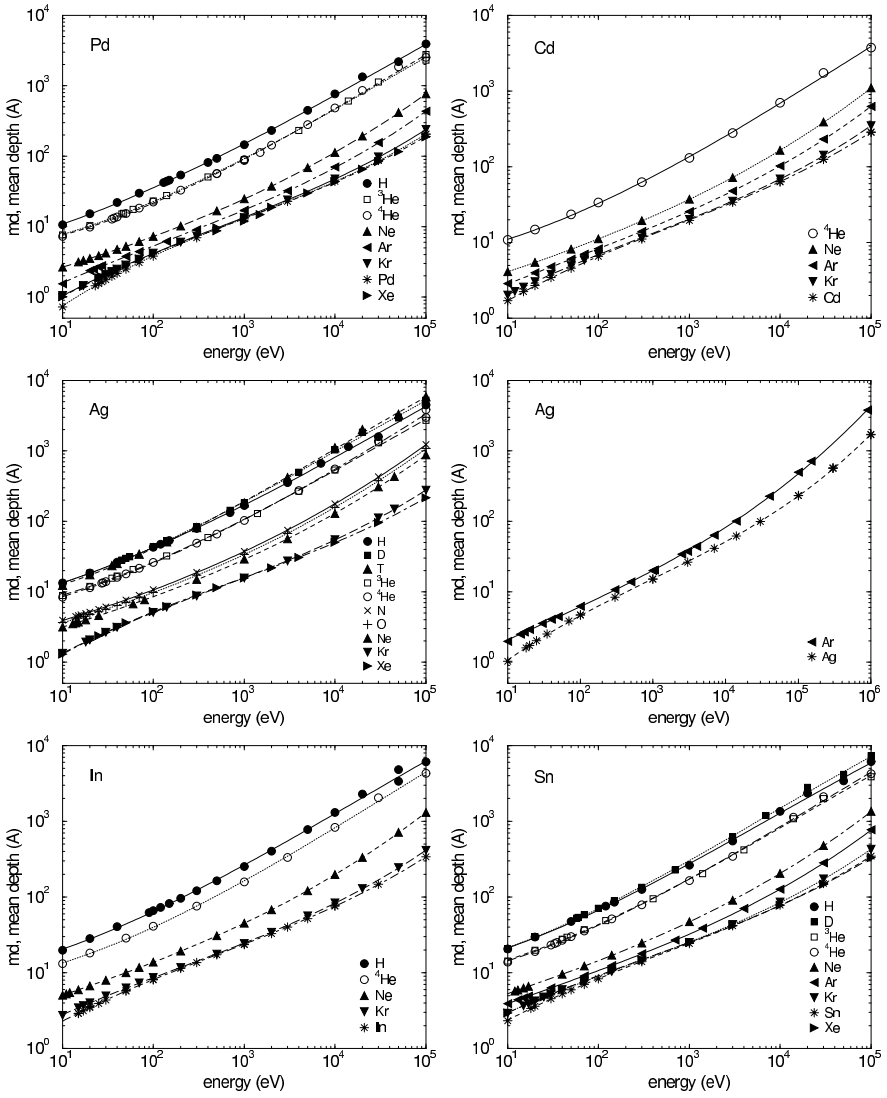

Figure 6: Calculated values for the energy dependence of the average depth of implanted projectiles at normal incidence for the bombardment of Pd, Cd, Ag, In and Sn with several incident ions [19, 20]. Lines are fits to the calculated values (parameters see tables 5 and 6).

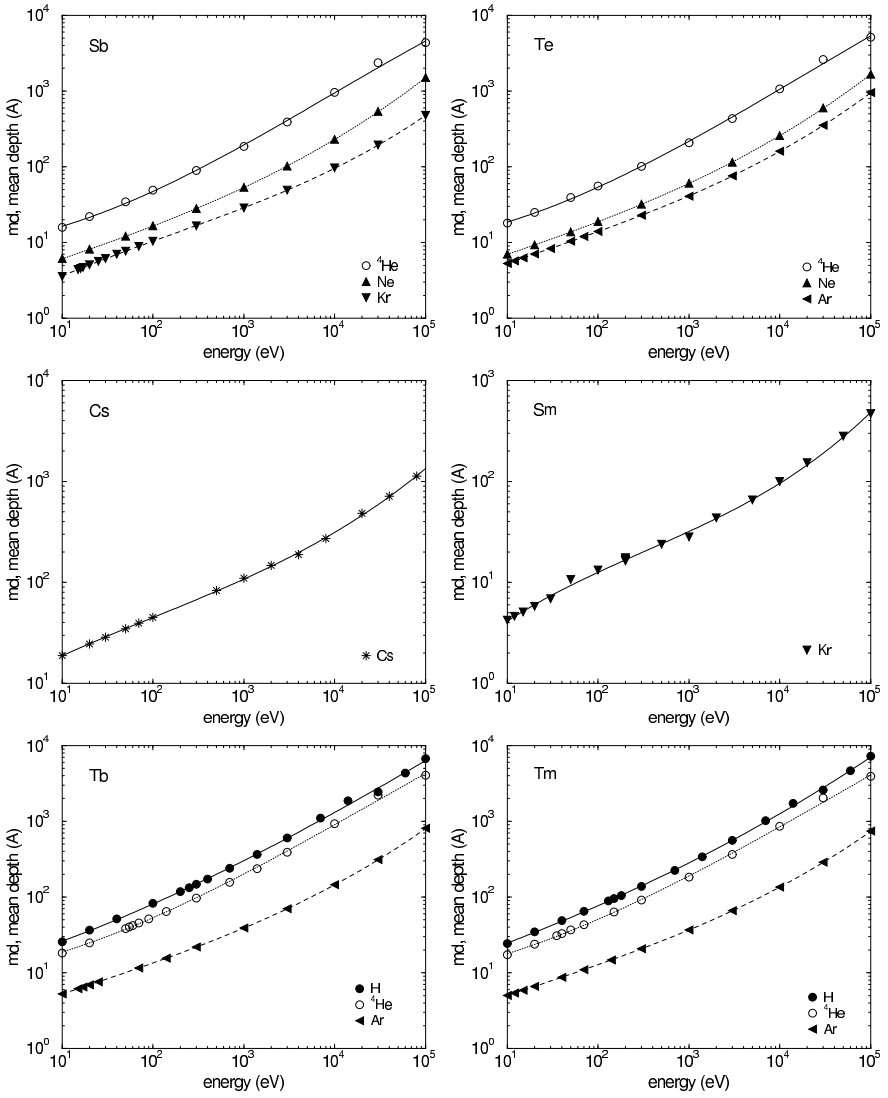

Figure 7: Calculated values for the energy dependence of the average depth of implanted projectiles at normal incidence for the bombardment of Sb, Te, Cs, Sm, Tb and Tm with several incident ions [19, 20]. Lines are fits to the calculated values (parameters see tables 6 and 7).

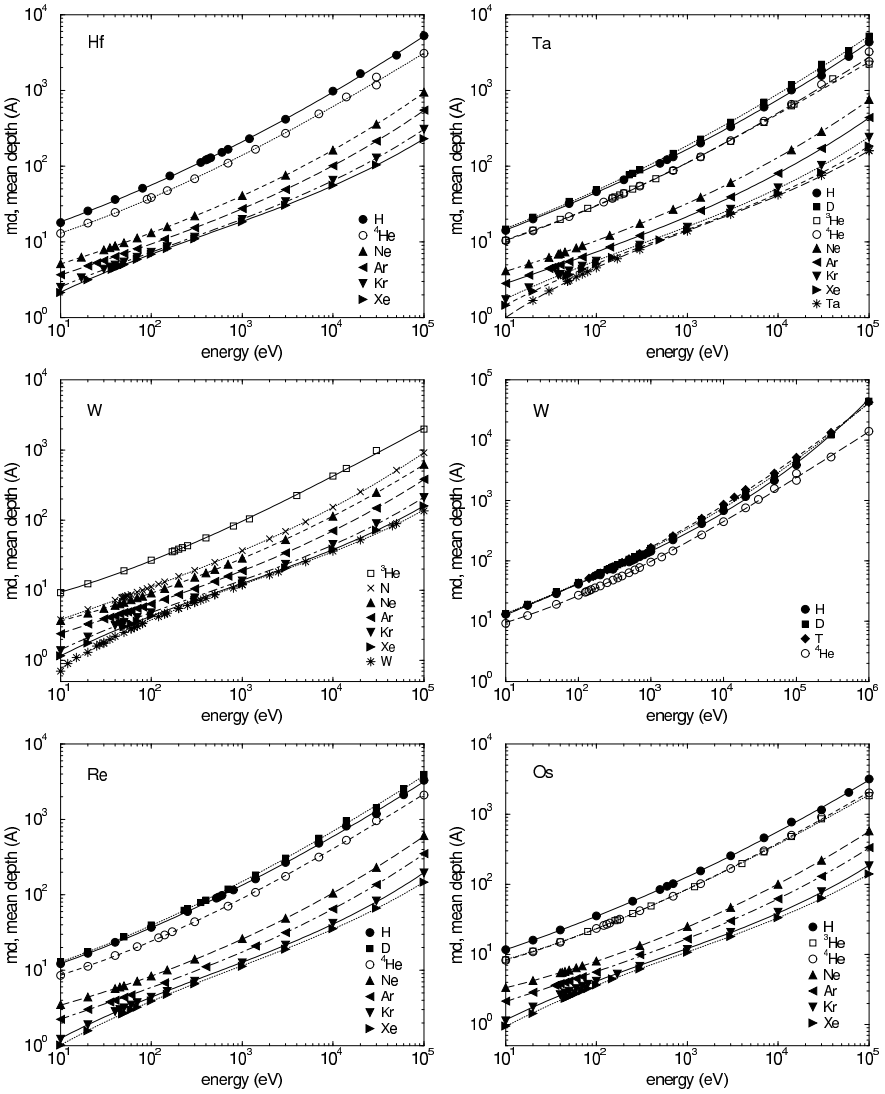

Figure 8: Calculated values for the energy dependence of the average depth of implanted projectiles at normal incidence for the bombardment of Hf, Ta, W, Re and Os with several incident ions [18, 19, 20]. Lines are fits to the calculated values (parameters see tables 7 and 8).

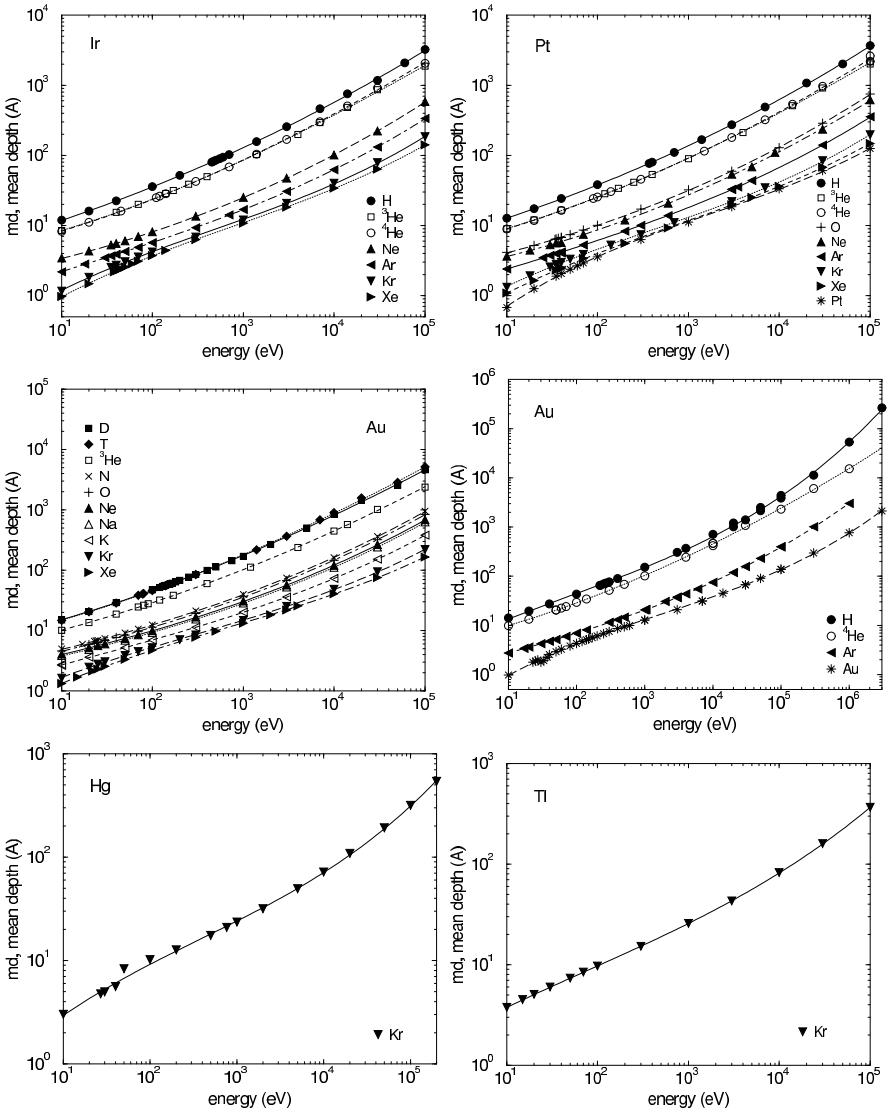

Figure 9: Calculated values for the energy dependence of the average depth of implanted projectiles at normal incidence for the bombardment of Ir, Pt, Au, Hg and Tl with several incident ions [19, 20]. Lines are fits to the calculated values (parameters see table 8).

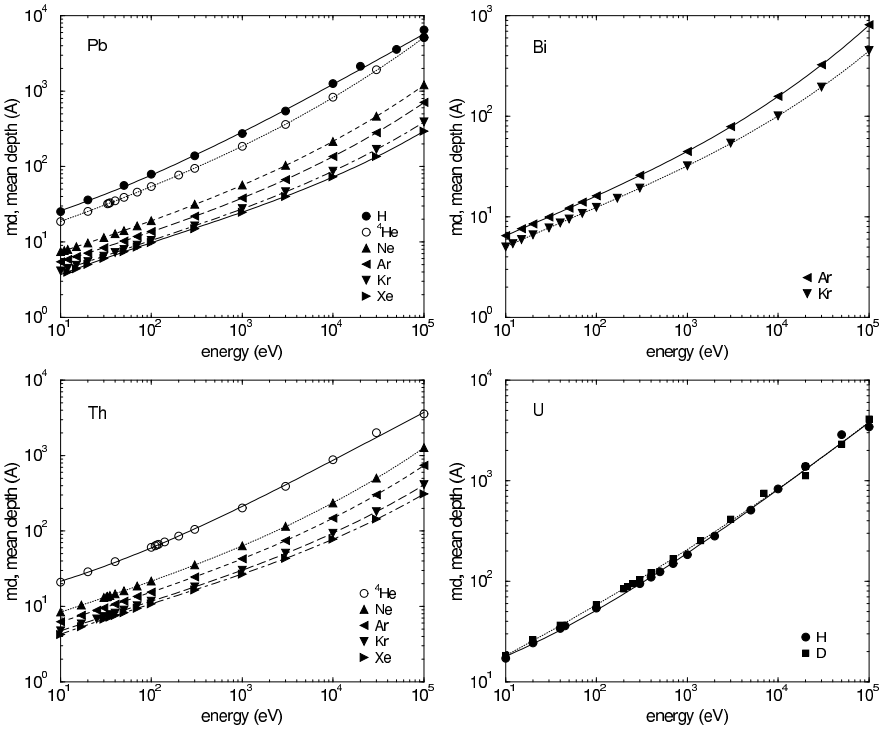

Figure 10: Calculated values for the energy dependence of the average depth of implanted projectiles at normal incidence for the bombardment of Pb, Bi, Th and U with several incident ions [19, 20]. Lines are fits to the calculated values (parameters see table 9).

6 Angular Dependence of the Mean Penetration Depths

Similarly as in the energy dependence, the angular dependence of the mean penetration depths is provided for each ion-target combination. Formula (2) can well describe the angular dependence. The fit is strongly dependent on the values at grazing incidence. Discrepancies appear sometimes at grazing incidence, but this may not be important because surface roughness may strongly influence the behaviour in this angular range.

The use of different interaction potentials in the calculations leeds to different values of the mean penetration depth; these differences are usually smaller than a factor of two, for the mostly used potentials (WHB [9] and ZBL [10] these differences are in most cases smaller than 20%, see the case of Si on Si in figure 18 and Ar on Cu in figure 22.

The fits of the angular dependence are shown in figures 11 to 31. Fitting parameters for $md(\alpha)$ are provided in tables 10 to 28.

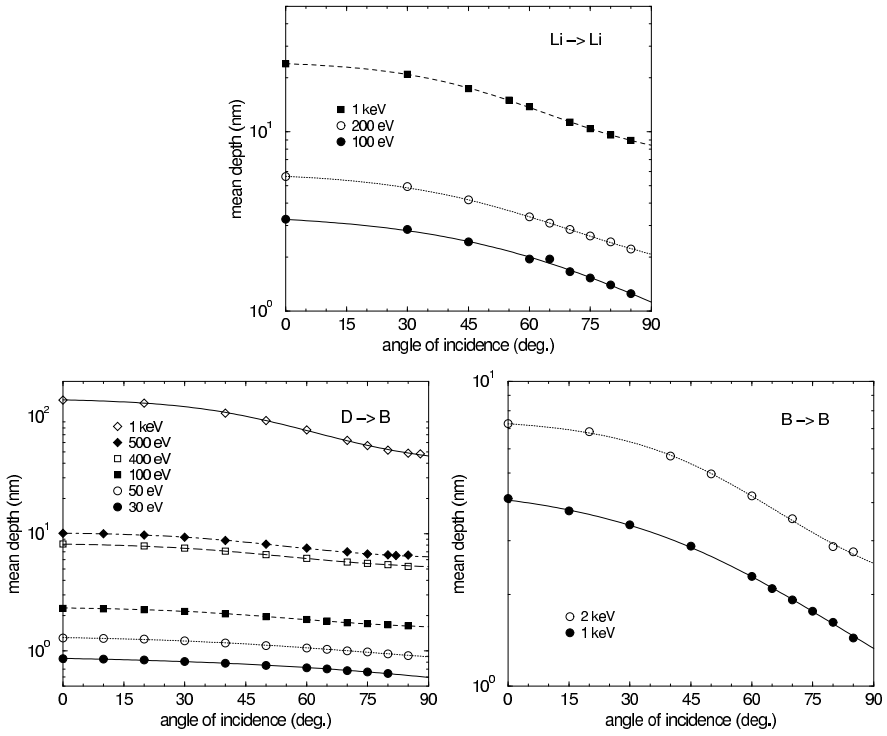

Figure 11: Calculated values for the angular dependence of the mean penetration depth at several incident energies for the bombardment of Li with Li and of B with D, B [18, 19, 20]. Lines are fits to the calculated values (parameters see tables 10 and 12).

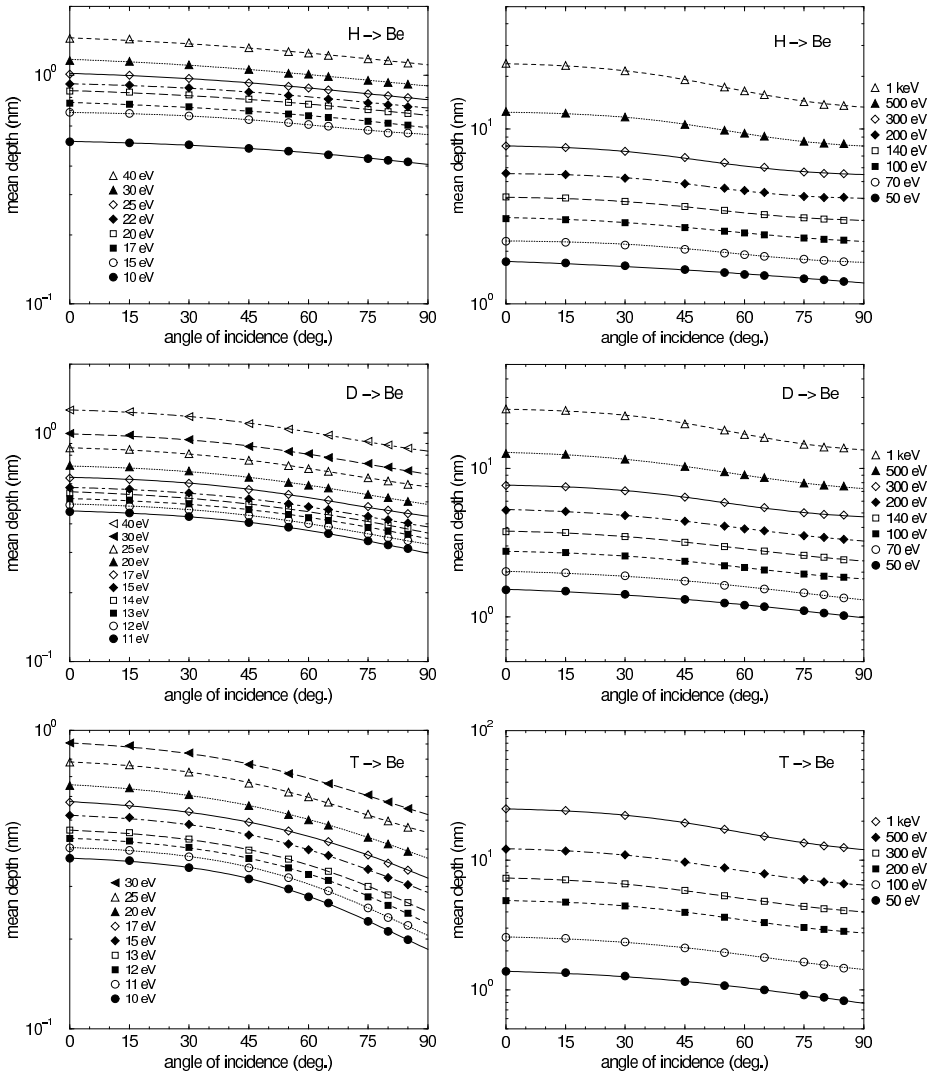

Figure 12: Calculated values for the angular dependence of the mean penetration depth at several incident energies for the bombardment of Be with H, D, T [18, 19, 20]. Lines are fits to the calculated values (parameters see tables 10 and 11).

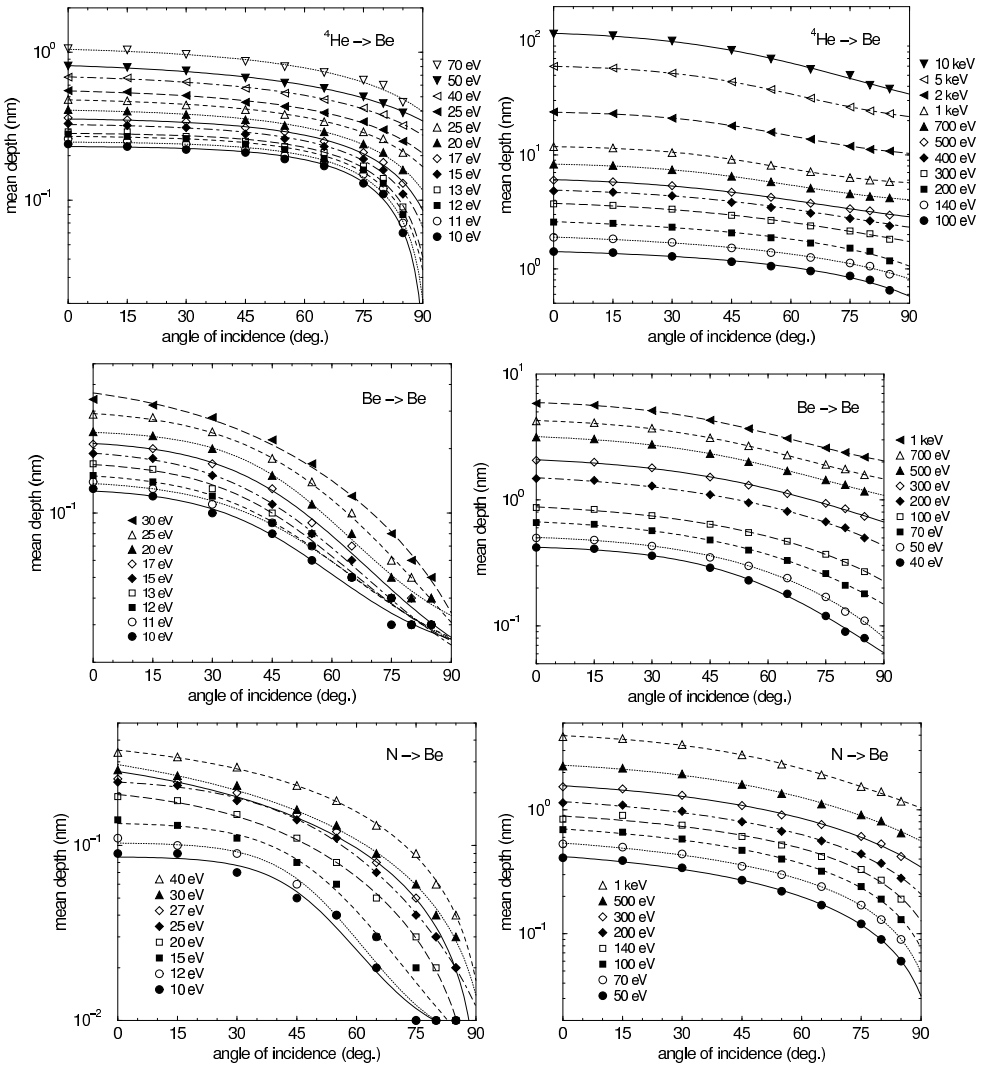

Figure 13: Calculated values for the angular dependence of the mean penetration depth at several incident energies for the bombardment of Be with ^{4}He, Be, N [18, 19, 20]. Lines are fits to the calculated values (parameters see tables 11 and 12).

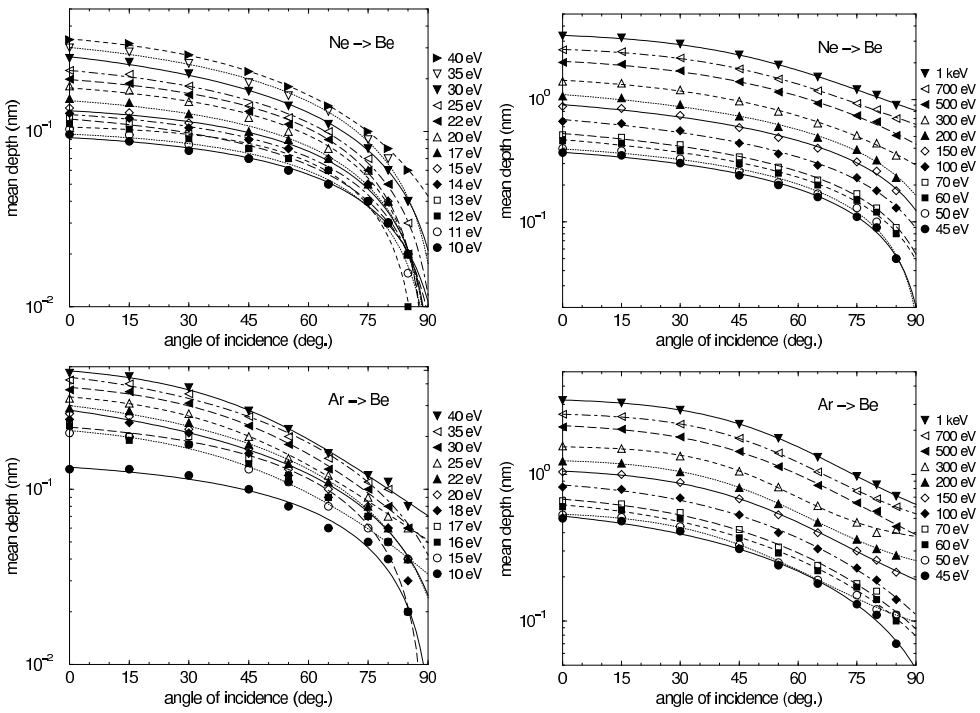

Figure 14: Calculated values for the angular dependence of the mean penetration depth at several incident energies for the bombardment of Be with Ne, Ar [18, 19, 20]. Lines are fits to the calculated values (parameters see table 13).

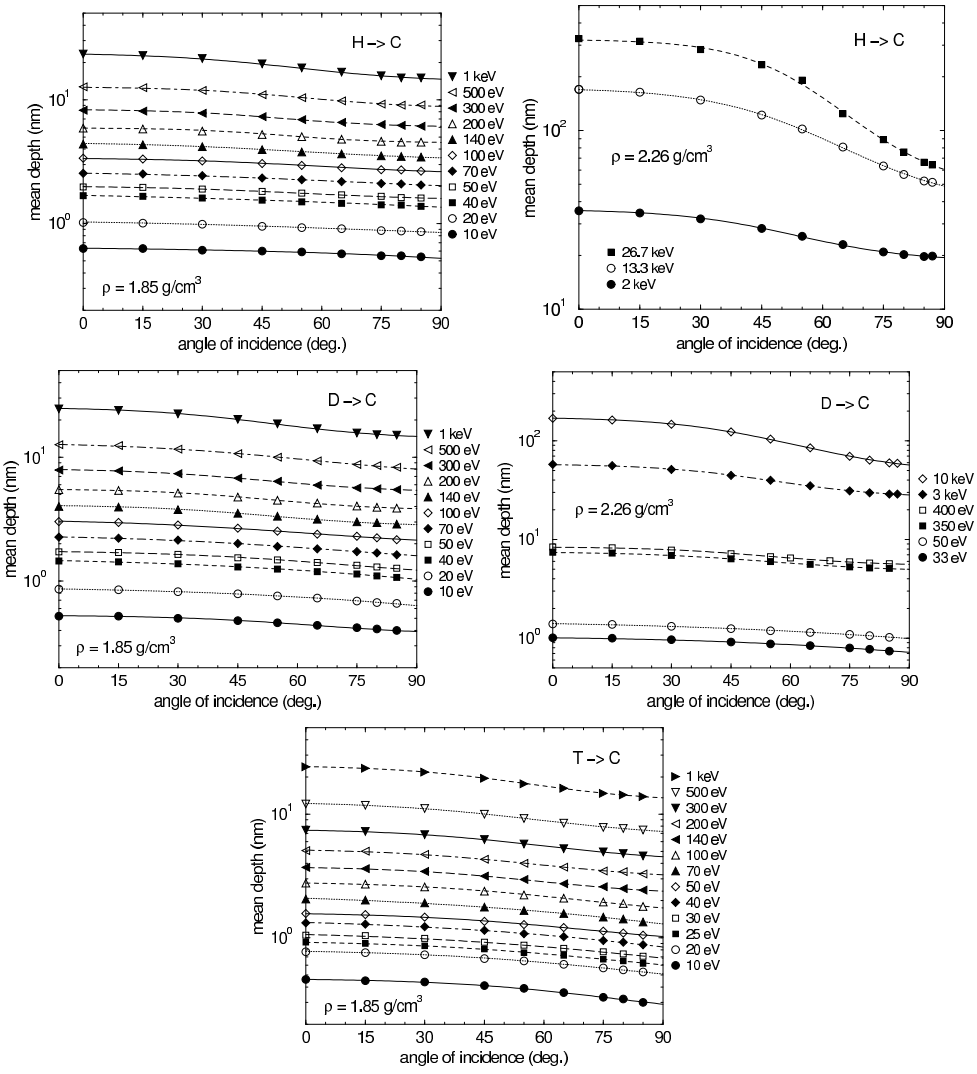

Figure 15: Calculated values for the angular dependence of the mean penetration depth at several incident energies for the bombardment of C with H, D, T [18, 19, 20] for two densities. Lines are fits to the calculated values (parameters see table 14).

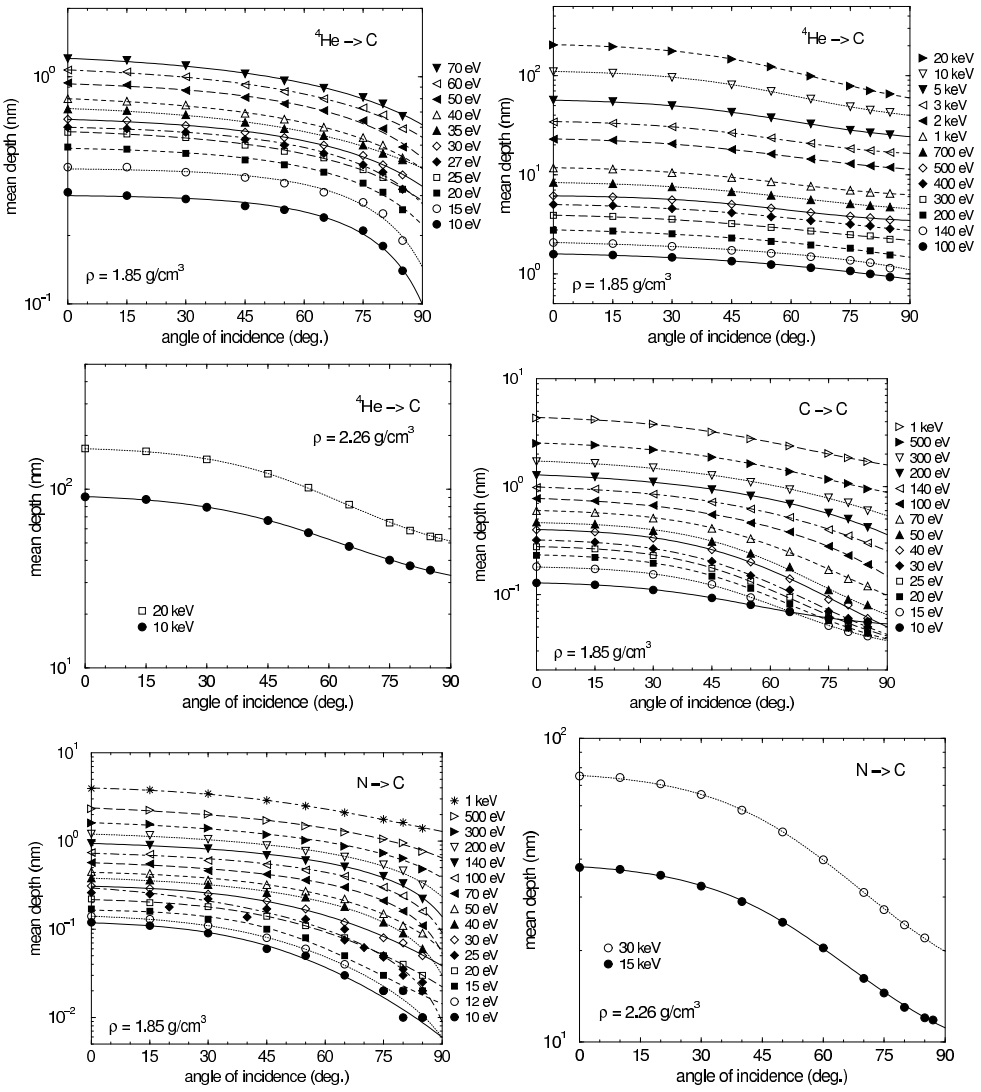

Figure 16: Calculated values for the angular dependence of the mean penetration depth at several incident energies for the bombardment of C with He, C, N [18, 19, 20] for two densities. Lines are fits to the calculated values (parameters see tables 15 and 16).

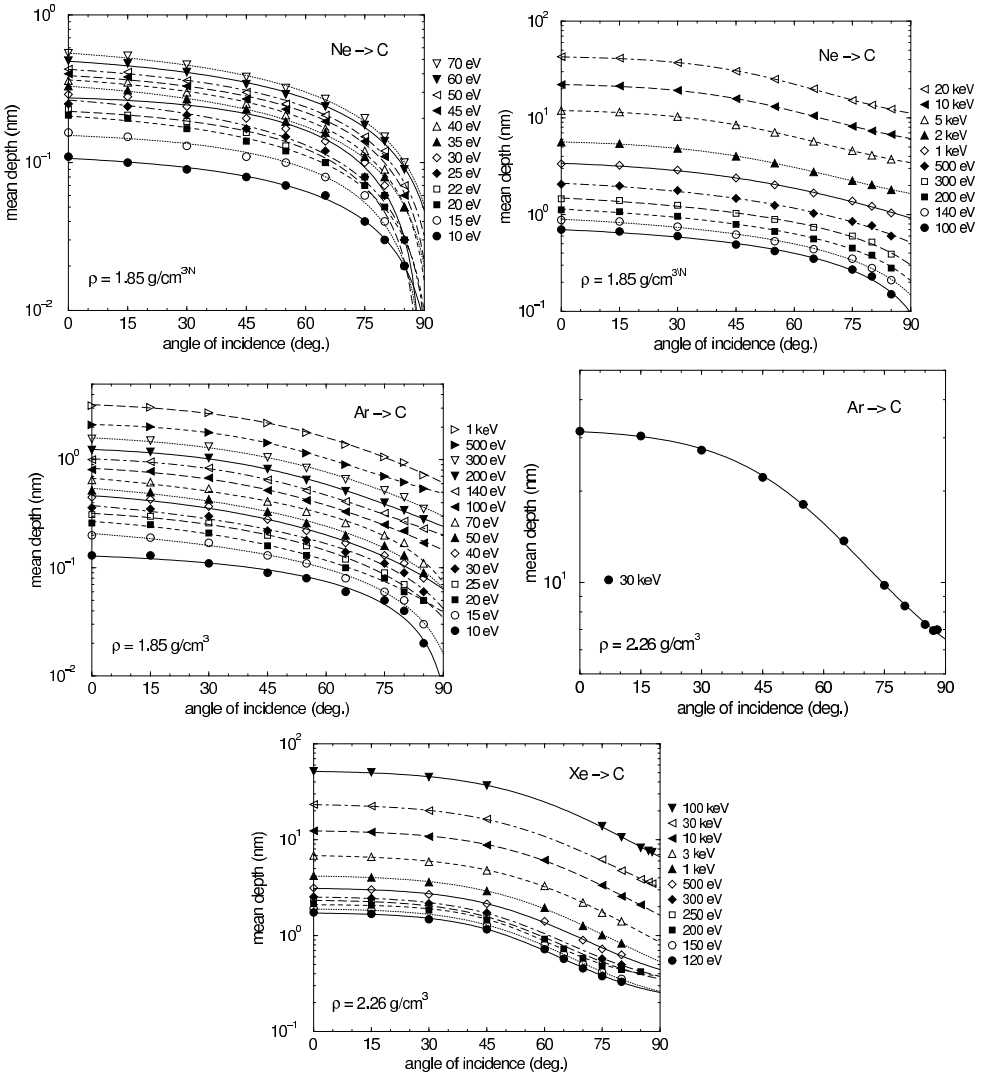

Figure 17: Calculated values for the angular dependence of the mean penetration depth at several incident energies for the bombardment of C with Ne, Ar, Xe [18, 19, 20] for two densities. Lines are fits to the calculated values (parameters see tables 16 and 17).

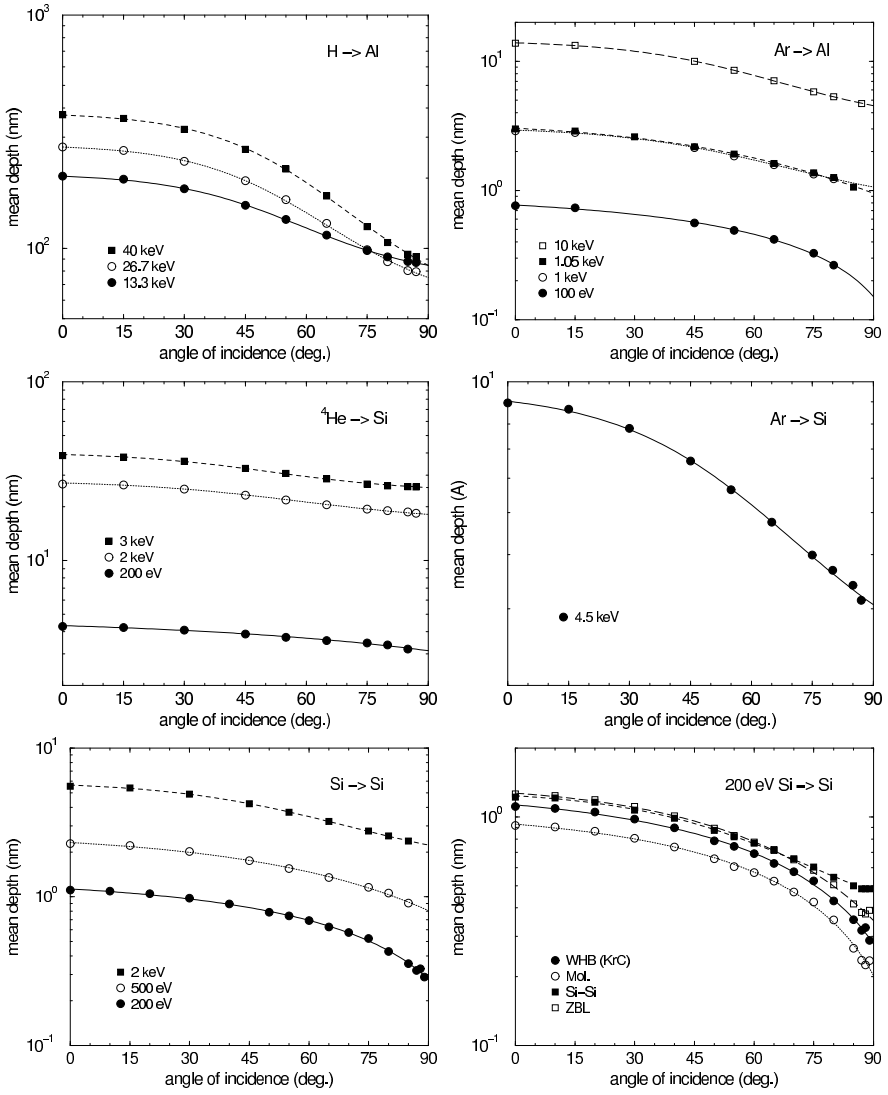

Figure 18: Calculated values for the angular dependence of the mean penetration depth at several incident energies for the bombardment of Al with H, Ar and of Si with ^{4}He, Si, Ar [19, 20]. Lines are fits to the calculated values (parameters see table 18).

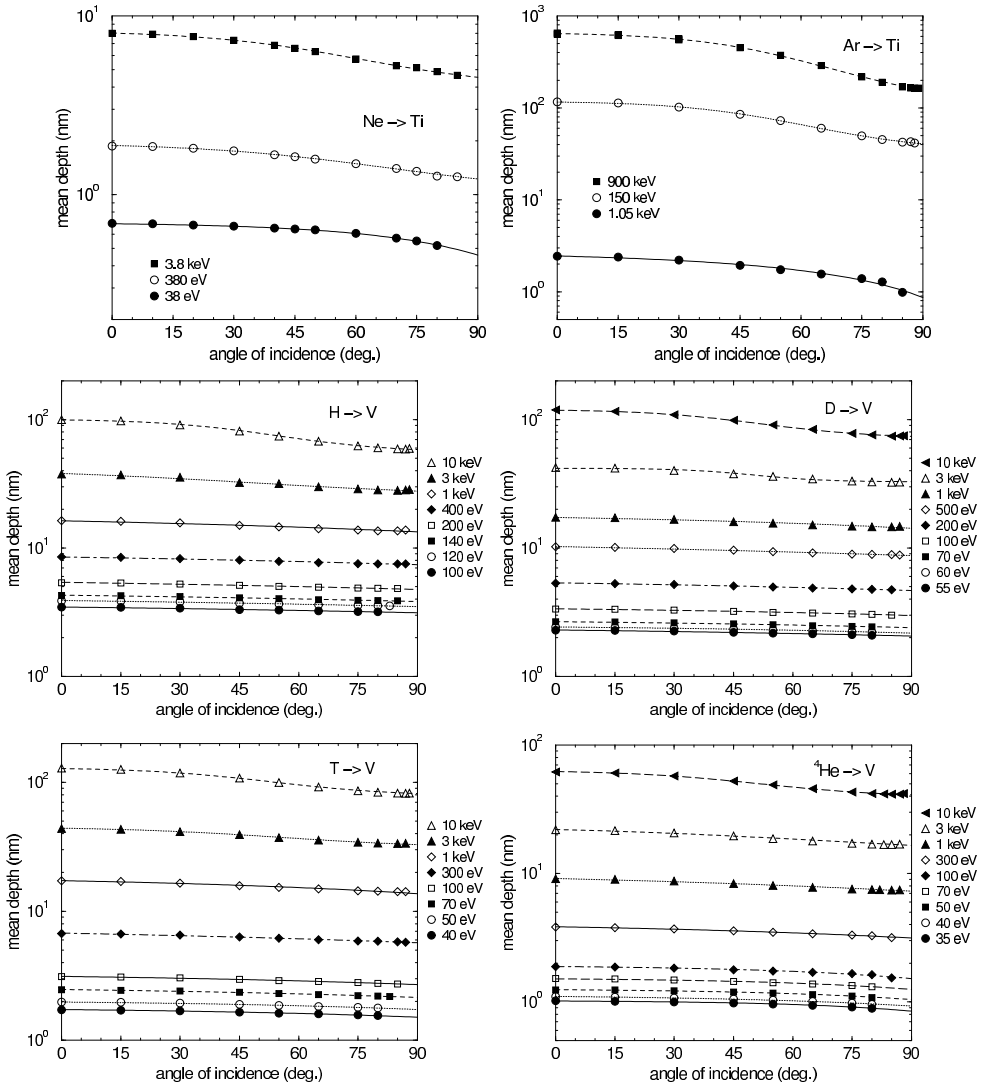

Figure 19: Calculated values for the angular dependence of the mean penetration depth at several incident energies for the bombardment of Ti with Ne, Ar and of V with H, D, T, ^{4}He [19, 20]. Lines are fits to the calculated values (parameters see tables 18 and 19).

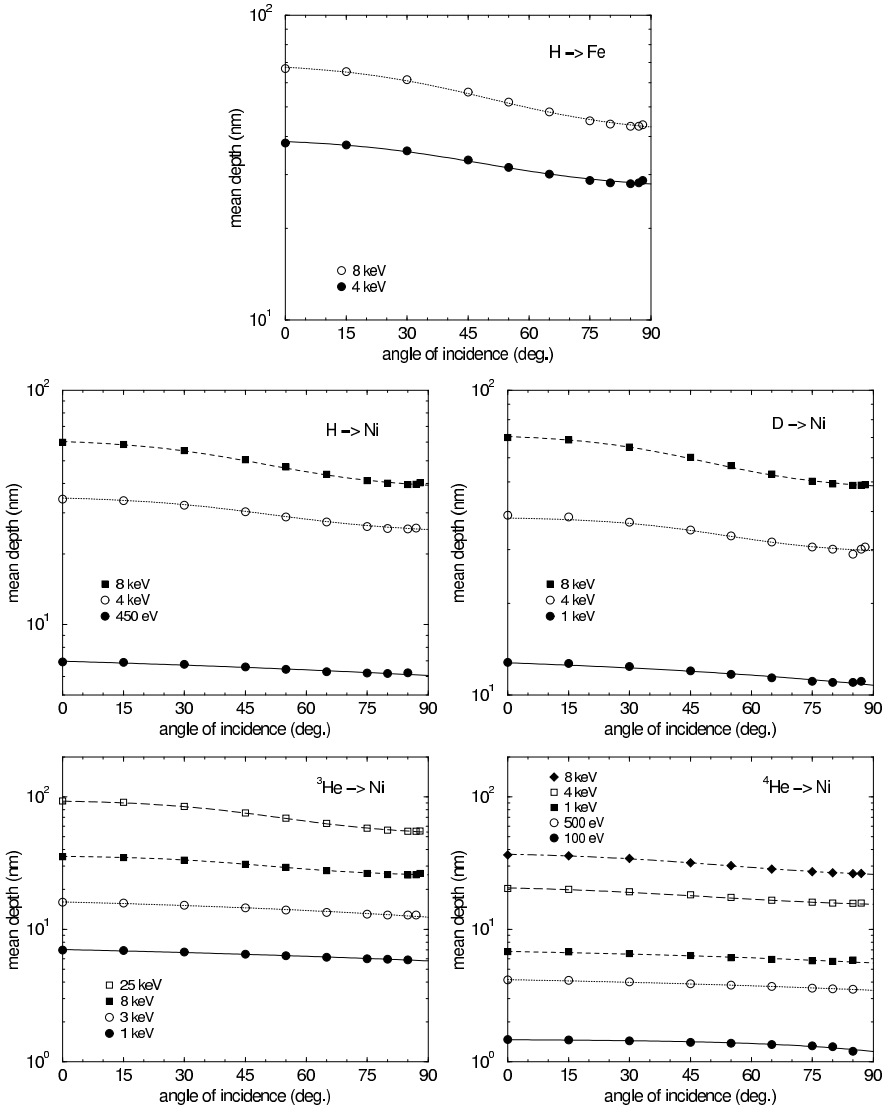

Figure 20: Calculated values for the angular dependence of the mean penetration depth at several incident energies for the bombardment of Fe with H and of Ni with H, D, ^{3}He, ^{4}He [19, 20]. Lines are fits to the calculated values (parameters see table 19).

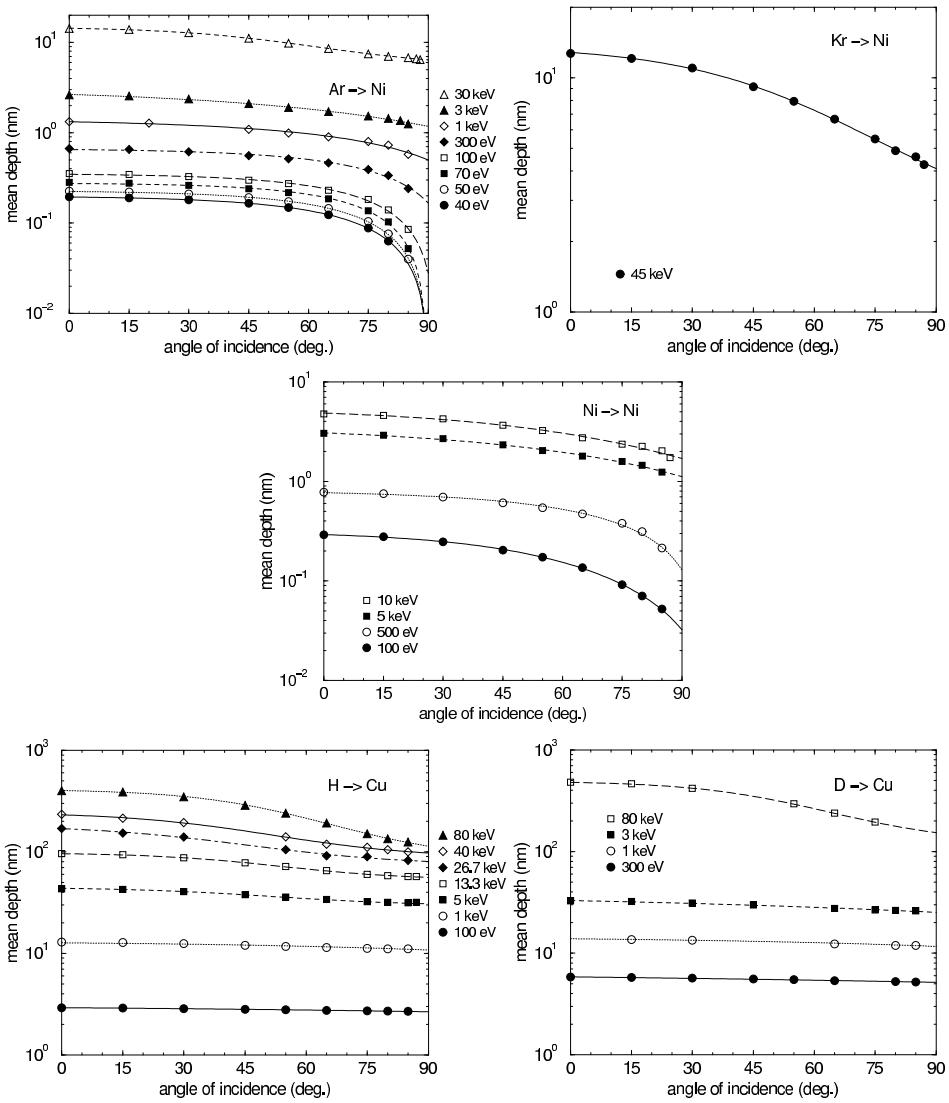

Figure 21: Calculated values for the angular dependence of the mean penetration depth at several incident energies for the bombardment of Ni with Ar, Kr, Ni and of Cu with H, D [19, 20]. Lines are fits to the calculated values (parameters see tables 19 and 20).

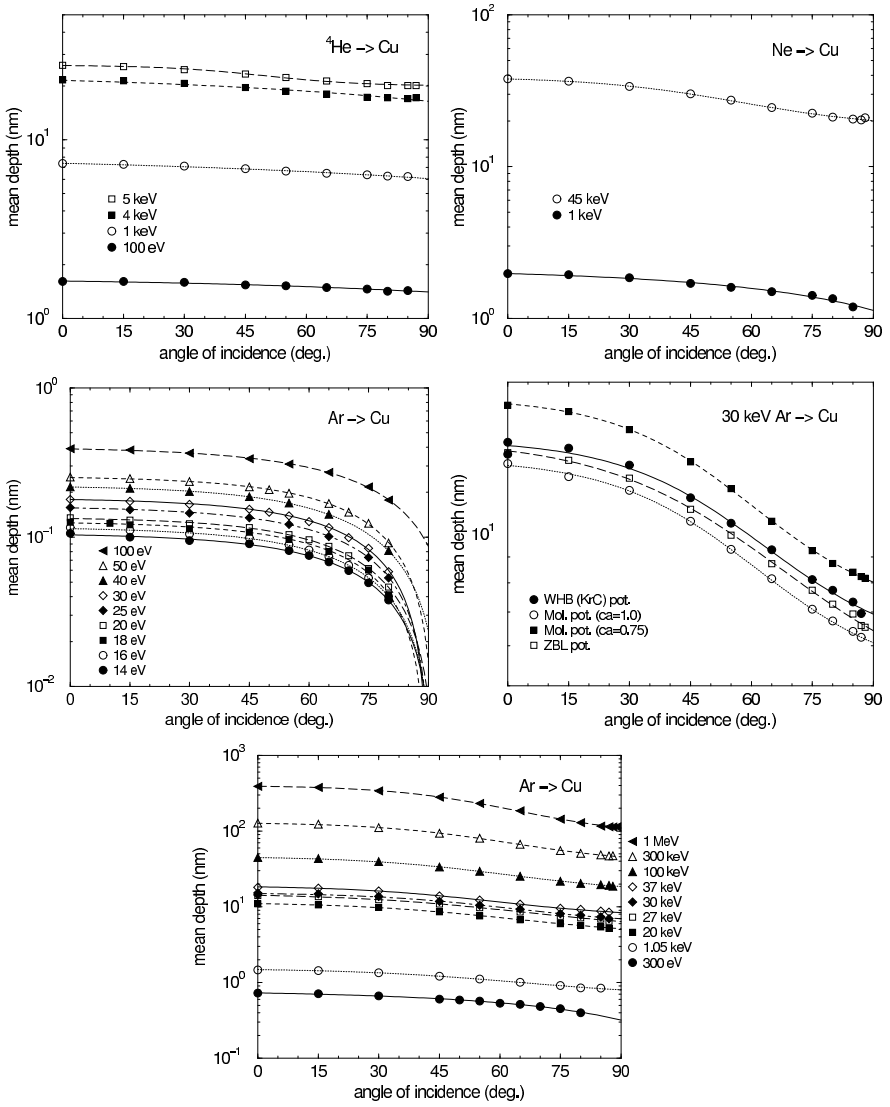

Figure 22: Calculated values for the angular dependence of the mean penetration depth at several incident energies for the bombardment of Cu with ^{4}He, Ne, Ar [19, 20]. Lines are fits to the calculated values (parameters see table 20).

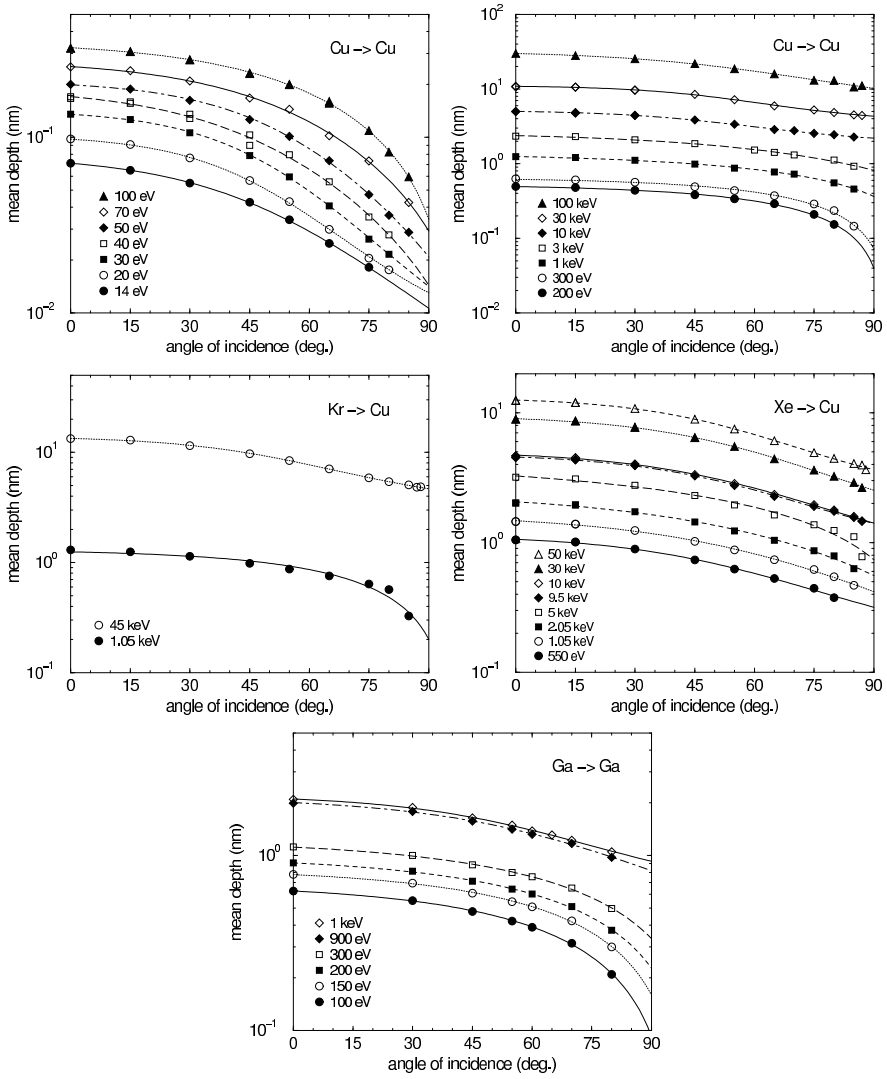

Figure 23: Calculated values for the angular dependence of the mean penetration depth at several incident energies for the bombardment of Cu with Cu, Kr, Xe and of Ga with Ga [19, 20]. Lines are fits to the calculated values (parameters see table 21).

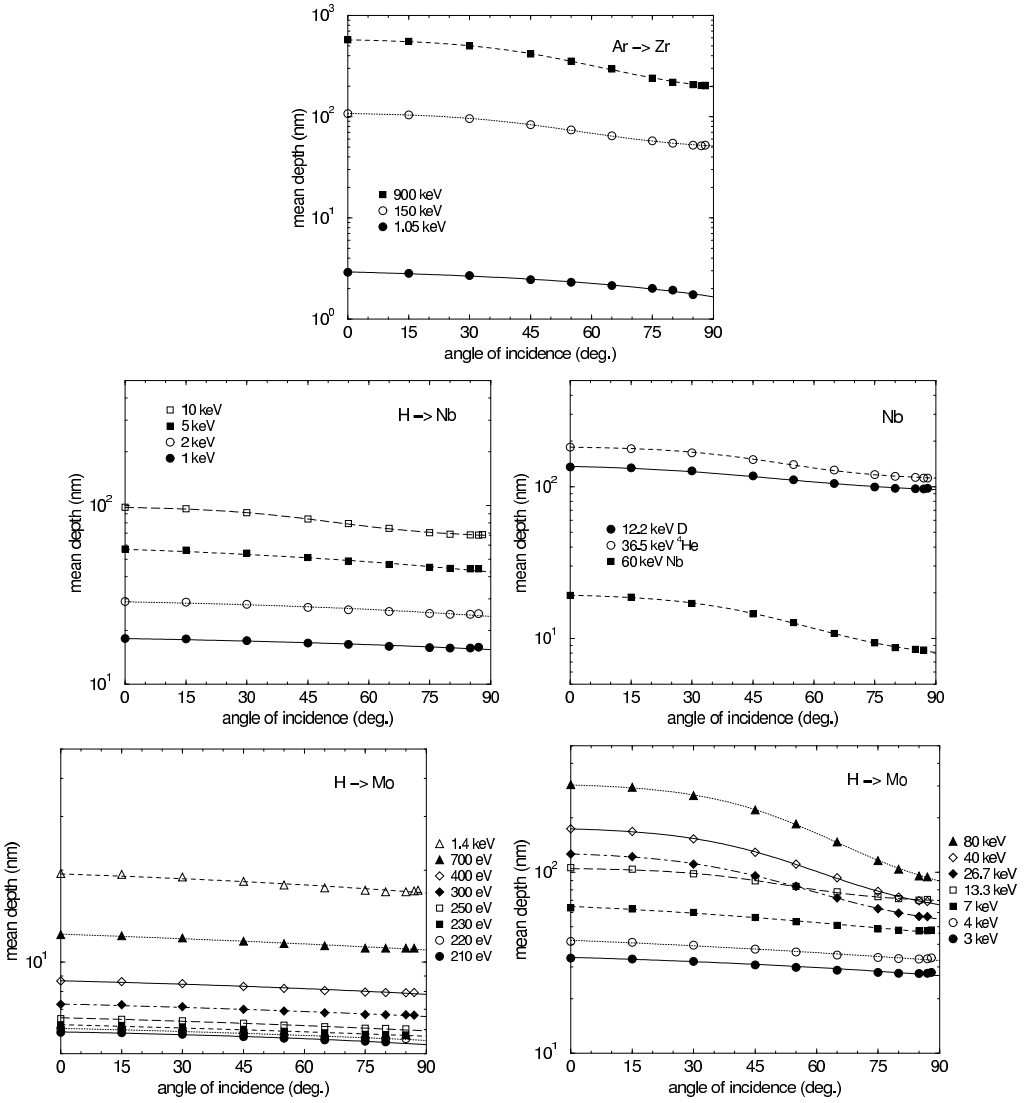

Figure 24: Calculated values for the angular dependence of the mean penetration depth at several incident energies for the bombardment of Zr with Ar and of Nb with H, D, ^{4}He, Nb and of Mo with H [19, 20]. Lines are fits to the calculated values (parameters see tables 21 and 22).

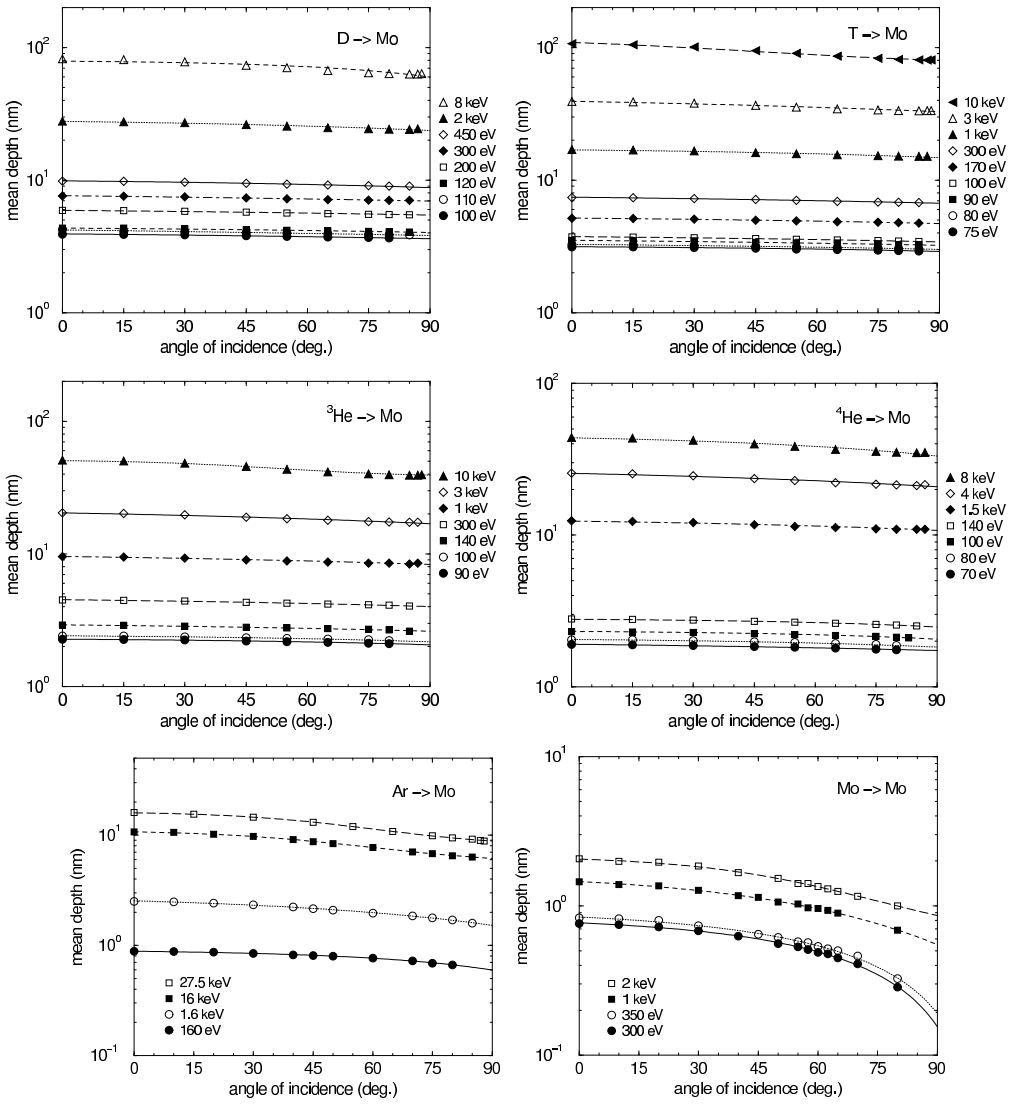

Figure 25: Calculated values for the angular dependence of the mean penetration depth at several incident energies for the bombardment of Mo with D, T, ^{3}He, ^{4}He, Ar, Mo [19, 20]. Lines are fits to the calculated values (parameters see tables 22 and 23).

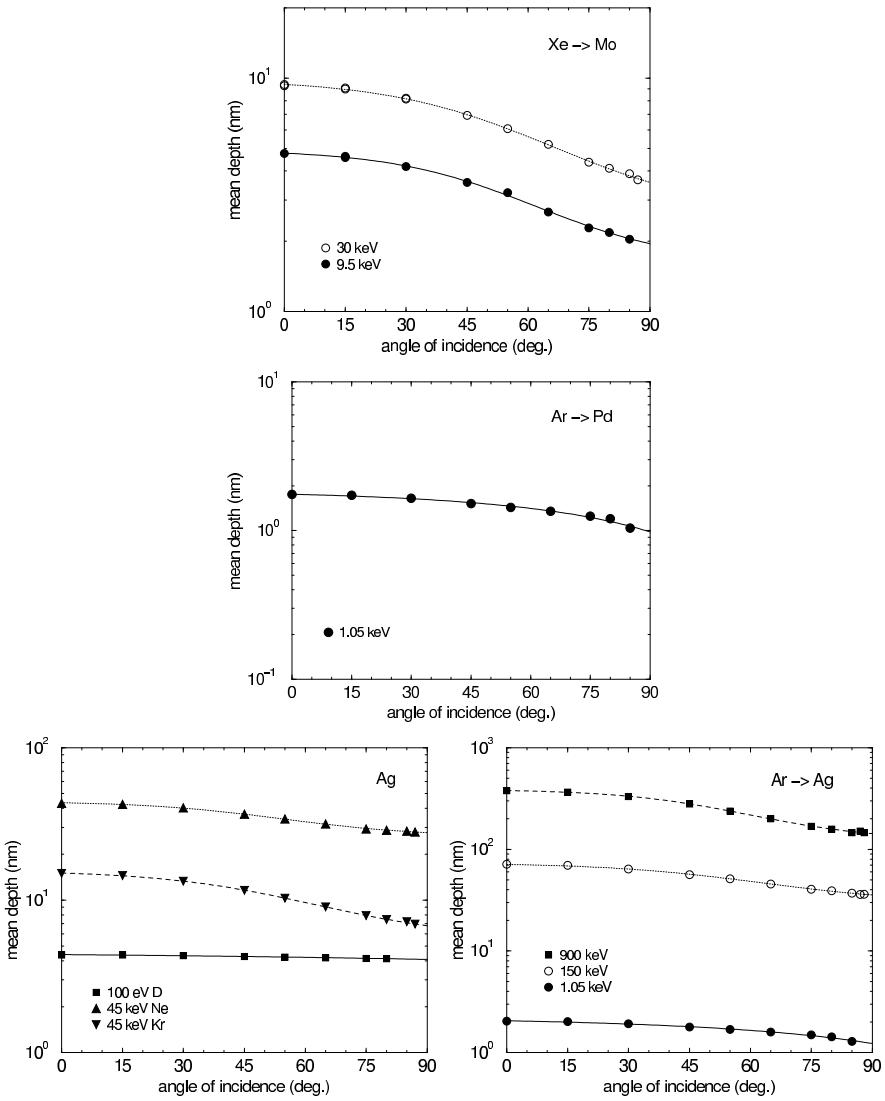

Figure 26: Calculated values for the angular dependence of the mean penetration depth at several incident energies for the bombardment of Mo with Xe and of Pd with Ar and of Ag with D, Ne, Ar, Kr [19, 20]. Lines are fits to the calculated values (parameters see table 23).

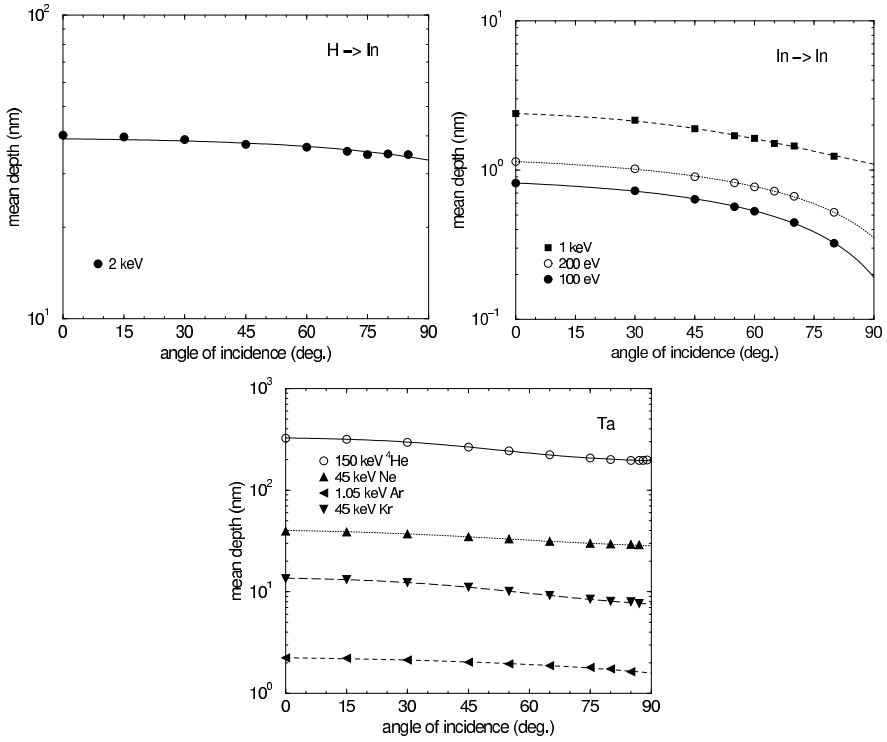

Figure 27: Calculated values for the angular dependence of the mean penetration depth at several incident energies for the bombardment of In with H, In and of Ta with ^{4}He, Ne, Ar, Kr [19, 20]. Lines are fits to the calculated values (parameters see table 23).

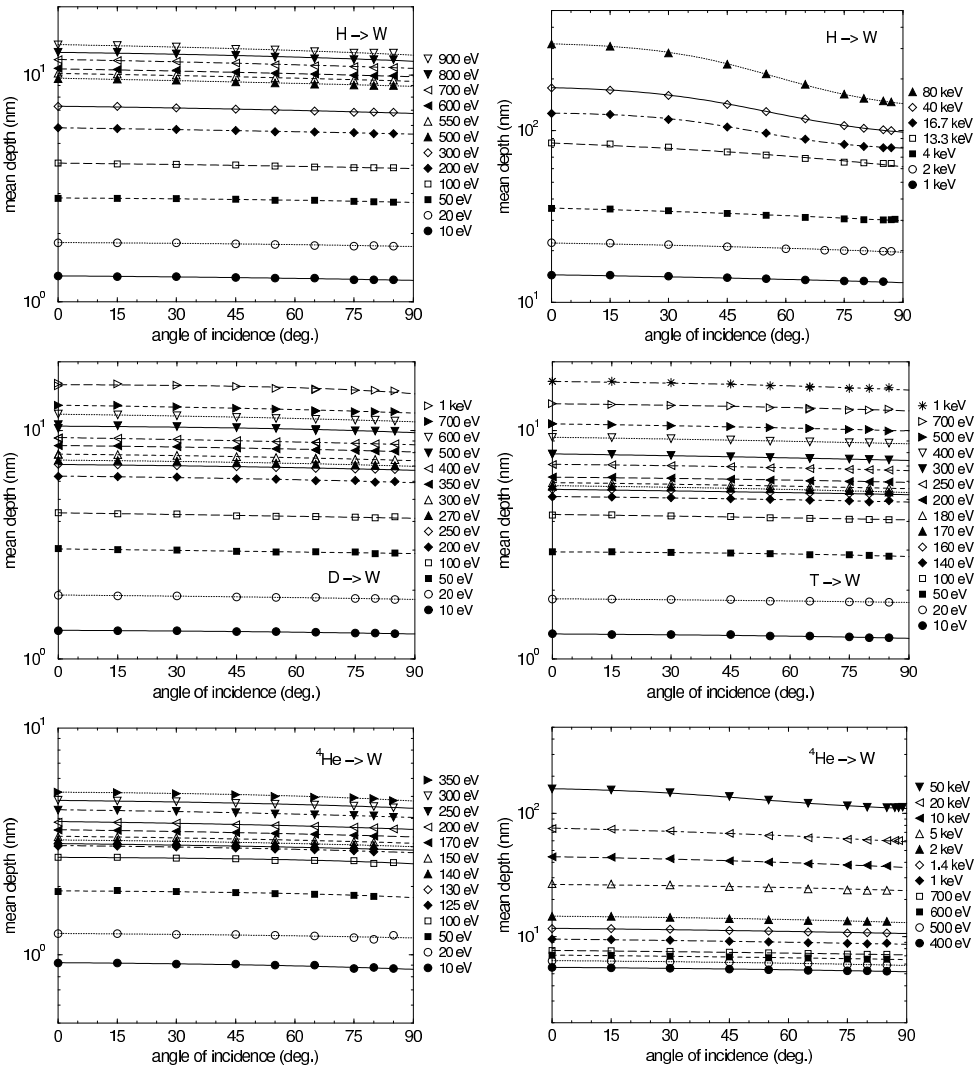

Figure 28: Calculated values for the angular dependence of the mean penetration depth at several incident energies for the bombardment of W with H, D, T, ^{4}He [18, 19, 20]. Lines are fits to the calculated values (parameters see tables 24 and 25).

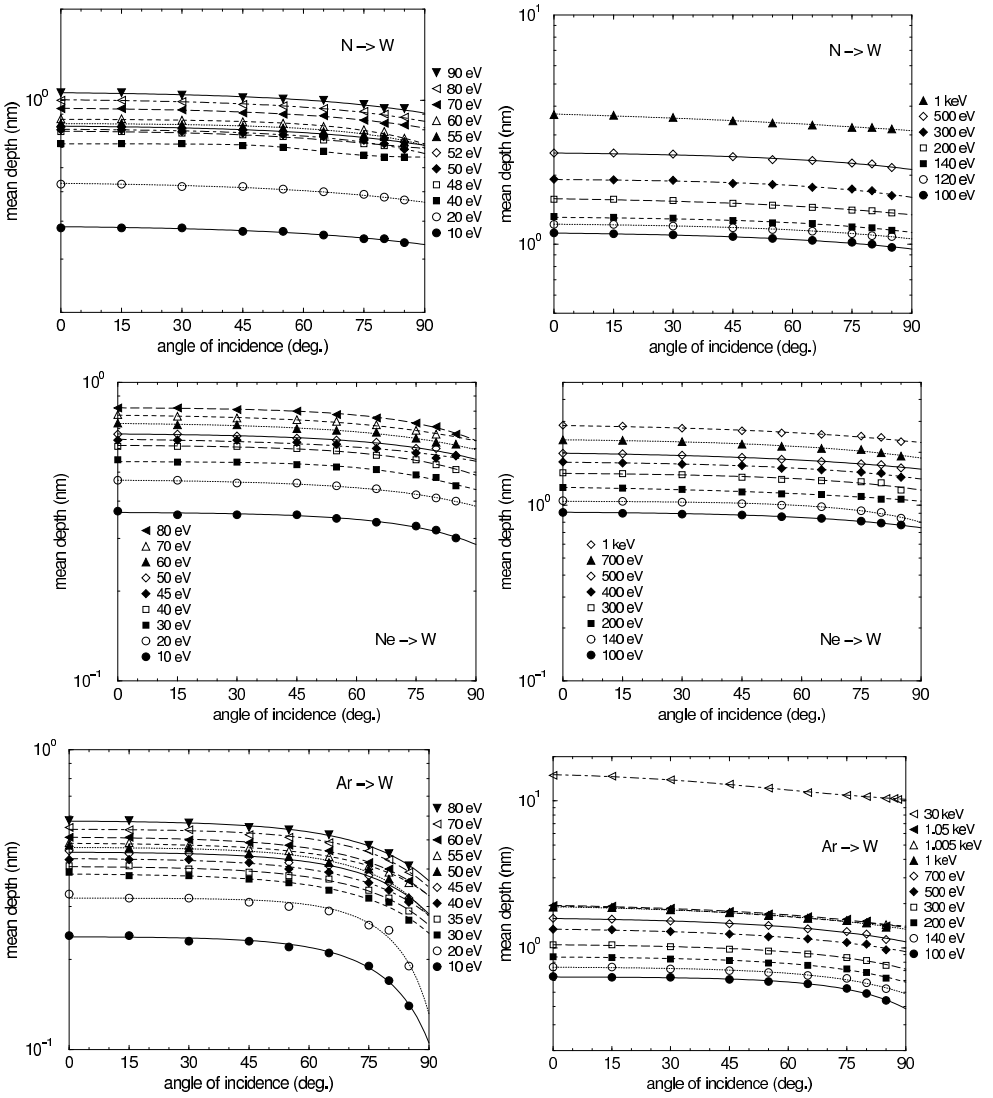

Figure 29: Calculated values for the angular dependence of the mean penetration depth at several incident energies for the bombardment of W with N, Ne, Ar [18, 19, 20]. Lines are fits to the calculated values (parameters see tables 25 and 26).

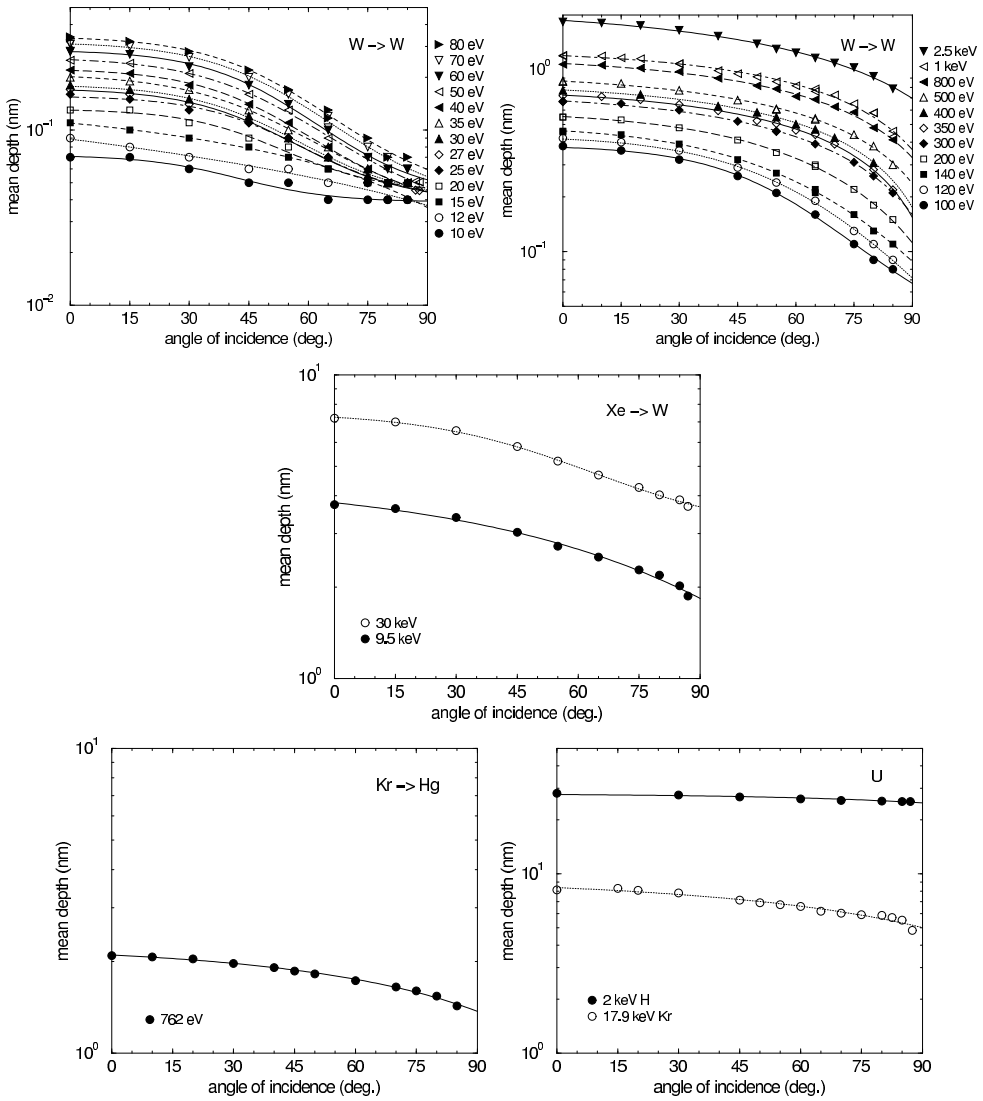

Figure 30: Calculated values for the angular dependence of the mean penetration depth at several incident energies for the bombardment of W with W, Xe, and of Hg with Kr, and of U with H, Kr [18, 19, 20]. Lines are fits to the calculated values (parameters see tables 27 and 28).

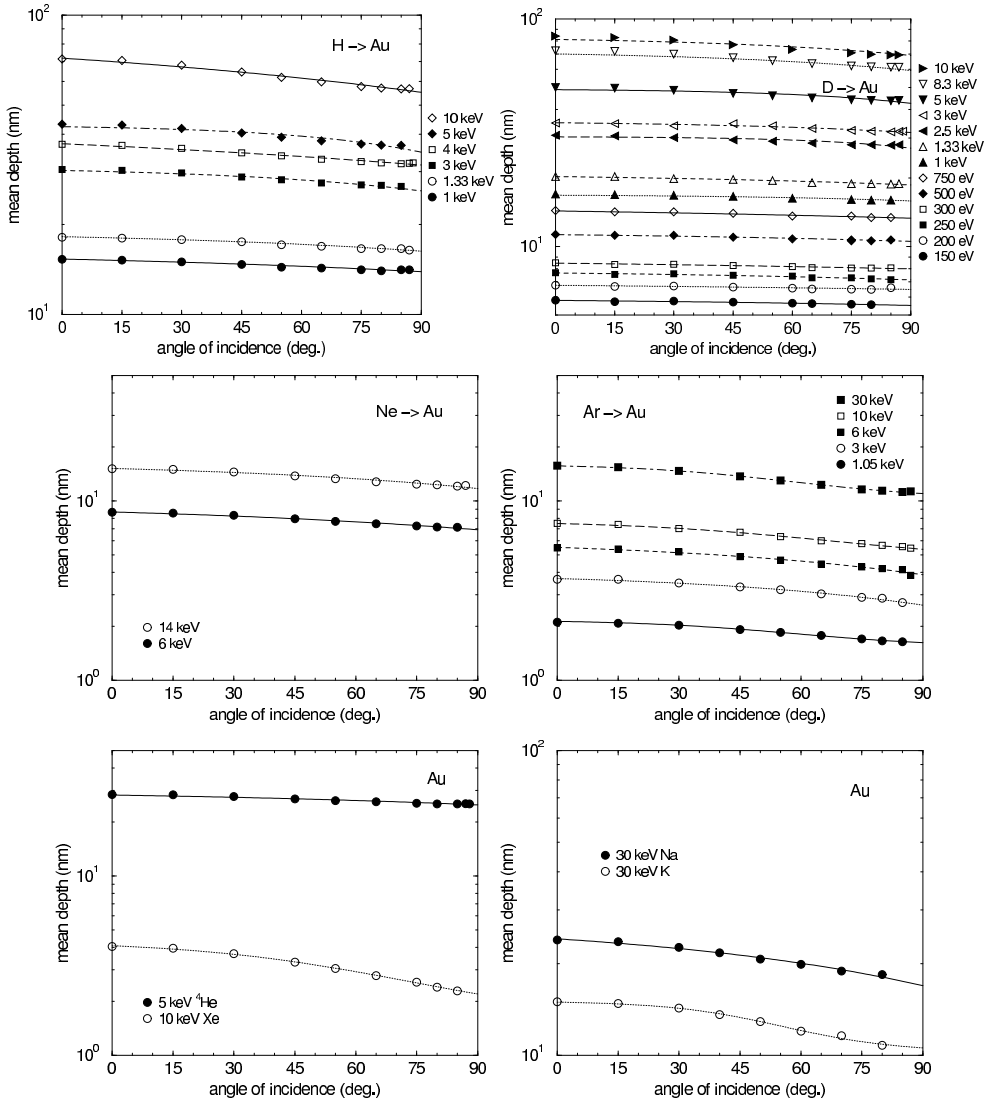

Figure 31: Calculated values for the angular dependence of the mean penetration depth at several incident energies for the bombardment of Au with H, D, ^{4}He, Ne, Na, Ar, K, Xe [19, 20]. Lines are fits to the calculated values (parameters see tables 27 and 28).

References

[1] R. Behrisch, W.Eckstein: *Sputtering*, (Springer, Berlin Heidelberg New York 2007)

[2] W. Eckstein, IPP Report 17/12, Garching (2009)

[3] W. Eckstein, W.von der Linden, V.Dose, Nucl. Instrum. Meth. B 95 (1995) 14

[4] J.F. Ziegler, In Helium Stopping Powers and Ranges in All Elements, The Stopping and Range of Ions in Matter, Vol. 4, ed. by J.F. Ziegler (Pergamon, New York 1977)

[5] W. Eckstein: *Computer Simulation of Ion-Solid Interactions*, Springer Series in Material Science, Vol.10, (Springer, Berlin Heidelberg New York 1991)

[6] J.P. Biersack, L.G. Haggmark, Nucl. Instrum. Meth. 174 (1980) 257

[7] J.P. Biersack, W. Eckstein, Appl. Phys. 34 (1984) 73

[8] W. Eckstein, R. Dohmen, A. Mutzke, R. Schneider, Report IPP 12/3, Garching 2007

[9] W.D.Wilson, L.G.Haggmark, J.P. Biersack, Phys. Rev. B 15 (1977) 2458

[10] J.F. Ziegler, J.P. Biersack, U. Littmark, The Stopping and Range of Ions in Solids, The Stopping and Range of Ions in Matter, Vol. 1, ed. by J.F. Ziegler (Pergamon, New York 1985)

[11] G. Molière, Z. Naturf. A2 (1947) 133

[12] W. Eckstein, S. Hackel, D. Heinemann, B. Fricke Z. Phys. D 24 (1992) 171

[13] O.S. Oen, M.T. Robinson, Nucl. Instrum. Meth. 132 (1976) 647

[14] E. Fermi, E. Teller, Phys. Rev. 72 (1947) 399

[15] J. Lindhard, M. Scharff, Phys. Rev. 124 (1961) 128

[16] H.H. Andersen, J.F. Ziegler, In Hydrogen Stopping Powers and Ranges in All Elements, The Stopping and Range of Ions in Matter, Vol. 3, ed. by J.F. Ziegler (Pergamon, New York 1977)

[17] W. Möller, W. Eckstein, J.P. Biersack, Comp. Phys. Commun. 51 (1988) 355

[18] W. Eckstein, IPP Report 9/117, Garching (1998)

[19] W. Eckstein, IPP Report 9/132, Garching (2002)

[20] W. Eckstein, calculated values can be retrieved from ftp: ftp.rzg.mpg.de/ftp/pub/ipp/eckstein/rep05

Table 1: Constants, a_i, for the energy dependence of the mean (penetration) depth, md, at normal incidence for different ions and targets. The lower limit of the fit is 10 eV, the upper limit, ul, is given in MeV.

ion	solid	a1	a2	a3	a4	ul (MeV)	ρ (g/cm^3)
D	Li	0.6617e+1	0.9577e+0	-0.4281e-2	-0.3931e-2	0.1	0.53
T	Li	0.6625e+1	0.9902e+0	-0.3831e-2	-0.4367e-2	0.1	0.53
^{4}He	Li	0.5937e+1	0.9773e+0	0.5874e-2	-0.4824e-2	0.1	0.53
Li	Li	0.5536e+1	0.9621e+0	0.1552e-1	-0.3992e-2	0.1	0.53
H	Be	0.5330e+1	0.7851e+0	0.1923e-2	-0.2722e-2	1.0	1.80
D	Be	0.5398e+1	0.8686e+0	-0.1029e-2	0.3849e-5	1.0	1.80
T	Be	0.5429e+1	0.9102e+0	-0.3072e-2	-0.1011e-2	1.0	1.80
^{3}He	Be	0.4835e+1	0.9760e+0	0.7735e-3	-0.6925e-2	0.1	1.80
^{4}He	Be	0.4773e+1	0.9390e+0	0.4912e-2	-0.3545e-2	1.0	1.80
Be	Be	0.4147e+1	0.8772e+0	0.1301e-1	0.1374e-2	0.1	1.80
N	Be	0.3715e+1	0.7958e+0	0.1752e-1	0.4472e-2	0.1	1.80
Ne	Be	0.3621e+1	0.7318e+0	0.1184e-1	0.5655e-2	0.1	1.80
Ar	Be	0.3491e+1	0.5949e+0	0.1522e-1	0.6959e-2	0.1	1.80
Kr	Be	0.3737e+1	0.4665e+0	0.2215e-1	0.3294e-2	0.1	1.80
Xe	Be	0.4027e+1	0.3998e+0	0.2035e-1	0.2312e-2	0.1	1.80
H	B	0.5236e+1	0.8774e+0	-0.5529e-2	-0.4447e-2	0.1	2.35
D	B	0.5324e+1	0.9743e+0	-0.8494e-2	-0.7248e-2	0.1	2.35
T	B	0.5297e+1	0.9898e+0	-0.7255e-2	-0.6521e-2	0.1	2.35
^{4}He	B	0.4613e+1	0.9800e+0	0.8103e-3	-0.7252e-2	0.1	2.35
B	B	0.3749e+1	0.8587e+0	0.1400e-1	0.1205e-2	0.1	2.35
Ne	B	0.3301e+1	0.7520e+0	0.1466e-1	0.4451e-2	0.1	2.35
H	C	0.5345e+1	0.7532e+0	0.1323e-2	0.2275e-2	1.0	1.85
H	C	0.5278e+1	0.8715e+0	-0.4675e-2	-0.4912e-2	0.1	2.26
D	C	0.5499e+1	0.9177e+0	-0.1663e-1	-0.8035e-2	0.1	1.85
D	C	0.5259e+1	0.8451e+0	-0.1153e-2	0.7802e-3	1.0	2.26
T	C	0.5424e+1	0.8924e+0	-0.1868e-2	-0.1698e-2	1.0	1.85
^{3}He	C	0.4623e+1	0.9508e+0	0.7801e-2	-0.8143e-2	0.1	2.26
^{4}He	C	0.4774e+1	0.8988e+0	0.5629e-2	-0.3826e-2	1.0	1.85
C	C	0.3787e+1	0.8096e+0	0.2240e-1	0.2166e-2	0.1	1.85
C	C	0.3582e+1	0.8423e+0	0.1992e-1	0.9773e-3	0.1	2.26
N	C	0.3740e+1	0.7773e+0	0.1586e-1	0.2973e-2	0.1	1.85
N	C	0.3549e+1	0.8014e+0	0.1500e-1	0.3037e-2	0.1	2.26
Ne	C	0.3562e+1	0.7250e+0	0.1841e-1	0.4572e-2	0.1	1.85
Ne	C	0.3345e+1	0.7319e+0	0.1709e-1	0.5136e-2	0.1	2.26
Ar	C	0.3274e+1	0.6161e+0	0.8864e-2	0.6316e-2	0.1	2.26
Xe	C	0.3729e+1	0.4277e+0	0.1755e-1	0.1766e-2	0.1	2.26
^{4}He	Mg	0.5261e+1	0.8655e+0	0.1423e-1	-0.5035e-2	0.1	1.74
Ne	Mg	0.3943e+1	0.6871e+0	0.2791e-1	0.2482e-2	0.1	1.74
Mg	Mg	0.3850e+1	0.6646e+0	0.2447e-1	0.3395e-2	0.1	1.74
Ar	Mg	0.3787e+1	0.5901e+0	0.2144e-1	0.4096e-2	0.1	1.74
Kr	Mg	0.3922e+1	0.4797e+0	0.1408e-1	0.3919e-2	0.1	1.74

Table 2: Constants, a_i, for the energy dependence of the mean (penetration) depth, md, at normal incidence for different ions and targets. The lower limit of the fit is 10 eV, the upper limit, ul, is given in MeV.

ion	solid	a1	a2	a3	a4	ul (MeV)	ρ (g/cm^3)
H	Al	0.5524e+1	0.7913e+0	0.6720e-2	-0.3386e-2	0.1	2.70
D	Al	0.5567e+1	0.8536e+0	0.5625e-2	-0.4912e-2	0.1	2.70
T	Al	0.5581e+1	0.8992e+0	0.5131e-2	-0.5833e-2	0.1	2.70
^{3}He	Al	0.4928e+1	0.8341e+0	0.1286e-1	-0.4771e-2	0.1	2.70
^{4}He	Al	0.4872e+1	0.8420e+0	0.2057e-1	-0.2843e-2	0.1	2.70
N	Al	0.3809e+1	0.7154e+0	0.2208e-1	0.3532e-2	0.1	2.70
Ne	Al	0.3569e+1	0.6885e+0	0.2456e-1	0.3052e-2	0.1	2.70
Al	Al	0.3456e+1	0.6782e+0	0.2108e-1	0.2703e-2	0.1	2.70
Ar	Al	0.3385e+1	0.5987e+0	0.1631e-1	0.4991e-2	0.1	2.70
Kr	Al	0.3505e+1	0.5094e+0	0.6648e-2	0.3869e-2	0.1	2.70
Xe	Al	0.3697e+1	0.4463e+0	0.7826e-2	0.3283e-2	0.1	2.70
H	Si	0.5685e+1	0.7923e+0	0.6689e-2	-0.3872e-2	0.1	2.32
D	Si	0.5741e+1	0.8478e+0	0.5614e-2	-0.4875e-2	0.1	2.32
T	Si	0.5731e+1	0.8877e+0	0.7028e-2	-0.5453e-2	0.1	2.32
^{3}He	Si	0.5083e+1	0.8186e+0	0.1489e-1	-0.4057e-2	0.1	2.32
^{4}He	Si	0.5031e+1	0.8337e+0	0.2186e-1	-0.2920e-2	0.1	2.32
N	Si	0.3967e+1	0.7090e+0	0.2445e-1	0.3017e-2	0.1	2.32
Ne	Si	0.3734e+1	0.6765e+0	0.2719e-1	0.2743e-2	0.1	2.32
(KrC)Si	Si	0.3449e+1	0.6880e+0	0.2288e-1	0.2453e-2	0.1	2.32
(Mol)Si	Si	0.3327e+1	0.6867e+0	0.1691e-1	0.5105e-2	0.1	2.32
(ZBL)Si	Si	0.3566e+1	0.6384e+0	0.1584e-1	0.5316e-2	0.1	2.32
Ar	Si	0.3560e+1	0.5987e+0	0.1728e-1	0.3593e-2	0.1	2.32
Kr	Si	0.3675e+1	0.5006e+0	0.9187e-2	0.3516e-2	0.1	2.32
Xe	Si	0.3845e+1	0.4464e+0	0.9855e-2	0.2896e-2	0.1	2.32
Ca	Ca	0.4115e+1	0.5622e+0	0.2377e-1	0.3338e-2	0.1	1.54
Sc	Sc	0.3513e+1	0.5713e+0	0.1725e-1	0.4154e-2	0.1	3.00
H	Ti	0.5387e+1	0.7391e+0	0.9920e-2	-0.2890e-2	0.1	4.52
D	Ti	0.5469e+1	0.7891e+0	0.1054e-1	-0.3473e-2	0.1	4.52
T	Ti	0.5450e+1	0.8243e+0	0.1138e-1	-0.4243e-2	0.1	4.52
^{3}He	Ti	0.4848e+1	0.7416e+0	0.1289e-1	-0.2067e-2	0.1	4.52
^{4}He	Ti	0.4817e+1	0.7805e+0	0.1746e-1	-0.3694e-1	0.1	4.52
N	Ti	0.3715e+1	0.6718e+0	0.2545e-1	0.2855e-2	0.1	4.52
Ne	Ti	0.3543e+1	0.6189e+0	0.2211e-1	0.3262e-2	0.1	4.52
Ar	Ti	0.3182e+1	0.5868e+0	0.1876e-1	0.4044e-2	0.1	4.52
Ti	Ti	0.3121e+1	0.5766e+0	0.1163e-1	0.4885e-2	0.1	4.52
Kr	Ti	0.3169e+1	0.5105e+0	0.6343e-2	0.4634e-2	0.1	4.52
Xe	Ti	0.3325e+1	0.4525e+0	0.1928e-2	0.4763e-2	0.1	4.52

Table 3: Constants, a_i, for the energy dependence of the mean (penetration) depth, md, at normal incidence for different ions and targets. The lower limit of the fit is 10 eV, the upper limit, ul, is given in MeV.

ion	solid	a1	a2	a3	a4	ul (MeV)	ρ (g/cm^3)
H	V	0.5127e+1	0.7352e+0	0.1223e-1	-0.2384e-2	0.1	6.10
D	V	0.5203e+1	0.7794e+0	0.1205e-1	-0.2996e-2	0.1	6.10
T	V	0.5204e+1	0.8190e+0	0.1228e-1	-0.3592e-2	0.1	6.10
^{4}He	V	0.4569e+1	0.7783e+0	0.1714e-1	-0.3945e-2	0.1	6.10
N	V	0.3473e+1	0.6658e+0	0.2346e-1	0.3388e-2	0.1	6.10
Ne	V	0.3210e+1	0.6479e+0	0.2610e-1	0.2669e-2	0.1	6.10
Ar	V	0.2916e+1	0.5946e+0	0.1587e-1	0.4372e-2	0.1	6.10
V	V	0.2848e+1	0.5766e+0	0.5234e-2	0.5975e-2	0.1	6.10
Kr	V	0.2859e+1	0.5334e+0	0.3138e-2	0.4597e-2	0.1	6.10
Xe	V	0.3012e+1	0.4723e+0	-0.2837e-2	0.5334e-2	0.1	6.10
H	Cr	0.4780e+1	0.6766e+0	0.5732e-1	0.9436e-2	0.1	7.19
^{4}He	Cr	0.4403e+1	0.7811e+0	0.1847e-1	-0.4219e-2	0.1	7.19
Ne	Cr	0.3056e+1	0.6422e+0	0.2408e-1	0.3162e-2	0.1	7.19
Ar	Cr	0.2744e+1	0.6018e+0	0.1427e-1	0.4314e-2	0.1	7.19
Cr	Cr	0.2674e+1	0.5716e+0	0.1421e-3	0.6965e-2	0.1	7.19
Kr	Cr	0.2667e+1	0.5492e+0	0.1549e-2	0.4375e-2	0.1	7.19
Xe	Cr	0.2813e+1	0.4984e+0	-0.4399e-2	0.4650e-2	0.1	7.19
^{4}He	Mn	0.4418e+1	0.7676e+0	0.1968e-1	-0.3435e-2	0.1	7.43
Ne	Mn	0.3069e+1	0.6424e+0	0.2452e-1	0.2864e-2	0.1	7.43
H	Fe	0.4922e+1	0.7252e+0	0.1748e-1	-0.9824e-3	0.1	7.87
D	Fe	0.4987e+1	0.7670e+0	0.1763e-1	-0.1555e-2	0.1	7.87
T	Fe	0.4983e+1	0.8025e+0	0.1877e-1	-0.2016e-2	0.1	7.87
^{4}He	Fe	0.4355e+1	0.7692e+0	0.2193e-1	-0.3343e-2	0.1	7.87
N	Fe	0.3274e+1	0.6529e+0	0.2264e-1	0.3683e-2	0.1	7.87
Ne	Fe	0.3002e+1	0.6343e+0	0.2577e-1	0.3104e-2	0.1	7.87
Ar	Fe	0.2706e+1	0.5970e+0	0.1351e-1	0.4348e-2	0.1	7.87
Fe	Fe	0.2615e+1	0.5624e+0	-0.2163e-2	0.7256e-2	0.1	7.87
Kr	Fe	0.2602e+1	0.5515e+0	0.1371e-2	0.4269e-2	0.1	7.87
Xe	Fe	0.2735e+1	0.5062e+0	-0.4834e-2	0.4260e-2	0.1	7.87
^{4}He	Co	0.4286e+1	0.7600e+0	0.2297e-1	-0.3067e-2	0.1	8.80
Ne	Co	0.2953e+1	0.6320e+0	0.2419e-1	0.3153e-2	0.1	8.80
Ar	Co	0.2629e+1	0.5984e+0	0.1350e-1	0.4240e-2	0.1	8.80
Kr	Co	0.2505e+1	0.5626e+0	0.1150e-2	0.3881e-2	0.1	8.80
Xe	Co	0.2626e+1	0.5203e+0	-0.5109e-2	0.3863e-2	0.1	8.80
H	Ni	0.4817e+1	0.7164e+0	0.1847e-1	-0.7206e-3	0.1	8.90
D	Ni	0.4887e+1	0.7620e+0	0.1830e-1	-0.1457e-2	0.1	8.90
T	Ni	0.4895e+1	0.7891e+0	0.1857e-1	-0.1560e-2	0.1	8.90
^{4}He	Ni	0.4252e+1	0.7554e+0	0.2365e-1	-0.2573e-2	0.1	8.90
N	Ni	0.3188e+1	0.6489e+0	0.2130e-1	0.3829e-2	0.1	8.90
O	Ni	0.3087e+1	0.6388e+0	0.2112e-1	0.3978e-2	0.1	8.90
Ne	Ni	0.2926e+1	0.6319e+0	0.2373e-1	0.3101e-2	0.1	8.90
Ar	Ni	0.2591e+1	0.5933e+0	0.1316e-1	0.4674e-2	0.1	8.90
Ni	Ni	0.2497e+1	0.5502e+0	-0.9765e-2	0.8881e-2	0.1	8.90
Kr	Ni	0.2486e+1	0.5509e+0	0.7731e-3	0.4394e-2	0.1	8.90
Xe	Ni	0.2607e+1	0.5203e+0	-0.4660e-2	0.3517e-2	0.1	8.90

Table 4: Constants, a_i, for the energy dependence of the mean (penetration) depth, md, at normal incidence for different ions and targets. The lower limit of the fit is 10 eV, the upper limit, ul, is given in MeV.

ion	solid	a1	a2	a3	a4	ul (MeV)	ρ (g/cm^3)
H	Cu	0.4882e+1	0.7090e+0	0.2085e-1	-0.9030e-3	0.1	8.95
T	Cu	0.4959e+1	0.7854e+0	0.1972e-1	-0.1914e-2	0.1	8.95
^{4}He	Cu	0.4311e+1	0.7332e+0	0.2677e-1	-0.1258e-2	0.1	8.95
N	Cu	0.3262e+1	0.6370e+0	0.2596e-1	0.3271e-2	0.1	8.95
Ne	Cu	0.3019e+1	0.6613e+0	0.2389e-1	0.1550e-3	1.0	8.95
Ar	Cu	0.2674e+1	0.6005e+0	0.1417e-1	0.3670e-2	0.1	8.95
Cu	Cu	0.2555e+1	0.5229e+0	-0.7749e-2	0.9795e-2	0.1	8.95
Kr	Cu	0.2543e+1	0.5564e+0	0.1215e-2	0.3730e-2	1.0	8.95
Xe	Cu	0.2653e+1	0.5128e+0	-0.4618e-2	0.3997e-2	1.0	8.95
^{4}He	Zn	0.4571e+1	0.7287e+0	0.2624e-1	-0.9954e-3	0.1	7.11
Ne	Zn	0.3257e+1	0.6259e+0	0.2768e-1	0.1956e-3	0.1	7.11
Ar	Zn	0.2941e+1	0.5675e+0	0.1747e-1	0.4369e-2	0.1	7.11
Zn	Zn	0.2807e+1	0.5403e+0	0.4703e-2	0.5220e-2	0.1	7.11
Kr	Cu	0.2811e+1	0.5276e+0	0.6022e-2	0.4026e-2	0.1	7.11
D	Ga	0.5472e+1	0.7352e+0	0.1366e-1	-0.2278e-2	0.1	5.91
T	Ga	0.5471e+1	0.7695e+0	0.1472e-1	-0.2808e-2	0.1	5.91
^{4}He	Ga	0.4832e+1	0.7168e+0	0.2398e-1	-0.1173e-3	0.1	5.91
Ne	Ga	0.3533e+1	0.6106e+0	0.2189e-1	0.3701e-2	0.1	5.91
Ga	Ga	0.3052e+1	0.5282e+0	0.8074e-2	0.4596e-2	0.1	5.91
H	Ge	0.5522e+1	0.6939e+0	0.1375e-1	-0.1775e-2	0.1	5.34
T	Ge	0.5605e+1	0.7312e+0	0.1264e-1	-0.2551e-2	0.1	5.34
^{4}He	Ge	0.4996e+1	0.7189e+0	0.1988e-1	-0.2162e-2	0.1	5.34
Ne	Ge	0.3659e+1	0.6119e+0	0.2968e-1	0.1797e-2	0.1	5.34
Na	Ge	0.3596e+1	0.6050e+0	0.2895e-1	0.1944e-2	0.1	5.34
Ar	Ge	0.3390e+1	0.5388e+0	0.1988e-1	0.3899e-2	0.1	5.34
K	Ge	0.3319e+1	0.5492e+0	0.2221e-1	0.3422e-2	0.1	5.34
Ge	Ge	0.3182e+1	0.5189e+0	0.9988e-2	0.4333e-2	0.1	5.34
Kr	Ge	0.3196e+1	0.4982e+0	0.1234e-1	0.3750e-2	0.1	5.34
^{4}He	Se	0.5183e+1	0.7105e+0	0.2088e-1	-0.1921e-2	0.1	4.79
Ne	Se	0.3860e+1	0.6051e+0	0.2961e-1	0.1552e-2	0.1	4.79
Ar	Se	0.3525e+1	0.5532e+0	0.2492e-1	0.2479e-2	0.1	4.79
H	Zr	0.5508e+1	0.6757e+0	0.1002e-1	-0.2679e-2	0.1	6.47
D	Zr	0.5634e+1	0.7106e+0	0.7586e-2	-0.3169e-2	0.1	6.47
T	Zr	0.5581e+1	0.7296e+0	0.2114e-1	-0.9727e-3	0.1	6.47
^{3}He	Zr	0.5042e+1	0.6821e+0	0.1219e-1	-0.3348e-2	0.1	6.47
^{4}He	Zr	0.5022e+1	0.6994e+0	0.1407e-1	-0.3501e-4	0.1	6.47
Ne	Zr	0.3682e+1	0.5926e+0	0.2931e-1	0.1539e-2	0.1	6.47
Ar	Zr	0.3360e+1	0.5626e+0	0.2249e-1	0.1452e-2	0.1	6.47
Kr	Zr	0.3148e+1	0.4905e+0	0.1292e-1	0.3311e-2	0.1	6.47
Zr	Zr	0.3121e+1	0.4952e+0	0.6232e-2	0.4348e-2	0.1	6.47
Xe	Zr	0.3251e+1	0.4230e+0	0.4965e-2	0.5189e-2	0.1	6.47

Table 5: Constants, a_i, for the energy dependence of the mean (penetration) depth, md, at normal incidence for different ions and targets. The lower limit of the fit is 10 eV, the upper limit, ul, is given in MeV.

ion	solid	a1	a2	a3	a4	ul (MeV)	ρ (g/cm^3)
H	Nb	0.5170e+1	0.6137e+0	0.1442e-1	0.1326e-2	3.0	8.60
D	Nb	0.5319e+1	0.6900e+0	0.7748e-2	-0.2449e-2	0.1	8.60
T	Nb	0.5353e+1	0.7341e+0	0.9259e-2	-0.3310e-2	0.1	8.60
^{3}He	Nb	0.4748e+1	0.6802e+0	0.1718e-1	-0.2338e-2	0.1	8.60
^{4}He	Nb	0.4702e+1	0.6814e+0	0.2637e-1	-0.6747e-4	0.1	8.60
Ne	Nb	0.3406e+1	0.5971e+0	0.2868e-1	0.1392e-2	0.1	8.60
Ar	Nb	0.3062e+1	0.5449e+0	0.2124e-1	0.3208e-2	0.1	8.60
Kr	Nb	0.2854e+1	0.5001e+0	0.9434e-2	0.3956e-2	0.1	8.60
Nb	Nb	0.2823e+1	0.5054e+0	0.1514e-2	0.4937e-2	0.1	8.60
Xe	Nb	0.2896e+1	0.4694e+0	0.2883e-2	0.4077e-2	0.1	8.60
H	Mo	0.5085e+1	0.6745e+0	0.1077e-1	-0.2330e-2	0.1	10.21
D	Mo	0.5176e+1	0.6986e+0	0.9708e-2	-0.2477e-2	0.1	10.21
T	Mo	0.5196e+1	0.7310e+0	0.1148e-1	-0.2887e-2	0.1	10.21
^{3}He	Mo	0.4588e+1	0.6735e+0	0.1869e-1	-0.2001e-2	0.1	10.21
^{4}He	Mo	0.4584e+1	0.6952e+0	0.2027e-1	-0.2255e-2	0.1	10.21
N	Mo	0.3542e+1	0.6030e+0	0.2481e-1	0.2619e-2	0.1	10.21
O	Mo	0.3436e+1	0.6054e+0	0.2396e-1	0.2396e-2	0.1	10.21
Ne	Mo	0.3257e+1	0.5970e+0	0.2875e-1	0.1328e-2	0.1	10.21
Ar	Mo	0.2977e+1	0.5308e+0	0.1623e-1	0.4293e-2	0.1	10.21
Kr	Mo	0.2717e+1	0.5035e+0	0.6650e-2	0.4308e-2	0.1	10.21
Mo	Mo	0.2664e+1	0.5252e+0	-0.3792e-2	0.4817e-2	0.1	10.21
Xe	Mo	0.2720e+1	0.4832e+0	0.9138e-3	0.3976e-2	0.1	10.21
H	Ru	0.4957e+1	0.6743e+0	0.1133e-1	-0.2285e-2	0.1	12.18
D	Ru	0.5053e+1	0.7022e+0	0.1087e-1	-0.2412e-2	0.1	12.18
^{4}He	Ru	0.4440e+1	0.6846e+0	0.2254e-1	-0.1597e-2	0.1	12.18
Ne	Ru	0.3134e+1	0.5960e+0	0.2840e-1	0.1182e-2	0.1	12.18
Ar	Ru	0.2779e+1	0.5397e+0	0.1859e-1	0.3998e-2	0.1	12.18
Kr	Ru	0.2538e+1	0.5175e+0	0.6624e-2	0.3825e-2	0.1	12.18
Xe	Ru	0.2546e+1	0.4935e+0	-0.2987e-3	0.3984e-2	0.1	12.18
H	Rh	0.4942e+1	0.6663e+0	0.1271e-1	-0.1830e-2	0.1	12.40
D	Rh	0.5036e+1	0.6964e+0	0.1254e-1	-0.2077e-2	0.1	12.40
^{3}He	Rh	0.4466e+1	0.6739e+0	0.1783e-1	-0.2529e-2	0.1	12.40
^{4}He	Rh	0.4451e+1	0.6833e+0	0.1967e-1	-0.2122e-2	0.1	12.40
Ne	Rh	0.3125e+1	0.5917e+0	0.2872e-1	0.1316e-2	0.1	12.40
Ar	Rh	0.2776e+1	0.5414e+0	0.1914e-1	0.3690e-2	0.1	12.40
Kr	Rh	0.2536e+1	0.5133e+0	0.6298e-2	0.4039e-2	0.1	12.40
Xe	Rh	0.2539e+1	0.4942e+0	-0.4445e-3	0.3894e-2	0.1	12.40
H	Pd	0.5008e+1	0.6629e+0	0.1506e-1	-0.1140e-2	0.1	11.96
^{3}He	Pd	0.4531e+1	0.6654e+0	0.1966e-1	-0.1734e-2	0.1	11.96
^{4}He	Pd	0.4502e+1	0.6812e+0	0.2234e-1	-0.1897e-2	0.1	11.96
Ne	Pd	0.3204e+1	0.5909e+0	0.2873e-1	0.1170e-2	0.1	11.96
Ar	Pd	0.2844e+1	0.5373e+0	0.2045e-1	0.3470e-2	0.1	11.96
Kr	Pd	0.2603e+1	0.5071e+0	0.7657e-2	0.4024e-2	0.1	11.96
Pd	Pd	0.2573e+1	0.5005e+0	-0.2567e-2	0.5209e-2	0.1	11.96
Xe	Pd	0.2567e+1	0.4890e+0	0.3218e-2	0.3751e-2	0.1	11.96

Table 6: Constants, a_i, for the energy dependence of the mean (penetration) depth, md, at normal incidence for different ions and targets. The lower limit of the fit is 10 eV, the upper limit, ul, is given in MeV.

ion	solid	a1	a2	a3	a4	ul (MeV)	ρ (g/cm^3)
H	Ag	0.5136e+1	0.6472e+0	0.1630e-1	-0.9835e-3	0.1	10.47
D	Ag	0.5245e+1	0.6909e+0	0.1584e-1	-0.2094e-2	0.1	10.47
T	Ag	0.5259e+1	0.7192e+0	0.1647e-1	-0.2555e-2	0.1	10.47
^{3}He	Ag	0.4676e+1	0.6606e+0	0.1867e-1	-0.1681e-2	0.1	10.47
^{4}He	Ag	0.4659e+1	0.6696e+0	0.2225e-1	-0.9890e-3	0.1	10.47
N	AG	0.3614e+1	0.6088e+0	0.2946e-1	0.7269e-3	0.1	10.47
O	Ag	0.3516e+1	0.6016e+0	0.2940e-1	0.8453e-3	0.1	10.47
Ne	Ag	0.3355e+1	0.5863e+0	0.2859e-1	0.1162e-2	9.1	10.47
(KrC)Ar	Ag	0.3000e+1	0.5534e+0	0.2092e-1	0.1719e-2	1.0	10.47
(Mol)Ar	Ag	0.2700e+1	0.5574e+0	0.2457e-1	0.3833e-2	0.1	10.47
(Mol,0.8)Ar	Ag	0.3042e+1	0.5267e+0	0.2926e-1	0.2492e-2	0.1	10.47
(ZBL)Ar	Ag	0.2836e+1	0.5664e+0	0.1240e-1	0.4325e-2	0.1	10.47
Kr	Ag	0.2762e+1	0.4952e+0	0.9336e-2	0.3954e-2	0.1	10.47
Ag	Ag	0.2726e+1	0.5061e+0	0.1090e-2	0.3603e-2	1.0	10.47
Xe	Ag	0.2763e+1	0.4695e+0	0.2980e-2	0.4044e-2	0.1	10.47
^{4}He	Cd	0.4913e+1	0.6711e+0	0.2000e-1	-0.1639e-2	0.1	8.58
Ne	Cd	0.3615e+1	0.5755e+0	0.2798e-1	0.1501e-2	0.1	8.58
Ar	Cd	0.3252e+1	0.5309e+0	0.2332e-1	0.2684e-2	0.1	8.58
Kr	Cd	0.3017e+1	0.4778e+0	0.1289e-1	0.3887e-2	0.1	8.58
Cd	Cd	0.2994e+1	0.4722e+0	0.5007e-2	0.4013e-2	0.1	8.58
H	In	0.5579e+1	0.6538e+0	0.1416e-1	-0.1529e-2	0.1	7.31
^{4}He	In	0.5099e+1	0.6654e+0	0.1945e-1	-0.1644e-2	0.1	7.31
Ne	In	0.3806e+1	0.5710e+0	0.2802e-1	0.1553e-2	0.1	7.31
Kr	In	0.3203e+1	0.4762e+0	0.1552e-1	0.3185e-2	0.1	7.31
In	In	0.3170e+1	0.4648e+0	0.7591e-2	0.3691e-2	0.1	7.31
H	Sn	0.5617e+1	0.6524e+0	0.1219e-1	-0.2006e-2	0.1	7.28
D	Sn	0.5717e+1	0.6756e+0	0.1202e-1	-0.2098e-2	0.1	7.28
^{3}He	Sn	0.5152e+1	0.6477e+0	0.1674e-1	-0.1797e-2	0.1	7.28
^{4}He	Sn	0.5153e+1	0.6609e+0	0.1809e-1	-0.1761e-2	0.1	7.28
Ne	Sn	0.3850e+1	0.5665e+0	0.2784e-1	0.1677e-2	0.1	7.28
Ar	Sn	0.3479e+1	0.5254e+0	0.2476e-1	0.2268e-2	0.1	7.28
Kr	Sn	0.3234e+1	0.4693e+0	0.1620e-1	0.3360e-2	0.1	7.28
Sn	Sn	0.3200e+1	0.4645e+0	0.7690e-2	0.3675e-2	0.1	7.28
Xe	Sn	0.3230e+1	0.4448e+0	0.1015e-1	0.3220e-2	0.1	7.28
^{4}He	Sb	0.5271e+1	0.6666e+0	0.1642e-1	-0.2611e-2	0.1	6.62
Ne	Sb	0.3978e+1	0.5620e+0	0.2793e-1	0.1754e-2	0.1	6.62
Kr	Sb	0.3360e+1	0.4656e+0	0.1745e-1	0.3101e-2	0.1	6.62
^{4}He	Te	0.5382e+1	0.6545e+0	0.1809e-1	-0.1853e-2	0.1	6.22
Ne	Te	0.4100e+1	0.5608e+0	0.2759e-1	0.1614e-2	0.1	6.22
Ar	Te	0.3723e+1	0.5196e+0	0.2556e-1	0.2087e-2	0.1	6.22
Cs	Cs	0.4682e+1	0.4073e+0	0.1807e-1	0.2622e-2	0.1	1.89

Table 7: Constants, a_i, for the energy dependence of the mean (penetration) depth, md, at normal incidence for different ions and targets. The lower limit of the fit is 10 eV, the upper limit, ul, is given in MeV.

ion	solid	a1	a2	a3	a4	ul (MeV)	ρ (g/cm^3)
Kr	Sm	0.3464e+1	0.4134e+0	0.1616e-1	0.4936e-2	0.1	7.56
H	Tb	0.5713e+1	0.6074e+0	0.1405e-1	-0.4853e-2	0.1	8.28
^{4}He	Tb	0.5303e+1	0.6222e+0	0.1653e-1	-0.1525e-2	0.1	8.28
Ar	Tb	0.3662e+1	0.5074e+0	0.2421e-1	0.1843e-2	0.1	8.28
H	Tm	0.5642e+1	0.6032e+0	0.1856e-1	0.5431e-3	0.1	9.33
^{4}He	Tm	0.5246e+1	0.6191e+0	0.1702e-1	-0.1381e-2	0.1	9.33
Ar	Tm	0.3605e+1	0.5010e+0	0.2378e-1	0.2015e-2	0.1	9.33
H	Hf	0.5348e+1	0.6127e+0	0.1853e-1	0.6716e-4	0.1	13.12
^{4}He	Hf	0.4937e+1	0.6066e+0	0.1755e-1	-0.5851e-3	0.1	13.12
Ne	Hf	0.3704e+1	0.5415e+0	0.2527e-1	0.1167e-2	0.1	13.12
Ar	Hf	0.3310e+1	0.5081e+0	0.2310e-1	0.1689e-2	0.1	13.12
Kr	Hf	0.2996e+1	0.4576e+0	0.1613e-1	0.2976e-2	0.1	13.12
Xe	Hf	0.2925e+1	0.4345e+0	0.8658e-2	0.3410e-2	0.1	13.12
H	Ta	0.5119e+1	0.6118e+0	0.1901e-1	0.3129e-3	0.1	16.60
D	Ta	0.5235e+1	0.6376e+0	0.1936e-1	-0.7863e-4	0.1	16.60
^{3}He	Ta	0.4713e+1	0.6094e+0	0.1728e-1	-0.1093e-2	0.1	16.60
^{4}He	Ta	0.4709e+1	0.6155e+0	0.2027e-1	-0.5194e-3	0.1	16.60
Ne	Ta	0.3473e+1	0.5455e+0	0.2559e-1	0.9228e-3	0.1	16.60
Ar	Ta	0.3073e+1	0.5108e+0	0.2309e-1	0.1711e-2	0.1	16.60
Kr	Ta	0.2765e+1	0.4595e+0	0.1286e-1	0.3559e-2	0.1	16.60
Xe	Ta	0.2676e+1	0.4442e+0	0.6012e-2	0.3785e-2	0.1	16.60
Ta	Ta	0.2643e+1	0.4510e+0	-0.4565e-2	0.4703e-2	0.1	16.60
H	W	0.4972e+1	0.5791e+0	0.2185e-1	0.2361e-2	1.0	19.29
D	W	0.5084e+1	0.6179e+0	0.2105e-1	0.9044e-3	1.0	19.29
T	W	0.5123e+1	0.6501e+0	0.2123e-1	0.2666e-4	1.0	19.29
^{3}He	W	0.4573e+1	0.6096e+0	0.1704e-1	-0.1123e-2	0.1	19.29
^{4}He	W	0.4583e+1	0.6217e+0	0.2046e-1	-0.9516e-3	1.0	19.29
N	W	0.3598e+1	0.5586e+0	0.2275e-1	0.1749e-2	0.1	19.29
Ne	W	0.3345e+1	0.5478e+0	0.2466e-1	0.4651e-3	0.1	19.29
Ar	W	0.2937e+1	0.5102e+0	0.2246e-1	0.1836e-2	0.1	19.29
Kr	W	0.2629e+1	0.4627e+0	0.1076e-1	0.3860e-2	0.1	19.29
Xe	W	0.2528e+1	0.4531e+0	0.3846e-2	0.3869e-2	0.1	19.29
W	W	0.2488e+1	0.4584e+0	-0.7259e-2	0.5088e-2	0.1	19.29
H	Re	0.4901e+1	0.6054e+0	0.1813e-1	-0.7699e-4	0.1	21.04
D	Re	0.5015e+1	0.6289e+0	0.1819e-1	-0.5475e-3	0.1	21.04
^{4}He	Re	0.4498e+1	0.6182e+0	0.1997e-1	-0.8224e-3	0.1	21.04
Ne	Re	0.3250e+1	0.5485e+0	0.2707e-1	0.5875e-3	0.1	21.04
Ar	Re	0.2857e+1	0.5124e+0	0.2255e-1	0.1727e-2	0.1	21.04
Kr	Re	0.2547e+1	0.4647e+0	0.9977e-2	0.4040e-2	0.1	21.04
Xe	Re	0.2439e+1	0.4591e+0	0.3432e-2	0.3852e-2	0.1	21.04

Table 8: Constants, a_i, for the energy dependence of the mean (penetration) depth, md, at normal incidence for different ions and targets. The lower limit of the fit is 10 eV, the upper limit, ul, is given in MeV.

ion	solid	a1	a2	a3	a4	ul (MeV)	ρ (g/cm^3)
H	Os	0.4849e+1	0.6049e+0	0.1876e-1	-0.4491e-4	0.1	22.56
^{3}He	Os	0.4439e+1	0.6060e+0	0.1885e-1	-0.8472e-3	0.1	22.56
^{4}He	Os	0.4445e+1	0.6156e+0	0.2052e-1	-0.6940e-3	0.1	22.56
Ne	Os	0.3203e+1	0.5487e+0	0.2704e-1	0.4405e-3	0.1	22.56
Ar	Os	0.2817e+1	0.5089e+0	0.2192e-1	0.1836e-2	0.1	22.56
Kr	Os	0.2493e+1	0.4639e+0	0.9273e-2	0.4126e-2	0.1	22.56
Xe	Os	0.2384e+1	0.4614e+0	0.2715e-2	0.3857e-2	0.1	22.56
H	Ir	0.4858e+1	0.6007e+0	0.1907e-1	0.2409e-3	0.1	22.51
^{3}He	Ir	0.4452e+1	0.6047e+0	0.1906e-1	-0.7894e-3	0.1	22.51
^{4}He	Ir	0.4457e+1	0.6124e+0	0.2039e-1	-0.5307e-3	0.1	22.51
Ne	Ir	0.3216e+1	0.5475e+0	0.2716e-1	0.4789e-3	0.1	22.51
Ar	Ir	0.2822e+1	0.5119e+0	0.2268e-1	0.1599e-2	0.1	22.51
Kr	Ir	0.2509e+1	0.4628e+0	0.9277e-2	0.4058e-2	0.1	22.51
Xe	Ir	0.2400e+1	0.4607e+0	0.2757e-2	0.3842e-2	0.1	22.51
H	Pt	0.4922e+1	0.6072e+0	0.2141e-1	0.2885e-3	0.1	21.44
^{3}He	Pt	0.4515e+1	0.6017e+0	0.1951e-1	-0.4434e-3	0.1	21.44
^{4}He	Pt	0.4518e+1	0.6086e+0	0.2198e-1	-0.8402e-4	0.1	21.44
O	Pt	0.3451e+1	0.5541e+0	0.2635e-1	0.5631e-3	0.1	21.44
Ne	Pt	0.3307e+1	0.5568e+0	0.2564e-1	0.2750e-4	0.1	21.44
Ar	Pt	0.2892e+1	0.5127e+0	0.2267e-1	0.1394e-2	0.1	21.44
Kr	Pt	0.2572e+1	0.4600e+0	0.1097e-1	0.3848e-2	0.1	21.44
Xe	Pt	0.2467e+1	0.4590e+0	0.3686e-2	0.3546e-2	0.1	21.44
Pt	Pt	0.2435e+1	0.4512e+0	-0.9029e-2	0.5376e-2	0.1	21.44
H	Au	0.5015e+1	0.5619e+0	0.2136e-1	0.2956e-2	3.0	19.31
D	Au	0.5168e+1	0.6236e+0	0.1932e-1	-0.1389e-3	0.1	19.31
T	Au	0.5195e+1	0.6452e+0	0.2032e-1	-0.4678e-3	0.1	19.31
^{3}He	Au	0.4628e+1	0.5937e+0	0.2032e-1	0.7440e-4	0.1	19.31
^{4}He	Au	0.4637e+1	0.5992e+0	0.1947e-1	-0.1380e-3	3.0	19.31
N	Au	0.3672e+1	0.5565e+0	0.2575e-1	0.7532e-3	0.1	19.31
O	Au	0.3575e+1	0.5537e+0	0.2570e-1	0.5633e-3	0.1	19.31
Ne	Au	0.3411e+1	0.5402e+0	0.2579e-1	0.8030e-3	0.1	19.31
Na	Au	0.3338e+1	0.5328e+0	0.2569e-1	0.1026e-2	0.1	19.31
Ar	Au	0.3023e+1	0.5121e+0	0.2221e-1	0.1237e-2	1.0	19.31
K	Au	0.3001e+1	0.5025e+0	0.2190e-1	0.1659e-2	0.1	19.31
Kr	Au	0.2696e+1	0.4602e+0	0.1243e-1	0.3354e-2	0.1	19.31
Xe	Au	0.2593e+1	0.4452e+0	0.4980e-2	0.3786e-2	0.1	19.31
Au	Au	0.2572e+1	0.4629e+0	-0.6371e-2	0.3543e-2	1.0	19.31
Kr	Hg	0.3182e+1	0.4232e+0	0.1103e-1	0.3958e-2	0.3	13.55
Kr	Tl	0.3250e+1	0.4511e+0	0.1743e-1	0.2218e-2	0.1	11.88

Table 9: Constants, a_i, for the energy dependence of the mean (penetration) depth, md, at normal incidence for different ions and targets. The lower limit of the fit is 10 eV, the upper limit, ul, is given in MeV.

ion	solid	a1	a2	a3	a4	ul (MeV)	ρ (g/cm^3)
H	Pb	0.5659e+1	0.6088e+0	0.1413e-1	-0.1087e-2	0.1	11.32
^{4}He	Pb	0.5228e+1	0.5846e+0	0.2408e-1	0.1259e-2	0.1	11.32
Ne	Pb	0.4035e+1	0.5182e+0	0.2407e-1	0.1575e-2	0.1	11.32
Ar	Pb	0.3642e+1	0.4893e+0	0.2284e-1	0.1816e-2	0.1	11.32
Kr	Pb	0.3312e+1	0.4488e+0	0.1815e-1	0.2133e-2	0.1	11.32
Xe	Pb	0.3211e+1	0.4200e+0	0.1366e-1	0.2690e-2	0.1	11.32
Ar	Bi	0.3801e+1	0.4854e+0	0.2287e-1	0.1806e-2	0.1	9.81
Kr	Bi	0.3472e+1	0.4448e+0	0.1846e-1	0.2046e-2	0.1	9.81
^{4}He	Th	0.5358e+1	0.5890e+0	0.1395e-1	-0.1375e-2	0.1	11.66
Ne	Th	0.4154e+1	0.5109e+0	0.2278e-1	0.1635e-2	0.1	11.66
Ar	Th	0.3754e+1	0.4813e+0	0.2182e-1	0.1786e-2	0.1	11.66
Kr	Th	0.3413e+1	0.4431e+0	0.1760e-1	0.1932e-2	0.1	11.66
Xe	Th	0.3293e+1	0.4146e+0	0.1429e-1	0.2427e-2	0.1	11.66
H	U	0.5251e+1	0.6087e+0	0.1490e-1	-0.1317e-2	0.1	19.04
D	U	0.5334e+1	0.5764e+0	0.1183e-1	0.2044e-3	0.1	19.04

Table 10: Constants for the angular dependence of the mean penetration depth at several energies and ion-target combinations.

ion	solid	energy (eV)	c1	c2	c3	c4	ρ (g/cm^3)
Li	Li	100	0.1859e+2	0.1645e+2	-0.1087e+1	0.1226e+1	0.53
Li	Li	200	0.3669e+2	0.2295e+2	-0.1370e+1	0.1297e+1	0.53
Li	Li	1000	0.1568e+3	0.9094e+2	-0.1663e+1	0.1513e+1	0.53
H	Be	10	0.4082e+1	0.1220e+1	-0.8417e+0	0.1316e+1	1.80
H	Be	15	0.6073e+1	0.8818e+0	-0.1447e+1	0.1509e+1	1.80
H	Be	17	0.2561e+1	0.5748e+1	-0.4497e+0	0.1366e+1	1.80
H	Be	20	0.6899e+1	0.2138e+1	-0.7305e+0	0.1046e+1	1.80
H	Be	22	0.7784e+1	0.1654e+1	-0.1019e+1	0.1228e+1	1.80
H	Be	25	0.8514e+1	0.2089e+1	-0.9210e+0	0.1101e+1	1.80
H	Be	30	0.9692e+1	-0.2799e+1	0.7592e+0	-0.9315e+0	1.80
H	Be	40	0.1171e+2	0.3961e+1	-0.6812e+0	0.9179e+0	1.80
H	Be	50	0.1384e+2	0.5515e+1	-0.5831e+0	0.7928e+0	1.80
H	Be	70	0.1992e+2	0.3162e+1	-0.1874e+1	0.1723e+1	1.80
H	Be	100	0.2669e+2	0.5221e+1	-0.1441e+1	0.1268e+1	1.80
H	Be	140	0.3519e+2	0.5999e+1	-0.1833e+1	0.1559e+1	1.80
H	Be	200	0.4772e+2	0.8187e+1	-0.2215e+1	0.1855e+1	1.80
H	Be	300	0.6727e+2	0.1373e+2	-0.1970e+1	0.1606e+1	1.80
H	Be	500	0.1013e+3	0.2481e+2	-0.1947e+1	0.1744e+1	1.80
H	Be	1000	0.1830e+3	0.5791e+2	-0.1822e+1	0.1581e+1	1.80
D	Be	11	0.3307e+1	0.1399e+1	-0.1076e+1	0.1452e+1	1.80
D	Be	12	0.3783e+1	0.1231e+1	-0.1225e+1	0.1471e+1	1.80
D	Be	13	0.3766e+1	0.1572e+1	-0.1032e+1	0.1419e+1	1.80
D	Be	14	0.3893e+1	0.1923e+1	-0.8906e+0	0.1273e+1	1.80
D	Be	15	0.4448e+1	-0.1498e+1	0.1157e+1	-0.1420e+1	1.80
D	Be	17	0.5126e+1	0.1424e+1	-0.1329e+1	0.1452e+1	1.80
D	Be	20	0.5623e+1	0.1742e+1	-0.1198e+1	0.1421e+1	1.80
D	Be	25	0.6847e+1	0.2030e+1	-0.1214e+1	0.1345e+1	1.80
D	Be	30	0.7711e+1	0.2481e+1	-0.1196e+1	0.1400e+1	1.80
D	Be	40	0.1001e+2	0.2966e+1	-0.1287e+1	0.1379e+1	1.80
D	Be	50	0.1125e+2	0.5441e+1	-0.7876e+0	0.9751e+0	1.80
D	Be	70	0.1559e+2	0.5542e+1	-0.1095e+1	0.1220e+0	1.80
D	Be	100	0.2237e+2	0.5887e+1	-0.1507e+1	0.1421e+0	1.80
D	Be	140	0.3014e+2	0.8943e+1	-0.1385e+1	0.1288e+0	1.80
D	Be	200	0.4182e+2	0.1304e+2	-0.1372e+1	0.1248e+0	1.80
D	Be	300	0.6162e+2	0.1680e+2	-0.1809e+1	0.1561e+0	1.80
D	Be	500	0.9948e+2	0.3282e+2	-0.1550e+1	0.1327e+0	1.80
D	Be	1000	0.1891e+3	0.6526e+2	-0.1884e+1	0.1671e+0	1.80

Table 11: Constants for the angular dependence of the mean penetration depth at several energies and ion-target combinations.

ion	solid	energy (eV)	c1	c2	c3	c4	ρ (g/cm^3)
T	Be	10	0.2441e+1	0.1385e+1	-0.1354e+1	0.1668e+1	1.80
T	Be	11	0.2664e+1	0.1485e+1	-0.1348e+1	0.1682e+1	1.80
T	Be	12	0.2684e+1	0.1828e+1	-0.1133e+1	0.1540e+1	1.80
T	Be	13	0.2989e+1	-0.1797e+1	0.1174e+1	-0.1546e+1	1.80
T	Be	15	0.3538e+1	0.1821e+1	-0.1214e+1	0.1520e+1	1.80
T	Be	17	0.3625e+1	0.2447e+1	-0.9764e+0	0.1358e+1	1.80
T	Be	20	0.4382e+1	-0.2532e+1	0.1006e+1	-0.1316e+1	1.80
T	Be	25	0.5763e+1	0.2320e+1	-0.1280e+1	0.1427e+1	1.80
T	Be	30	0.6450e+1	0.3010e+1	-0.1124e+1	0.1332e+1	1.80
T	Be	50	0.9767e+1	0.5046e+1	-0.9898e+0	0.1165e+1	1.80
T	Be	100	0.1918e+2	0.7538e+1	-0.1289e+1	0.1279e+1	1.80
T	Be	200	0.3761e+2	0.1248e+2	-0.1654e+1	0.1483e+1	1.80
T	Be	300	0.5573e+2	0.1992e+2	-0.1523e+1	0.1323e+1	1.80
T	Be	500	0.9242e+2	0.3420e+2	-0.1630e+1	0.1406e+1	1.80
T	Be	1000	0.1814e+3	0.7417e+2	-0.1691e+1	0.1511e+1	1.80
^{4}He	Be	10	-0.1137e+2	-0.1369e+2	0.1595e+1	-0.3724e+1	1.80
^{4}He	Be	11	-0.1195e+2	-0.1444e+2	0.1539e+1	-0.3646e+1	1.80
^{4}He	Be	12	-0.1144e+2	-0.1417e+2	0.1420e+1	-0.3422e+1	1.80
^{4}He	Be	13	-0.1392e+2	0.1678e+2	-0.1419e+1	0.3500e+1	1.80
^{4}He	Be	15	-0.1512e+2	0.1843e+2	-0.1203e+1	0.3168e+1	1.80
^{4}He	Be	17	-0.1527e+2	0.1889e+2	-0.1154e+1	0.3082e+1	1.80
^{4}He	Be	20	-0.1932e+2	0.2351e+2	-0.1023e+1	0.2945e+1	1.80
^{4}He	Be	25	-0.1208e+2	0.1705e+2	-0.9193e+0	0.2563e+1	1.80
^{4}He	Be	30	-0.2403e+2	0.2981e+2	-0.8192e+0	0.2644e+1	1.80
^{4}He	Be	40	-0.1741e+2	0.2469e+2	-0.7549e+0	0.2332e+1	1.80
^{4}He	Be	50	-0.2219e+2	0.3109e+2	-0.6506e+0	0.2191e+1	1.80
^{4}He	Be	70	-0.3932e+2	-0.5045e+2	0.7827e+0	-0.2515e+1	1.80
^{4}He	Be	100	-0.5618e+2	0.7185e+2	-0.6286e+0	0.2289e+1	1.80
^{4}He	Be	140	-0.4153e+2	0.6392e+2	-0.4903e+0	0.1810e+1	1.80
^{4}He	Be	200	-0.7554e+2	0.1059e+3	-0.5048e+0	0.1930e+1	1.80
^{4}He	Be	300	0.2394e+2	0.1701e+2	-0.8634e+0	0.1107e+1	1.80
^{4}He	Be	400	0.3320e+2	0.1873e+2	-0.1172e+1	0.1247e+1	1.80
^{4}He	Be	500	0.4267e+2	0.2186e+2	-0.1234e+1	0.1177e+1	1.80
^{4}He	Be	700	0.6057e+2	0.2526e+2	-0.1608e+1	0.1432e+1	1.80
^{4}He	Be	1000	0.8659e+2	0.3428e+2	-0.1853e+1	0.1599e+1	1.80
^{4}He	Be	2000	0.1666e+3	0.7708e+2	-0.1720e+1	0.1539e+1	1.80
^{4}He	Be	5000	0.3970e+3	0.2226e+3	-0.1671e+1	0.1498e+1	1.80
^{4}He	Be	10000	0.7062e+2	0.5347e+3	-0.1350e+1	0.1288e+1	1.80

Table 12: Constants for the angular dependence of the mean penetration depth at several energies and ion-target combinations.

ion	solid	energy (eV)	c1	c2	c3	c4	ρ (g/cm^3)
Be	Be	10	0.7571e+0	-0.5519e+0	0.1995e+1	-0.1624e+1	1.80
Be	Be	11	0.7973e+0	-0.6311e+0	0.1803e+1	-0.1553e+1	1.80
Be	Be	12	0.8675e+0	-0.6867e+0	0.1852e+1	-0.1517e+1	1.80
Be	Be	13	0.9625e+0	-0.7942e+0	0.1895e+1	-0.1535e+1	1.80
Be	Be	15	0.1064e+1	-0.9355e+0	0.1808e+1	-0.1466e+1	1.80
Be	Be	17	0.1170e+1	-0.1030e+1	0.1892e+1	-0.1588e+1	1.80
Be	Be	20	0.1335e+1	-0.1104e+1	0.2143e+1	-0.1843e+1	1.80
Be	Be	25	0.1547e+1	-0.1527e+1	0.1661e+1	-0.1477e+1	1.80
Be	Be	30	0.1889e+1	-0.2425e+1	0.1066e+1	-0.9192e+0	1.80
Be	Be	40	0.2202e+1	0.2159e+1	-0.1652e+1	0.1651e+1	1.80
Be	Be	50	0.2338e+1	0.3019e+1	-0.1279e+1	0.1451e+1	1.80
Be	Be	70	0.3317e+1	0.3930e+1	-0.1145e+1	0.1293e+1	1.80
Be	Be	100	0.3668e+1	0.6171e+1	-0.9053e+0	0.1189e+1	1.80
Be	Be	200	0.6586e+1	0.1046e+2	-0.8486e+0	0.1114e+0	1.80
Be	Be	300	0.1206e+2	0.1068e+2	-0.1098e+1	0.1170e+1	1.80
Be	Be	500	0.1986e+2	0.1394e+2	-0.1298e+1	0.1273e+1	1.80
Be	Be	700	0.2733e+2	0.1764e+1	-0.1423e+1	0.1336e+1	1.80
Be	Be	1000	0.3833e+2	0.2385e+1	-0.1489e+1	0.1364e+1	1.80
N	Be	10	0.4676e+0	-0.3952e+0	0.3063e+1	-0.2600e+1	1.80
N	Be	12	0.5509e+0	-0.4854e+0	0.3027e+1	-0.2574e+1	1.80
N	Be	15	0.6893e+0	-0.6620e+0	0.2477e+1	-0.2164e+1	1.80
N	Be	20	0.9177e+0	-0.1288e+1	0.1249e+1	-0.1107e+1	1.80
N	Be	25	0.1136e+1	-0.1286e+1	0.1642e+1	-0.1508e+1	1.80
N	Be	27	0.1028e+1	-0.2779e+1	0.6579e+0	-0.6665e+0	1.80
N	Be	30	0.1282e+1	-0.3054e+1	0.6237e+0	-0.5866e+0	1.80
N	Be	40	0.8475e+0	-0.3414e+1	0.7890e+0	-0.1038e+1	1.80
N	Be	50	0.7826e-1	0.5263e+1	-0.6405e+0	0.1051e+1	1.80
N	Be	70	-0.8176e+1	0.1551e+2	-0.4599e+0	0.1353e+1	1.80
N	Be	100	-0.8201e+1	0.1722e+2	-0.5166e+0	0.1389e+1	1.80
N	Be	140	-0.7532e-1	0.1866e+2	-0.5512e+0	0.1378e+1	1.80
N	Be	200	-0.2151e+1	0.1701e+2	-0.5557e+0	0.1127e+1	1.80
N	Be	300	0.5696e+1	0.1286e+2	-0.7647e+0	0.1024e+1	1.80
N	Be	500	0.1121e+2	0.1470e+2	-0.9431e+0	0.1080e+1	1.80
N	Be	1000	0.2230e+2	0.2082e+2	-0.1170e+1	0.1186e+1	1.80
D	B	30	0.5121e+1	-0.4094e+1	0.6888e+0	-0.1286e+1	1.80
D	B	50	0.1025e+2	0.3285e+1	-0.1041e+1	0.1207e+1	1.80
D	B	100	0.1944e+2	0.4291e+1	-0.1585e+1	0.1435e+1	1.80
D	B	400	0.6633e+2	0.1696e+2	-0.1669e+1	0.1455e+1	1.80
D	B	500	0.8173e+2	0.2105e+2	-0.1853e+1	0.1603e+1	1.80
D	B	8000	0.9035e+3	0.5210e+3	-0.1852e+1	0.1658e+1	1.80
B	B	1000	0.2535e+2	0.2020e+2	-0.1077e+1	0.1004e+1	1.80
B	B	2000	0.4697e+2	0.2834e+2	-0.1589e+1	0.1488e+1	1.80

Table 13: Constants for the angular dependence of the mean penetration depth at several energies and ion-target combinations.

ion	solid	energy (eV)	c1	c2	c3	c4	ρ (g/cm^3)
Ne	Be	10	-0.3997e+1	-0.5029e+1	0.7070e+0	-0.2255e+1	1.80
Ne	Be	11	-0.2290e+1	-0.3339e+1	0.8370e+0	-0.2186e+1	1.80
Ne	Be	12	-0.9688e+0	-0.2071e+1	0.1147e+1	-0.2277e+1	1.80
Ne	Be	13	-0.3960e+1	-0.5398e+1	0.5590e+0	-0.1851e+1	1.80
Ne	Be	14	-0.2953e+1	-0.4380e+1	0.6969e+0	-0.1940e+1	1.80
Ne	Be	15	-0.2278e+1	-0.3737e+1	0.7790e+0	-0.1959e+1	1.80
Ne	Be	17	-0.3604e+1	-0.5357e+1	0.6532e+0	-0.1860e+1	1.80
Ne	Be	20	-0.2510e+1	-0.4562e+1	0.7011e+0	-0.1726e+1	1.80
Ne	Be	22	-0.2664e+1	-0.4976e+1	0.6884e+0	-0.1680e+1	1.80
Ne	Be	25	-0.1221e+1	-0.3963e+1	0.6277e+0	-0.1337e+1	1.80
Ne	Be	30	-0.2740e+1	-0.6562e+1	0.4380e+0	-0.1172e+1	1.80
Ne	Be	35	-0.1842e+1	-0.5726e+1	0.5634e+0	-0.1253e+1	1.80
Ne	Be	40	0.1424e+1	-0.2431e+1	0.9817e+0	-0.1106e+1	1.80
Ne	Be	45	-0.6951e+1	-0.1180e+2	0.4998e+0	-0.1488e+1	1.80
Ne	Be	50	-0.6122e+1	-0.1099e+2	0.5819e+0	-0.1565e+1	1.80
Ne	Be	60	-0.6555e+1	-0.1339e+2	0.4059e+0	-0.1222e+1	1.80
Ne	Be	70	-0.4916e+1	-0.1248e+2	0.4317e+0	-0.1147e+1	1.80
Ne	Be	100	-0.4174e+1	-0.1425e+2	0.4201e+0	-0.1031e+1	1.80
Ne	Be	150	-0.2112e+2	0.3498e+2	-0.3516e+0	0.1309e+1	1.80
Ne	Be	200	-0.1569e+2	0.3178e+2	-0.3881e+0	0.1221e+1	1.80
Ne	Be	300	0.7218e+1	0.9001e+1	-0.1025e+1	0.1089e+1	1.80
Ne	Be	500	0.1037e+2	0.1273e+2	-0.1032e+1	0.1104e+1	1.80
Ne	Be	700	0.1489e+2	0.1240e+2	-0.1403e+1	0.1346e+1	1.80
Ne	Be	1000	0.1937e+2	0.1627e+2	-0.1386e+1	0.1326e+1	1.80
Ar	Be	10	-0.3392e+1	-0.4915e+1	0.6970e+0	-0.1969e+1	1.80
Ar	Be	15	0.1164e+1	-0.1239e+1	0.1231e+1	-0.1113e+1	1.80
Ar	Be	17	-0.1192e+1	-0.3813e+1	0.7522e+0	-0.1502e+1	1.80
Ar	Be	20	0.2141e+0	-0.4413e+1	0.4289e+0	-0.6813e+0	1.80
Ar	Be	22	0.1046e+1	-0.2806e+1	0.7371e+0	-0.8622e+0	1.80
Ar	Be	25	0.1898e+1	-0.1790e+1	0.1393e+1	-0.1155e+1	1.80
Ar	Be	30	0.2043e+1	0.2163e+1	-0.1307e+1	0.1154e+1	1.80
Ar	Be	35	0.1955e+0	-0.3532e+1	0.8259e+0	-0.8320e+0	1.80
Ar	Be	40	0.2664e+1	-0.2532e+1	0.1392e+1	-0.1157e+1	1.80
Ar	Be	45	0.2257e+1	-0.4240e+1	0.8265e+0	-0.8485e+0	1.80
Ar	Be	50	0.3126e+1	-0.2489e+1	0.1746e+1	-0.1447e+1	1.80
Ar	Be	60	0.3200e+1	0.4073e+1	-0.1033e+1	0.9412e+0	1.80
Ar	Be	70	0.3502e+1	-0.4186e+1	0.1133e+1	-0.1045e+1	1.80
Ar	Be	100	0.4355e+1	-0.5139e+1	0.1172e+1	-0.1095e+1	1.80
Ar	Be	150	0.5976e+1	-0.5077e+1	0.1616e+1	-0.1436e+1	1.80
Ar	Be	200	0.7336e+1	0.5426e+1	-0.1925e+1	0.1659e+1	1.80
Ar	Be	300	0.9487e+1	0.6149e+1	-0.2323e+1	0.1998e+1	1.80
Ar	Be	500	0.1198e+2	0.1062e+2	-0.1549e+1	0.1430e+1	1.80
Ar	Be	700	0.1505e+2	0.1139e+2	-0.1878e+1	0.1700e+1	1.80
Ar	Be	1000	0.1827e+2	0.1500e+2	-0.1735e+1	0.1621e+1	1.80

Table 14: Constants for the angular dependence of the mean penetration depth at several energies and ion-target combinations.

ion	solid	energy (eV)	c1	c2	c3	c4	ρ (g/cm^3)
H	C	10	-0.1882e+1	0.8478e+1	-0.5390e+0	0.2072e+1	1.85
H	C	20	0.8981e+1	0.1816e+1	-0.7699e+0	0.9300e+0	1.85
H	C	40	0.8066e+1	0.1181e+2	-0.2959e+0	0.9706e+0	1.85
H	C	50	0.1778e+2	0.2424e+1	-0.1439e+1	0.1304e+1	1.85
H	C	70	0.2219e+2	0.4457e+1	-0.9267e+0	0.9862e+0	1.85
H	C	100	0.2950e+2	0.4512e+1	-0.1483e+1	0.1442e+1	1.85
H	C	140	0.3885e+2	0.6605e+1	-0.1376e+1	0.1222e+1	1.85
H	C	200	0.5204e+2	0.7237e+1	-0.2299e+1	0.1962e+1	1.85
H	C	300	0.7192e+2	0.1190e+2	-0.2019e+1	0.1666e+1	1.85
H	C	500	0.1063e+3	0.2116e+2	-0.1856e+1	0.1681e+1	1.85
H	C	1000	0.1888e+3	0.5048e+2	-0.1657e+1	0.1399e+1	1.85
H	C	2000	0.2734e+3	0.8869e+2	-0.1979e+1	0.1676e+1	2.26
H	C	13333	0.1056e+4	0.6772e+3	-0.1884e+1	0.1739e+1	2.26
H	C	26667	0.1854e+4	-0.1382e+4	0.2392e+1	-0.2263e+1	2.26
D	C	10	0.4474e+1	0.8341e+0	-0.1591e+1	0.1685e+1	1.85
D	C	20	0.5469e+1	0.3637e+1	-0.7006e+0	0.1344e+1	1.85
D	C	40	0.1013e+2	0.5500e+1	-0.7060e+0	0.1148e+1	1.85
D	C	50	0.1397e+2	0.3739e+1	-0.1211e+1	0.1409e+1	1.85
D	C	70	0.1838e+2	0.5419e+1	-0.9989e+0	0.1108e+1	1.85
D	C	100	0.2522e+2	0.6621e+1	-0.1105e+1	0.1074e+1	1.85
D	C	140	0.3440e+2	0.6896e+1	-0.1746e+1	0.1503e+1	1.85
D	C	200	0.4631e+2	0.9222e+1	-0.1844e+1	0.1617e+1	1.85
D	C	300	0.6642e+2	0.1489e+2	-0.1621e+1	0.1361e+1	1.85
D	C	500	0.1007e+3	0.3111e+2	-0.1271e+1	0.1208e+1	1.85
D	C	1000	0.1962e+3	0.5748e+2	-0.1742e+1	0.1464e+1	1.85
D	C	33	0.7447e+1	0.2991e+1	-0.9290e+0	0.1376e+1	2.26
D	C	50	0.9289e+1	0.5893e+1	-0.6412e+0	0.1117e+1	2.26
D	C	350	0.6122e+2	0.1385e+2	-0.1707e+1	0.1521e+1	2.26
D	C	400	0.6918e+2	0.1523e+2	-0.1924e+1	0.1731e+1	2.26
D	C	3000	0.4230e+3	0.1605e+3	-0.1933e+1	0.1687e+1	2.26
D	C	10000	0.1107e+4	-0.6373e+3	0.1834e+1	-0.1642e+1	2.26
T	C	10	0.3454e+1	-0.1243e+1	0.1354e+1	-0.1650e+1	1.85
T	C	20	0.5849e+1	0.2198e+1	-0.1090e+1	0.1356e+1	1.85
T	C	25	0.7032e+1	0.2514e+1	-0.1087e+1	0.1294e+1	1.85
T	C	30	0.7570e+1	0.3822e+1	-0.8220e+0	0.1100e+1	1.85
T	C	40	0.8583e+1	0.5987e+1	-0.6990e+0	0.1071e+1	1.85
T	C	50	0.1231e+2	0.3805e+1	-0.1270e+1	0.1383e+1	1.85
T	C	70	0.1267e+2	0.1109e+2	-0.5938e+0	0.9569e+0	1.85
T	C	100	0.2147e+2	0.7126e+1	-0.1287e+1	0.1378e+1	1.85
T	C	140	0.2986e+2	0.7971e+1	-0.1552e+1	0.1436e+1	1.85
T	C	200	0.4106e+2	0.1163e+2	-0.1466e+1	0.1329e+1	1.85
T	C	300	0.5850e+2	0.1731e+2	-0.1503e+1	0.1392e+1	1.85
T	C	500	0.9575e+2	0.3083e+2	-0.1446e+1	0.1284e+1	1.85
T	C	1000	0.1866e+3	0.6171e+2	-0.1700e+1	0.1484e+1	1.85

Table 15: Constants for the angular dependence of the mean penetration depth at several energies and ion-target combinations.

ion	solid	energy (eV)	c1	c2	c3	c4	ρ (g/cm^3)
^{4}He	C	10	-0.1023e+2	-0.1325e+2	0.1443e+1	-0.3513e+1	1.85
^{4}He	C	15	-0.1408e+2	0.1804e+2	-0.1414e+1	0.3518e+1	1.85
^{4}He	C	20	-0.1526e+2	0.2021e+2	-0.1044e+1	0.2953e+1	1.85
^{4}He	C	25	-0.2444e+2	0.3046e+2	-0.7810e+0	0.2676e+1	1.85
^{4}He	C	27	-0.1570e+2	0.2186e+2	-0.9810e+0	0.2778e+1	1.85
^{4}He	C	30	-0.9105e+1	0.1588e+2	-0.8341e+0	0.2357e+1	1.85
^{4}He	C	35	0.2322e+1	0.5297e+1	-0.8505e+0	0.1655e+1	1.85
^{4}He	C	40	-0.3994e+2	0.4847e+2	-0.7023e+0	0.2604e+1	1.85
^{4}He	C	50	-0.3064e+2	0.4034e+2	-0.8449e+0	0.2654e+1	1.85
^{4}He	C	60	-0.2309e+2	0.3454e+2	-0.6941e+0	0.2263e+1	1.85
^{4}He	C	70	-0.4942e+2	0.6250e+2	-0.6220e+0	0.2394e+1	1.85
^{4}He	C	100	0.1021e+2	0.6662e+1	-0.9498e+0	0.1284e+1	1.85
^{4}He	C	140	-0.2767e+2	0.5103e+2	-0.5260e+0	0.1818e+1	1.85
^{4}He	C	200	0.1588e+2	0.1447e+2	-0.8017e+0	0.1179e+1	1.85
^{4}He	C	300	0.2887e+2	0.1228e+2	-0.1181e+1	0.1195e+1	1.85
^{4}He	C	400	0.3663e+2	0.1569e+2	-0.1248e+1	0.1292e+1	1.85
^{4}He	C	500	0.4709e+2	0.1534e+2	-0.1770e+1	0.1630e+1	1.85
^{4}He	C	700	0.6278e+2	0.2332e+2	-0.1506e+1	0.1413e+1	1.85
^{4}He	C	1000	0.8886e+2	0.3241e+2	-0.1622e+1	0.1441e+1	1.85
^{4}He	C	2000	0.1681e+3	0.7148e+2	-0.1482e+1	0.1330e+1	1.85
^{4}He	C	3000	0.2511e+3	0.1045e+3	-0.1689e+1	0.1453e+1	1.85
^{4}He	C	5000	0.3949e+3	0.1901e+3	-0.1630e+1	0.1457e+1	1.85
^{4}He	C	10000	0.7309e+3	0.4082e+3	-0.1718e+1	0.1553e+1	1.85
^{4}He	C	20000	0.1274e+4	0.8498e+3	-0.1692e+1	0.1567e+1	1.85
^{4}He	C	10000	0.6015e+3	0.3386e+3	-0.1674e+1	0.1520e+1	2.26
^{4}He	C	20000	0.1067e+4	0.6607e+3	-0.1861e+1	0.1702e+1	2.26
C	C	10	0.9018e+0	-0.4229e+0	0.1789e+1	-0.1477e+1	1.85
C	C	15	0.1062e+1	-0.7746e+0	0.2061e+1	-0.1824e+1	1.85
C	C	20	0.1331e+1	-0.1063e+1	0.1998e+1	-0.1725e+1	1.85
C	C	25	0.1564e+1	-0.1297e+1	0.1997e+1	-0.1724e+1	1.85
C	C	30	0.1768e+1	-0.1547e+1	0.1893e+1	-0.1651e+1	1.85
C	C	40	0.2153e+1	0.2003e+1	-0.1785e+1	0.1630e+1	1.85
C	C	50	0.2532e+1	0.2219e+1	-0.1947e+1	0.1806e+1	1.85
C	C	70	0.3265e+1	0.2948e+1	-0.1710e+1	0.1655e+1	1.85
C	C	100	0.3612e+1	0.4774e+1	-0.1161e+1	0.1344e+1	1.85
C	C	140	0.5075e+1	-0.5599e+1	0.1147e+1	-0.1312e+1	1.85
C	C	200	0.5728e+1	0.8606e+1	-0.9163e+0	0.1186e+1	1.85
C	C	300	0.9067e+1	0.1001e+2	-0.9863e+0	0.1163e+1	1.85
C	C	500	0.1584e+2	0.1114e+2	-0.1288e+1	0.1283e+1	1.85
C	C	1000	0.2837e+2	0.1786e+2	-0.1380e+1	0.1302e+1	1.85

Table 16: Constants for the angular dependence of the mean penetration depth at several energies and ion-target combinations.

ion	solid	energy (eV)	c1	c2	c3	c4	ρ (g/cm^3)
N	C	10	0.6124e+0	-0.6376e+0	0.1760e+1	-0.1443e+1	1.85
N	C	12	0.6990e+0	-0.8100e+0	0.1534e+1	-0.1339e+1	1.85
N	C	15	0.8698e+0	-0.8184e+0	0.2062e+1	-0.1824e+1	1.85
N	C	20	0.1100e+1	-0.1186e+1	0.1541e+1	-0.1470e+1	1.85
N	C	25	0.1460e+1	-0.2231e+1	0.9629e+0	-0.7967e+0	1.85
N	C	30	0.1542e+1	-0.1704e+1	0.1464e+1	-0.1470e+1	1.85
N	C	40	0.5578e+0	-0.3638e+1	0.9461e+0	-0.1415e+1	1.85
N	C	50	0.1650e+1	-0.3067e+1	0.1174e+1	-0.1481e+1	1.85
N	C	70	-0.1897e+2	0.2555e+2	-0.6392e+0	0.2008e+1	1.85
N	C	100	-0.2757e+2	-0.3580e+2	0.6762e+0	-0.2149e+1	1.85
N	C	140	-0.1660e+2	0.2725e+2	-0.6863e+0	0.1871e+1	1.85
N	C	200	-0.3006e+2	0.4399e+2	-0.6071e+0	0.1896e+1	1.85
N	C	300	-0.2160e+2	0.4128e+2	-0.5339e+0	0.1557e+1	1.85
N	C	500	0.1881e+1	0.2707e+2	-0.6002e+0	0.1112e+1	1.85
N	C	10e3	0.2394e+2	0.1937e+2	-0.1167e+1	0.1180e+1	1.85
N	C	15000	0.2357e+3	0.1547e+3	-0.1714e+1	0.1581e+1	2.26
N	C	30000	0.4555e+3	0.3258e+3	-0.1694e+1	0.1593e+1	2.26
Ne	C	10	-0.3657e+1	-0.4854e+1	0.7231e+0	-0.2156e+1	1.85
Ne	C	15	-0.1744e+1	-0.3393e+1	0.9131e+0	-0.2010e+1	1.85
Ne	C	20	-0.3671e+1	-0.6121e+1	0.6356e+0	-0.1717e+1	1.85
Ne	C	22	-0.3005e+1	-0.5474e+1	0.8211e+0	-0.1895e+1	1.85
Ne	C	25	-0.2120e+1	-0.5408e+1	0.6085e+0	-0.1388e+1	1.85
Ne	C	30	-0.1041e+1	-0.3932e+1	0.1105e+1	-0.1997e+1	1.85
Ne	C	35	-0.7548e+1	-0.1158e+2	0.5701e+0	-0.1705e+1	1.85
Ne	C	40	-0.4577e+1	-0.8855e+1	0.6652e+0	-0.1642e+1	1.85
Ne	C	45	-0.1632e+2	-0.2087e+2	0.6285e+0	-0.2065e+1	1.85
Ne	C	50	-0.5813e+1	-0.1080e+2	0.6682e+0	-0.1694e+1	1.85
Ne	C	60	-0.1175e+2	0.1758e+2	-0.5886e+0	0.1783e+1	1.85
Ne	C	70	-0.1444e+2	-0.2125e+2	0.5449e+0	-0.1731e+1	1.85
Ne	C	100	-0.2715e+2	0.3576e+2	-0.5230e+0	0.1883e+1	1.85
Ne	C	140	-0.2473e+2	0.3660e+2	-0.4438e+0	0.1596e+1	1.85
Ne	C	200	-0.2845e+2	0.4390e+2	-0.4181e+0	0.1515e+1	1.85
Ne	C	300	-0.2793e+2	0.4827e+2	-0.4119e+0	0.1407e+1	1.85
Ne	C	500	0.8893e+1	0.1621e+2	-0.7771e+0	0.9855e+0	1.85
Ne	C	1000	0.1906e+2	0.1820e+2	-0.1118e+1	0.1152e+1	1.85
Ne	C	2000	0.3457e+2	0.2454e+2	-0.1504e+1	0.1421e+1	1.85
Ne	C	5000	0.7379e+2	0.4989e+2	-0.1653e+1	0.1525e+1	1.85
Ne	C	10000	0.1356e+3	0.9277e+2	-0.1732e+1	0.1611e+1	1.85
Ne	C	20000	0.2585e+3	0.1801e+3	-0.1811e+1	0.1701e+1	1.85

Table 17: Constants for the angular dependence of the mean penetration depth at several energies and ion-target combinations.

ion	solid	energy (eV)	c1	c2	c3	c4	ρ (g/cm^3)
Ar	C	10	-0.2901e+1	-0.4352e+1	0.7213e+0	-0.1969e+1	1.85
Ar	C	15	-0.4173e+1	-0.7363e+1	0.3657e+0	-0.1250e+1	1.85
Ar	C	20	0.1404e+1	-0.1834e+1	0.9470e+0	-0.8640e+0	1.85
Ar	C	25	0.1378e+1	-0.2340e+1	0.9575e+0	-0.1030e+1	1.85
Ar	C	30	0.8845e+0	-0.4832e+1	0.4981e+0	-0.6859e+0	1.85
Ar	C	40	0.2390e+1	0.3193e+1	-0.9537e+0	0.8803e+0	1.85
Ar	C	50	0.2145e+1	0.5039e+1	-0.6904e+0	0.7782e+0	1.85
Ar	C	70	-0.9399e+1	0.2183e+2	-0.2842e+0	0.9488e+0	1.85
Ar	C	100	0.4556e+1	-0.4673e+1	0.1209e+1	-0.1102e+1	1.85
Ar	C	140	0.5830e+1	0.5153e+1	-0.1397e+1	0.1241e+1	1.85
Ar	C	200	0.6961e+1	-0.6478e+1	0.1349e+1	-0.1249e+1	1.85
Ar	C	300	0.8523e+1	0.9011e+1	-0.1186e+1	0.1150e+1	1.85
Ar	C	500	0.1254e+2	0.9699e+1	-0.1595e+1	0.1435e+1	1.85
Ar	C	1000	0.1709e+2	0.1782e+2	-0.1262e+1	0.1264e+1	1.85
Ar	C	30000	0.1809e+3	0.1404e+3	-0.1907e+1	0.1822e+1	2.26
Xe	C	120	0.9660e+1	-0.7691e+1	0.2402e+1	-0.2151e+1	2.26
Xe	C	150	0.1050e+2	-0.8660e+1	0.2311e+1	-0.2101e+1	2.26
Xe	C	200	0.1222e+2	0.8903e+1	-0.2711e+1	0.2429e+1	2.26
Xe	C	250	0.1314e+2	0.1048e+2	-0.2317e+1	0.2069e+1	2.26
Xe	C	300	0.1415e+2	0.1142e+2	-0.2273e+1	0.2047e+1	2.26
Xe	C	500	0.1711e+2	0.1443e+2	-0.2149e+1	0.2005e+1	2.26
Xe	C	1000	0.2228e+2	0.2039e+2	-0.1964e+1	0.1895e+1	2.26
Xe	C	3000	0.3546e+2	0.3447e+2	-0.1840e+1	0.1837e+1	2.26
Xe	C	10000	0.6460e+2	0.6169e+2	-0.1877e+1	0.1895e+1	2.26
Xe	C	30000	0.1238e+3	0.1141e+3	-0.1873e+1	0.1824e+1	2.26
Xe	C	1e5	0.2701e+3	0.2584e+3	-0.1879e+1	0.1881e+1	2.26

Table 18: Constants for the angular dependence of the mean penetration depth at several energies and ion-target combinations.

ion	solid	energy (eV)	c1	c2	c3	c4	ρ (g/cm^3)
H	Al	13333	0.1418e+4	0.6737e+3	-0.1818e+1	0.1606e+1	2.70
H	Al	26667	0.1679e+4	0.1110e+4	-0.1862e+1	0.1714e+1	2.70
H	Al	40000	0.2176e+4	-0.1646e+4	0.1836e+1	-0.1763e+1	2.70
Ar	Al	100	-0.1386e+2	0.2320e+2	-0.5482e+0	0.1658e+1	2.70
Ar	Al	1000	0.1911e+2	0.1183e+2	-0.1407e+1	0.1311e+1	2.70
Ar	Al	1050	0.1629e+2	0.1798e+2	-0.9208e+0	0.1051e+1	2.70
Ar	Al	10000	0.8853e+2	0.5654e+2	-0.1551e+1	0.1430e+1	2.70
^{4}He	Si	200	-0.2689e+2	0.7519e+2	-0.4112e+0	0.1675e+1	2.32
^{4}He	Si	2000	0.2224e+3	0.5758e+2	-0.1382e+1	0.1272e+1	2.32
^{4}He	Si	3000	0.3229e+3	0.7977e+2	-0.1601e+1	0.1312e+1	2.32
KrC Si	Si	200	-0.6350e+1	0.1967e+2	-0.6080e+0	0.1458e+1	2.32
Mol Si	Si	200	-0.1082e+2	0.2163e+2	-0.6217e+0	0.1660e+1	2.32
SiSi Si	Si	200	0.7884e+1	-0.5210e+1	0.1287e+1	-0.1302e+1	2.32
ZBL Si	Si	200	0.4876e+1	0.9093e+1	-0.9225e+0	0.1299e+1	2.32
Si	Si	500	0.9281e+1	0.1728e+2	-0.7508e+0	0.1110e+1	2.32
Si	Si	2000	0.3740e+2	0.2220e+2	-0.1342e+1	0.1280e+1	2.32
Ar	Si	4500	0.5732e+2	0.3773e+2	-0.1416e+1	0.1344e+1	2.32
Ne	Ti	38	-0.2872e+1	0.9868e+1	-0.9806e+0	0.2527e+1	4.52
Ne	Ti	380	0.1485e+2	0.4617e+1	-0.1242e+1	0.1312e+1	4.52
Ne	Ti	3798	0.6118e+2	0.2142e+2	-0.1503e+1	0.1418e+1	4.52
Ar	Ti	1050	-0.4341e+2	0.7094e+2	-0.6230e+0	0.1916e+1	4.52
Ar	Ti	1.5e5	0.7634e+3	0.4213e+3	-0.1883e+0	0.1717e+1	4.52
Ar	Ti	9e5	0.3848e+4	0.2769e+4	-0.1821e+1	0.1689e+1	4.52
H	V	100	0.2828e+1	0.3629e+2	-0.1986e+0	0.1365e+1	6.10
H	V	120	0.9758e+1	0.3530e+2	-0.1839e+0	0.1181e+1	6.10
H	V	140	0.9535e+1	0.3906e+2	-0.2090e+0	0.1266e+1	6.10
H	V	200	0.2771e+2	0.3414e+2	-0.2286e+0	0.1021e+1	6.10
H	V	400	0.7031e+1	0.9092e+2	-0.2195e+0	0.1287e+1	6.10
H	V	1000	-0.6316e+0	0.1941e+3	-0.2429e+0	0.1229e+1	6.10
H	V	3000	0.3330e+3	0.8320e+2	-0.9311e+0	0.6468e+1	6.10
H	V	10000	0.7824e+3	0.2282e+3	-0.1923e+1	0.1683e+1	6.10
D	V	55	-0.6764e+0	0.2626e+2	-0.2232e+0	0.1477e+1	6.10
D	V	60	0.4835e+1	0.2065e+2	-0.3800e+0	0.1743e+1	6.10
D	V	70	0.4611e+1	0.2385e+2	-0.3149e+0	0.1620e+1	6.10
D	V	100	0.4600e+1	0.3133e+2	-0.3287e+0	0.1624e+1	6.10
D	V	200	0.1072e+2	0.5033e+2	-0.2319e+0	0.1257e+1	6.10
D	V	500	-0.7940e+1	0.1404e+3	-0.1530e+0	0.1064e+1	6.10
D	V	1000	0.2691e+2	0.1626e+3	-0.3656e+0	0.1459e+1	6.10
D	V	3000	0.3725e+3	0.4518e+2	-0.3113e+1	0.2670e+1	6.10
D	V	10000	0.9576e+3	-0.2434e+3	0.1962e+1	-0.1650e+1	6.10

Table 19: Constants for the angular dependence of the mean penetration depth at several energies and ion-target combinations.

ion	solid	energy (eV)	c1	c2	c3	c4	ρ (g/cm^3)
T	V	40	0.3363e+1	0.1476e+2	-0.4415e+0	0.1775e+1	6.10
T	V	50	0.4767e+1	0.1580e+2	-0.4805e+0	0.1834e+1	6.10
T	V	70	0.1834e+1	0.2519e+2	-0.3073e+0	0.1525e+1	6.10
T	V	100	0.1382e+2	0.1990e+2	-0.3611e+0	0.1361e+1	6.10
T	V	300	-0.6945e+1	0.8996e+2	-0.1909e+0	0.1188e+1	6.10
T	V	1000	0.2280e+2	0.1691e+3	-0.3743e+0	0.1406e+1	6.10
T	V	3000	0.3799e+3	0.7196e+2	-0.1362e+1	0.1235e+1	6.10
T	V	10000	0.1041e+4	0.2615e+3	-0.1772e+1	0.1516e+1	6.10
^{4}He	V	35	0.3089e+1	0.7166e+1	-0.9620e+0	0.2481e+1	6.10
^{4}He	V	40	0.4389e+1	0.6994e+1	-0.6044e+0	0.1818e+1	6.10
^{4}He	V	50	0.3799e+1	0.8887e+1	-0.7541e+0	0.2145e+1	6.10
^{4}He	V	70	0.1654e+1	0.1376e+2	-0.7567e+0	0.2235e+1	6.10
^{4}He	V	100	-0.2048e+0	0.1952e+2	-0.7316e+0	0.2214e+1	6.10
^{4}He	V	300	0.4390e+1	0.3832e+2	-0.3478e+0	0.1422e+1	6.10
^{4}He	V	1000	0.5076e+1	0.1081e+3	-0.2305e+0	0.1096e+1	6.10
^{4}He	V	3000	0.1860e+3	-0.5086e+2	0.7929e+0	-0.8120e+0	6.10
^{4}He	V	10000	0.5138e+4	0.1216e+3	-0.1727e+1	0.1440e+1	6.10
H	Fe	4000	0.3324e+3	0.6306e+2	-0.1544e+1	0.1212e+1	7.87
H	Fe	8000	0.5520e+3	0.1459e+3	-0.1554e+1	0.1227e+1	7.87
H	Ni	450	0.2416e+2	0.5994e+2	-0.1854e+0	0.9981e+0	8.90
H	Ni	4000	0.2992e+3	0.5362e+2	-0.1643e+1	0.1383e+1	8.90
H	Ni	8000	0.4980e+3	0.1204e+3	-0.1718e+1	0.1367e+1	8.90
D	Ni	1000	0.1710e+2	0.1232e+3	-0.3272e+0	0.1456e+1	8.90
D	Ni	4000	0.3374e+3	0.4613e+2	-0.1932e+1	0.1728e+1	8.90
D	Ni	8000	0.5946e+3	0.1232e+3	-0.1811e+1	0.1437e+1	8.90
^{3}He	Ni	1000	0.4812e+1	0.8370e+2	-0.1956e+0	0.1054e+1	8.90
^{3}He	Ni	3000	0.1747e+2	0.1757e+3	-0.2862e+0	0.1149e+1	8.90
^{3}He	Ni	8000	0.3060e+3	0.5433e+2	-0.1853e+1	0.1537e+1	8.90
^{3}He	Ni	25000	0.7287e+3	0.2189e+3	-0.1783e+1	0.1515e+1	8.90
^{4}He	Ni	100	0.2368e+1	0.1243e+2	-0.1026e+1	0.2637e+1	8.90
^{4}He	Ni	500	0.4416e+1	0.4411e+2	-0.2535e+0	0.1238e+1	8.90
^{4}He	Ni	1000	0.1102e+2	0.6512e+2	-0.3284e+0	0.1357e+1	8.90
^{4}He	Ni	4000	0.1804e+3	0.3366e+2	-0.1252e+1	0.9543e+0	8.90
^{4}He	Ni	8000	0.3127e+3	0.6742e+2	-0.1407e+1	0.1179e+1	8.90
Ar	Ni	40	-0.5286e+1	-0.7281e+1	0.1195e+1	-0.2804e+1	8.90
Ar	Ni	50	-0.6062e+1	-0.8345e+1	0.1271e+1	-0.2918e+1	8.90
Ar	Ni	70	-0.1020e+2	-0.1298e+2	0.1399e+1	-0.3253e+1	8.90
Ar	Ni	100	-0.1445e+2	0.1799e+2	-0.1234e+1	0.3091e+1	8.90
Ar	Ni	300	-0.2479e+2	-0.3146e+2	0.1131e+1	-0.3000e+1	8.90
Ar	Ni	1000	-0.2848e+2	0.4271e+2	-0.7438e+0	0.2222e+1	8.90
Ar	Ni	3000	0.8781e+1	0.2224e+2	-0.6162e+0	0.1102e+1	8.90
Ar	Ni	30000	0.1008e+3	0.4763e+2	-0.1598e+1	0.1482e+1	8.90

Table 20: Constants for the angular dependence of the mean penetration depth at several energies and ion-target combinations.

ion	solid	energy (eV)	c1	c2	c3	c4	ρ (g/cm^3)
Ni	Ni	100	0.1032e+1	-0.2116e+1	0.1134e+1	-0.1432e+1	8.90
Ni	Ni	500	-0.2657e+2	0.3478e+2	-0.8656e+0	-0.2461e+1	8.90
Ni	Ni	5000	0.9351e+1	0.2738e+2	-0.6263e+0	0.1050e+1	8.90
Ni	Ni	10000	0.2391e+2	0.3050e+2	-0.8620e+0	0.1123e+1	8.90
Kr	Ni	45000	0.7937e+2	0.5731e+2	-0.1322e+1	0.1266e+1	8.90
H	Cu	100	0.4184e+1	0.2719e+2	-0.2671e+0	0.1588e+1	8.95
H	Cu	1000	0.1564e+2	0.1171e+3	-0.5005e+0	0.1855e+1	8.95
H	Cu	5000	0.3712e+3	0.7740e+2	-0.1566e+1	0.1305e+1	8.95
H	Cu	13333	0.7545e+3	0.2239e+3	-0.1833e+1	0.1568e+1	8.95
H	Cu	26667	0.1289e+4	0.5529e+3	-0.1458e+1	0.9335e+0	8.95
H	Cu	40000	0.1662e+4	0.7921e+3	-0.1594e+1	0.1184e+1	8.95
H	Cu	80000	0.2488e+4	0.1652e+4	-0.1788e+1	0.1663e+1	8.95
D	Cu	300	0.1679e+2	0.5363e+2	-0.1682e+0	0.1039e+1	8.95
D	Cu	1000	0.1222e+2	0.1345e+3	-0.4456e+0	0.1736e+1	8.95
D	Cu	3000	-0.1324e+3	0.5460e+3	-0.2340e+0	0.1243e+1	8.95
D	Cu	80000	0.3070e+4	0.1866e+4	-0.1785e+1	0.1635e+1	8.95
^{4}He	Cu	100	0.1213e+2	0.4646e+1	-0.5755e+0	0.1345e+1	8.95
^{4}He	Cu	1000	0.9699e+1	0.7235e+2	-0.3367e+0	0.1405e+1	8.95
^{4}He	Cu	4000	0.2330e+2	0.2149e+3	-0.4127e+0	0.1434e+1	8.95
^{4}He	Cu	5000	0.2306e+3	0.3082e+2	-0.2308e+1	0.1926e+1	8.95
Ne	Cu	1000	-0.6187e+2	0.8334e+2	-0.5816e+0	0.2280e+1	8.95
Ne	Cu	45000	0.2851e+3	0.1057e+3	-0.1577e+1	0.1389e+1	8.95
Ar	Cu	14	-0.4752e+1	-0.5816e+1	0.1173e+1	-0.3022e+1	8.95
Ar	Cu	16	-0.2330e+1	-0.3499e+1	0.1219e+1	-0.2749e+1	8.95
Ar	Cu	18	-0.6560e+1	-0.7835e+1	0.1235e+1	-0.3148e+1	8.95
Ar	Cu	20	-0.7713e+0	-0.2130e+1	0.1353e+1	-0.2550e+1	8.95
Ar	Cu	25	-0.7982e+1	-0.9596e+1	0.1172e+1	-0.3049e+1	8.95
Ar	Cu	30	-0.8990e+1	-0.1082e+2	0.1222e+1	-0.3111e+1	8.95
Ar	Cu	40	-0.1460e+1	-0.3676e+1	0.1272e+1	-0.2497e+1	8.95
Ar	Cu	50	-0.6586e+1	0.9147e+1	-0.1253e+1	0.2910e+1	8.95
Ar	Cu	100	-0.1198e+2	-0.1600e+2	0.1076e+1	-0.2797e+1	8.95
Ar	Cu	300	-0.1921e+2	0.2725e+2	-0.6228e+0	0.2140e+1	8.95
Ar	Cu	1050	0.1096e+2	0.4408e+1	-0.1383e+1	0.1353e+1	8.95
Ar	Cu	20000	0.7802e+2	0.3699e+2	-0.1429e+1	0.1331e+1	8.95
Ar	Cu	27000	0.9846e+2	0.5086e+2	-0.1333e+1	0.1259e+1	8.95
Ar	Cu	30000	0.1059e+3	0.4801e+2	-0.1623e+1	0.1550e+1	8.95
Ar	Cu	37000	0.1313e+3	0.5862e+2	-0.1617e+1	0.1415e+1	8.95
Ar	Cu	1e5	0.3082e+3	0.1544e+3	-0.1625e+1	0.1463e+1	8.95
Ar	Cu	3e5	0.8370e+3	0.4625e+3	-0.1770e+1	0.1615e+1	8.95
Ar	Cu	1e6	0.2425e+4	0.1574e+4	-0.1889e+1	0.1737e+1	8.95
MolaAr	Cu	30000	0.9617e+2	0.4484e+2	-0.1635e+1	0.1502e+1	8.95
MolbAr	Cu	30000	0.1277e+3	0.5878e+2	-0.1688e+1	0.1531e+1	8.95
ZBL Ar	Cu	30000	0.1004e+3	0.5354e+2	-0.1336e+1	0.1279e+1	8.95

Table 21: Constants for the angular dependence of the mean penetration depth at several energies and ion-target combinations.

ion	solid	energy (eV)	c1	c2	c3	c4	ρ (g/cm^3)
Cu	Cu	14	0.3989e+0	-0.3857e+0	0.1347e+1	-0.1124e+1	8.95
Cu	Cu	20	0.5485e+0	-0.4799e+0	0.1749e+1	-0.1409e+1	8.95
Cu	Cu	30	0.7297e+0	-0.6937e+0	0.1708e+1	-0.1434e+1	8.95
Cu	Cu	40	0.8694e+0	-0.1035e+1	0.1260e+1	-0.1110e+1	8.95
Cu	Cu	50	0.1008e+1	-0.1088e+1	0.1533e+1	-0.1469e+1	8.95
Cu	Cu	70	0.1112e+1	-0.1635e+1	0.1182e+1	-0.1306e+1	8.95
Cu	Cu	100	0.7102e+0	-0.2799e+1	0.1020e+1	-0.1470e+1	8.95
Cu	Cu	200	-0.1862e+2	0.2394e+2	-0.8458e+0	0.2412e+1	8.95
Cu	Cu	300	-0.2236e+2	0.2889e+2	-0.9195e+0	0.2540e+1	8.95
Cu	Cu	1000	-0.3720e+2	0.5130e+2	-0.6245e+0	0.2069e+1	8.95
Cu	Cu	3000	0.8998e+1	0.1729e+2	-0.8408e+0	0.1273e+1	8.95
Cu	Cu	10000	0.3529e+2	0.1649e+2	-0.1655e+1	0.1482e+1	8.95
Cu	Cu	30000	0.7394e+2	0.3728e+2	-0.1807e+1	0.1680e+1	8.95
Cu	Cu	1e5	0.1885e+3	0.1327e+3	-0.1257e+1	0.1201e+1	8.95
Kr	Cu	1050	-0.4082e+2	0.5400e+2	-0.9207e+0	0.2526e+1	8.95
Kr	Cu	45000	0.8670e+2	0.5297e+2	-0.1526e+1	0.1416e+1	8.95
Xe	Cu	550	0.6505e+1	0.4947e+1	-0.1277e+1	0.1191e+1	8.95
Xe	Cu	1050	0.8269e+1	0.8212e+1	-0.1022e+1	0.1060e+1	8.95
Xe	Cu	2050	0.9782e+1	0.1424e+2	-0.8278e+0	0.9958e+1	8.95
Xe	Cu	5000	-0.7555e+2	0.1200e+3	-0.4003e+0	0.1479e+1	8.95
Xe	Cu	9500	0.2822e+2	0.2013e+2	-0.1397e+1	0.1321e+1	8.95
Xe	Cu	10000	0.2851e+2	0.2218e+2	-0.1279e+1	0.1238e+1	8.95
Xe	Cu	30000	0.5314e+2	0.4253e+2	-0.1344e+1	0.1329e+1	8.95
Xe	Cu	50000	0.7693e+2	0.5457e+2	-0.1512e+1	0.1418e+1	8.95
Ga	Ga	100	-0.1082e+2	0.1778e+2	-0.7423e+0	0.1960e+1	5.91
Ga	Ga	150	-0.2462e+2	0.3318e+2	-0.7214e+0	0.2204e+1	5.91
Ga	Ga	200	-0.2863e+2	0.3875e+2	-0.6714e+0	0.2146e+1	5.91
Ga	Ga	300	-0.2120e+2	0.3370e+2	-0.6535e+0	0.1952e+1	5.91
Ga	Ga	900	0.1188e+2	0.9548e+1	-0.1066e+1	0.1266e+1	5.91
Ga	Ga	1000	0.1397e+2	0.8204e+2	-0.1237e+1	0.1289e+1	5.91
Ar	Zr	1050	-0.5373e+1	0.3856e+2	-0.5153e+0	0.1453e+1	6.47
Ar	Zr	1.5e5	0.7827e+3	0.3168e+3	-0.1826e+1	0.1596e+1	6.47
Ar	Zr	9e5	0.3762e+4	0.2145e+4	-0.1798e+1	0.1619e+1	6.47
H	Nb	1000	0.2019e+2	0.1751e+3	-0.3219e+0	0.1542e+1	8.60
H	Nb	2000	0.1147e+2	0.2987e+3	-0.4136e+0	0.1652e+1	8.60
H	Nb	5000	0.3583e+3	0.2818e+3	-0.4612e+0	0.9629e+0	8.60
H	Nb	10000	0.8242e+3	0.1634e+3	-0.1902e+1	0.1594e+1	8.60
D	Nb	12200	0.1157e+4	0.2440e+3	-0.1485e+1	0.1204e+1	8.60
^{4}He	Nb	36500	0.1474e+4	0.3693e+3	-0.2072e+1	0.1754e+1	8.60
Nb	Nb	60000	0.1343e+3	0.6293e+2	-0.1847e+1	0.1643e+1	8.60

Table 22: Constants for the angular dependence of the mean penetration depth at several energies and ion-target combinations.

ion	solid	energy (eV)	c1	c2	c3	c4	ρ (g/cm^3)
H	Mo	210	0.3959e+1	0.5766e+2	-0.3677e+0	0.1875e+1	10.21
H	Mo	220	0.9647e+1	0.5666e+2	-0.2216e+0	0.1465e+1	10.21
H	Mo	230	0.8550e+1	0.6468e+2	-0.1369e+0	0.1190e+1	10.21
H	Mo	250	0.8629e+1	0.6571e+2	-0.1885e+0	0.1325e+1	10.21
H	Mo	300	0.9108e+1	0.7318e+2	-0.1825e+0	0.1336e+1	10.21
H	Mo	400	0.1257e+2	0.8239e+2	-0.2420e+0	0.1476e+1	10.21
H	Mo	700	0.1028e+1	0.1556e+3	-0.1265e+0	0.1062e+1	10.21
H	Mo	1400	0.2095e+2	0.1976e+3	-0.2559e+0	0.1368e+1	10.21
H	Mo	2000	0.2754e+2	0.2522e+3	-0.3107e+0	0.1395e+1	10.21
H	Mo	3000	-0.8715e+1	0.4020e+3	-0.2963e+0	0.1311e+1	10.21
H	Mo	4000	0.3409e+3	0.1562e+3	-0.4244e+0	0.5639e+0	10.21
H	Mo	7000	0.5255e+3	0.2060e+3	-0.6441e+0	0.6822e+0	10.21
H	Mo	13333	0.8680e+3	0.1888e+3	-0.2110e+1	0.1827e+1	10.21
H	Mo	26667	0.8925e+3	0.4048e+3	-0.1767e+1	0.1546e+1	10.21
H	Mo	40000	0.1174e+4	0.6052e+3	-0.1844e+1	0.1563e+1	10.21
H	Mo	80000	0.1899e+4	0.1208e+4	-0.1864e+1	0.1734e+1	10.21
D	Mo	100	0.1206e+1	0.4135e+2	-0.2316e+0	0.1604e+1	10.21
D	Mo	110	0.2570e+1	0.5026e+2	-0.1120e+0	0.1063e+1	10.21
D	Mo	120	0.4722e+1	0.4071e+2	-0.3255e+0	0.1860e+1	10.21
D	Mo	200	0.1166e+2	0.5148e+2	-0.2612e+0	0.1607e+1	10.21
D	Mo	300	0.7957e+1	0.7980e+2	-0.1643e+0	0.1282e+1	10.21
D	Mo	450	0.4308e+1	0.1001e+3	-0.3652e+0	0.1777e+1	10.21
D	Mo	2000	0.2977e+2	0.2638e+3	-0.4285e+0	0.1729e+1	10.21
D	Mo	8000	0.2392e+2	0.7791e+3	-0.9017e+0	0.2363e+1	10.21
T	Mo	75	0.4901e+1	0.2736e+2	-0.4697e+0	0.2114e+1	10.21
T	Mo	80	0.5421e+1	0.2932e+2	-0.2914e+0	0.1679e+1	10.21
T	Mo	90	0.5167e+1	0.3247e+2	-0.2629e+0	0.1613e+1	10.21
T	Mo	100	0.4401e+1	0.3538e+2	-0.3030e+0	0.1706e+1	10.21
T	Mo	170	0.5608e+1	0.4912e+2	-0.3194e+0	0.1733e+1	10.21
T	Mo	300	0.9592e+1	0.7197e+2	-0.2440e+0	0.1474e+1	10.21
T	Mo	1000	0.2381e+2	0.1532e+3	-0.4445e+0	0.1821e+1	10.21
T	Mo	3000	0.4781e+1	0.4544e+3	-0.2448e+0	0.1275e+1	10.21
T	Mo	10000	0.9663e+3	0.2286e+3	-0.9703e+0	0.6199e+0	10.21
^{3}He	Mo	90	0.5157e+1	0.1815e+2	-0.5150e+0	0.2073e+1	10.21
^{3}He	Mo	100	0.7090e+1	0.1766e+2	-0.5268e+0	0.2010e+1	10.21
^{3}He	Mo	140	0.1045e+2	0.2057e+2	-0.3361e+0	0.1527e+1	10.21
^{3}He	Mo	300	0.4790e+1	0.4356e+2	-0.3205e+0	0.1632e+1	10.21
^{3}He	Mo	1000	0.1564e+2	0.8903e+2	-0.2995e+0	0.1465e+1	10.21
^{3}He	Mo	3000	0.2490e+2	0.2073e+3	-0.2863e+0	0.1308e+1	10.21
^{3}He	Mo	10000	0.4462e+3	0.6609e+2	-0.1631e+1	0.1429e+1	10.21

Table 23: Constants for the angular dependence of the mean penetration depth at several energies and ion-target combinations.

ion	solid	energy (eV)	c1	c2	c3	c4	ρ (g/cm^3)
^{4}He	Mo	70	0.4016e+1	0.1658e+2	-0.2597e+0	0.1518e+1	10.21
^{4}He	Mo	80	0.7529e+1	0.1350e+2	-0.5546e+0	0.1959e+1	10.21
^{4}He	Mo	100	-0.5179e+1	0.2873e+2	-0.6615e+0	0.2500e+1	10.21
^{4}He	Mo	140	0.1201e+2	0.1629e+2	-0.6933e+0	0.2148e+1	10.21
^{4}He	Mo	1500	0.9049e+1	0.1222e+3	-0.3823e+0	0.1715e+1	10.21
^{4}He	Mo	4000	-0.9545e+2	0.3859e+3	-0.2894e+0	0.1521e+1	10.21
^{4}He	Mo	8000	-0.5184e+1	0.4714e+3	-0.5269e+0	0.1728e+1	10.21
Ar	Mo	160	-0.1226e+2	0.2143e+2	-0.7420e+0	0.2424e+1	10.21
Ar	Mo	1600	0.5248e+1	0.2364e+2	-0.5150e+0	0.1258e+1	10.21
Ar	Mo	16000	0.8267e+2	0.2817e+2	-0.1469e+1	0.1342e+1	10.21
Ar	Mo	27500	0.1211e+3	0.4265e+2	-0.1596e+1	0.1499e+1	10.21
Mo	Mo	300	-0.8075e+1	0.1659e+2	-0.7489e+0	0.1839e+1	10.21
Mo	Mo	350	-0.2972e+2	0.3934e+2	-0.6244e+0	0.2090e+1	10.21
Mo	Mo	1000	0.5845e+1	0.1057e+2	-0.7645e+0	0.1168e+1	10.21
Mo	Mo	2000	0.1343e+2	0.8176e+1	-0.1289e+1	0.1351e+1	10.21
Xe	Mo	9500	0.3266e+2	0.1660e+2	-0.1639e+1	0.1497e+1	10.21
Xe	Mo	30000	0.6233e+2	0.3633e+2	-0.1452e+1	0.1348e+1	10.21
Ar	Pd	1050	-0.3723e+2	0.5598e+2	-0.6641e+0	0.2264e+1	11.96
D	Ag	100	0.4125e+1	0.4226e+2	-0.2739e+0	0.1759e+1	10.47
Ne	Ag	45000	0.3531e+3	0.9149e+2	-0.1691e+1	0.1475e+1	10.47
Ar	Ag	1050	-0.5359e+2	0.7619e+2	-0.5368e+0	0.2155e+1	10.47
Ar	Ag	1.5e5	0.5154e+3	0.2184e+3	-0.1514e+1	0.1441e+1	10.47
Ar	Ag	9e5	0.2557e+4	0.1331e+4	-0.1830e+1	0.1623e+1	10.47
Kr	Ag	45000	0.1060e+3	0.5019e+2	-0.1528e+1	0.1408e+1	10.47
H	IN	2000	0.1086e+2	0.3847e+3	-0.8803e+0	0.2595e+1	7.31
In	IN	100	-0.1178e+2	0.2091e+2	-0.7024e+0	0.1887e+1	7.31
In	IN	200	-0.3916e+2	0.5199e+2	-0.6227e+0	0.2138e+1	7.31
In	IN	1000	0.1590e+2	0.9394e+1	-0.1179e+1	0.1268e+1	7.31
^{4}He	Ta	1.5e5	0.2589e+4	0.7337e+3	-0.1858e+1	0.1551e+1	16.60
Ne	Ta	45000	0.3394e+3	0.7706e+2	-0.1281e+1	0.1109e+1	16.60
Ar	Ta	1050	0.3693e+1	0.2000e+2	-0.6330e+0	0.1702e+1	16.60
Kr	Ta	45000	0.1035e+3	0.3718e+2	-0.1488e+1	0.1369e+1	16.60

Table 24: Constants for the angular dependence of the mean penetration depth at several energies and ion-target combinations.

ion	solid	energy (eV)	c1	c2	c3	c4	ρ (g/cm^3)
H	W	10	0.1334e+1	0.1204e+2	-0.3101e+0	0.2081e+1	19.29
H	W	20	0.2774e+1	0.1572e+2	-0.4397e+0	0.2409e+1	19.29
H	W	50	-0.3810e+2	0.6717e+2	-0.4709e+0	0.2931e+1	19.29
H	W	100	0.5358e+1	0.3763e+2	-0.2386e+0	0.1774e+1	19.29
H	W	200	0.9046e+1	0.5770e+2	-0.1283e+0	0.1286e+1	19.29
H	W	300	0.9570e+1	0.6781e+2	-0.2586e+0	0.1689e+1	19.29
H	W	500	0.1358e+2	0.1095e+3	-0.9436e-1	0.9977e+0	19.29
H	W	550	0.1108e+2	0.1004e+3	-0.2010e+0	0.1485e+1	19.29
H	W	600	0.1150e+2	0.1065e+3	-0.1829e+0	0.1429e+1	19.29
H	W	700	0.1177e+2	0.1191e+3	-0.1923e+0	0.1401e+1	19.29
H	W	800	0.1187e+2	0.1193e+3	-0.3749e+0	0.1902e+1	19.29
H	W	900	0.9030e+1	0.1369e+3	-0.3016e+0	0.1656e+1	19.29
H	W	1000	0.1995e+2	0.1402e+3	-0.2270e+0	0.1415e+1	19.29
H	W	2000	0.1752e+2	0.2232e+3	-0.2909e+0	0.1547e+1	19.29
H	W	4000	-0.9475e+1	0.4328e+3	-0.2121e+0	0.1219e+1	19.29
H	W	13333	0.2111e+2	0.1000e+4	-0.3113e+0	0.1173e+1	19.29
H	W	26667	0.1023e+4	0.2564e+3	-0.2091e+1	0.1768e+1	19.29
H	W	40000	0.1363e+4	-0.4603e+3	0.1720e+1	-0.1498e+1	19.29
H	W	80000	0.2287e+4	-0.9852e+3	0.1876e+1	-0.1641e+1	19.29
D	W	10	0.4927e+1	0.8610e+1	-0.4255e+0	0.2276e+1	19.29
D	W	20	0.3697e+1	0.1621e+2	-0.2250e+0	0.1810e+1	19.29
D	W	50	0.8226e+1	0.3491e+2	-0.4094e-1	0.7472e+0	19.29
D	W	100	0.9064e+1	0.4458e+2	-0.7610e-1	0.1034e+1	19.29
D	W	200	0.5416e+1	0.6013e+2	-0.3280e+0	0.1955e+1	19.29
D	W	250	0.5593e+1	0.6759e+2	-0.3448e+0	0.2058e+1	19.29
D	W	270	0.4757e+1	0.7158e+2	-0.3726e+0	0.2100e+1	19.29
D	W	300	0.4626e+1	0.7704e+2	-0.3341e+0	0.1987e+1	19.29
D	W	350	0.5528e+1	0.8378e+2	-0.3171e+0	0.1947e+1	19.29
D	W	400	0.4700e+1	0.9947e+2	-0.1599e+0	0.1419e+1	19.29
D	W	500	0.6596e+1	0.9908e+2	-0.6129e+0	0.2559e+1	19.29
D	W	600	0.6847e+1	0.1164e+3	-0.3166e+0	0.1869e+1	19.29
D	W	700	0.4644e+1	0.1305e+3	-0.3154e+0	0.1863e+1	19.29
D	W	1000	0.1192e+2	0.1476e+3	-0.9689e+0	0.2994e+1	19.29
T	W	10	0.3538e+1	0.9516e+1	-0.4566e+0	0.2325e+1	19.29
T	W	20	0.3791e+1	0.1552e+2	-0.1739e+0	0.1724e+1	19.29
T	W	50	0.3760e+1	0.2596e+2	-0.5819e+0	0.2627e+1	19.29
T	W	100	0.2217e+1	0.4850e+2	-0.8967e-1	0.1219e+1	19.29
T	W	140	0.5041e+1	0.4910e+2	-0.2358e+0	0.1782e+1	19.29
T	W	160	0.1010e+2	0.5169e+2	-0.1261e+0	0.1350e+1	19.29
T	W	170	0.4874e+1	0.5497e+2	-0.3083e+0	0.1885e+1	19.29
T	W	180	0.4416e+1	0.5880e+2	-0.2096e+0	0.1667e+1	19.29
T	W	200	0.4267e+1	0.6022e+2	-0.3137e+0	0.2041e+1	19.29
T	W	250	0.4482e+1	0.6889e+2	-0.3538e+0	0.2049e+1	19.29
T	W	300	0.9818e+1	0.7893e+2	-0.1446e+0	0.1363e+1	19.29
T	W	400	0.1089e+2	0.9159e+2	-0.1715e+0	0.1478e+1	19.29
T	W	500	0.1317e+2	0.1014e+3	-0.2258e+0	0.1618e+1	19.29
T	W	700	0.5829e+1	0.1294e+3	-0.3721e+0	0.2041e+1	19.29
T	W	1000	0.1146e+2	0.1575e+3	-0.4334e+0	0.2066e+1	19.29

Table 25: Constants for the angular dependence of the mean penetration depth at several energies and ion-target combinations.

ion	solid	energy (eV)	c1	c2	c3	c4	ρ (g/cm^3)
^{4}He	W	10	0.2818e+1	0.6573e+1	-0.5180e+0	0.2203e+1	19.29
^{4}He	W	20	0.2243e+1	0.1043e+2	-0.3746e+0	0.2197e+1	19.29
^{4}He	W	50	-0.3216e+1	0.2251e+2	-0.7163e+0	0.2840e+1	19.29
^{4}He	W	100	0.1242e+2	0.1466e+2	-0.7874e+0	0.2578e+1	19.29
^{4}He	W	125	-0.1954e+1	0.3323e+2	-0.3877e+0	0.2123e+1	19.29
^{4}He	W	130	0.4137e+1	0.2811e+2	-0.3111e+0	0.1875e+1	19.29
^{4}He	W	140	0.6335e+1	0.2668e+2	-0.3958e+0	0.2029e+1	19.29
^{4}He	W	150	0.4512e+1	0.3036e+2	-0.3059e+0	0.1830e+1	19.29
^{4}He	W	170	0.6001e+1	0.3180e+2	-0.2581e+0	0.1671e+1	19.29
^{4}He	W	200	0.4358e+1	0.3600e+2	-0.3436e+0	0.1879e+1	19.29
^{4}He	W	250	0.4333e+1	0.4152e+2	-0.3076e+0	0.1803e+1	19.29
^{4}He	W	300	0.8201e+1	0.4124e+2	-0.4193e+0	0.2014e+1	19.29
^{4}He	W	350	0.4740e+1	0.4820e+2	-0.6358e+0	0.2429e+1	19.29
^{4}He	W	400	0.4592e+1	0.5502e+2	-0.2888e+0	0.1748e+1	19.29
^{4}He	W	500	0.8706e+1	0.5847e+2	-0.3294e+0	0.1775e+1	19.29
^{4}He	W	600	0.9454e+1	0.6809e+2	-0.2109e+0	0.1479e+1	19.29
^{4}He	W	700	0.9747e+1	0.7643e+2	-0.1831e+0	0.1393e+1	19.29
^{4}He	W	1000	0.4957e+1	0.1027e+3	-0.1906e+0	0.1384e+1	19.29
^{4}He	W	1400	0.2231e+2	0.1088e+3	-0.1986e+0	0.1329e+1	19.29
^{4}He	W	2000	0.1593e+2	0.1379e+3	-0.4026e+0	0.1806e+1	19.29
^{4}He	W	5000	-0.2619e+2	0.3010e+3	-0.4493e+0	0.2041e+1	19.29
^{4}He	W	10000	-0.1551e+2	0.5150e+3	-0.3215e+0	0.1445e+1	19.29
^{4}He	W	20000	0.9736e+2	0.8112e+3	-0.2819e+0	0.1142e+1	19.29
^{4}He	W	50000	0.1332e+4	0.3008e+3	-0.1459e+1	0.1213e+1	19.29
N	W	10	0.2670e+1	0.1202e+1	-0.9111e+0	0.2070e+1	19.29
N	W	20	0.2100e+1	0.3297e+1	-0.8187e+0	0.2287e+1	19.29
N	W	40	0.6834e+1	-0.3533e+0	0.3948e+1	-0.4322e+1	19.29
N	W	48	0.7163e+1	0.7792e+0	-0.1435e+1	0.1962e+1	19.29
N	W	50	-0.2446e+1	0.1052e+2	-0.1134e+1	0.3103e+1	19.29
N	W	52	0.2173e+1	0.6112e+1	-0.9717e+0	0.2643e+1	19.29
N	W	55	-0.9424e+1	0.1783e+2	-0.1328e+1	0.3723e+1	19.29
N	W	60	-0.1501e+1	0.1018e+2	-0.1470e+1	0.3577e+1	19.29
N	W	70	0.6177e+1	0.3305e+1	-0.1027e+1	0.2285e+1	19.29
N	W	80	-0.7281e+1	0.1743e+2	-0.9041e+0	0.2929e+1	19.29
N	W	90	0.1342e+1	0.9359e+1	-0.9082e+0	0.2602e+1	19.29
N	W	100	0.3135e+1	0.8236e+1	-0.7660e+0	0.2241e+1	19.29
N	W	120	0.6880e+1	0.5504e+1	-0.8409e+0	0.2131e+1	19.29
N	W	140	0.1680e+1	0.1156e+2	-0.8747e+0	0.2559e+1	19.29
N	W	200	0.5608e+1	0.1064e+2	-0.6204e+0	0.1917e+1	19.29
N	W	300	0.1093e+2	0.8383e+1	-0.1037e+1	0.2336e+1	19.29
N	W	500	-0.1982e+0	0.2556e+2	-0.7956e+0	0.2460e+1	19.29
N	W	1000	0.6966e-1	0.4206e+2	-0.2602e+0	0.1364e+1	19.29

Table 26: Constants for the angular dependence of the mean penetration depth at several energies and ion-target combinations.

ion	solid	energy (eV)	c1	c2	c3	c4	ρ (g/cm^3)
Ne	W	10	-0.7113e+1	0.1079e+2	-0.1357e+1	0.3752e+1	19.29
Ne	W	20	-0.4455e+1	0.9188e+1	-0.1070e+1	0.3171e+1	19.29
Ne	W	30	0.4423e+1	0.1004e+1	-0.1957e+1	0.3025e+1	19.29
Ne	W	40	-0.1319e+1	0.7491e+1	-0.1262e+1	0.3165e+1	19.29
Ne	W	45	0.7771e+0	0.5736e+1	-0.8858e+1	0.2529e+1	19.29
Ne	W	50	-0.1635e+1	0.8390e+1	-0.1101e+1	0.2997e+1	19.29
Ne	W	60	0.1030e+1	0.6314e+1	-0.1016e+1	0.2639e+1	19.29
Ne	W	70	0.4100e+1	0.3729e+1	-0.1023e+1	0.2312e+1	19.29
Ne	W	80	-0.4547e+1	0.1279e+2	-0.1346e+1	0.3387e+1	19.29
Ne	W	100	0.4845e+1	0.4354e+1	-0.1030e+1	0.2307e+1	19.29
Ne	W	140	-0.5037e+1	0.1558e+2	-0.1437e+1	0.3468e+1	19.29
Ne	W	200	0.4379e+1	0.8769e+1	-0.5520e+0	0.1740e+1	19.29
Ne	W	300	0.4183e+1	0.1114e+2	-0.9745e+0	0.2436e+1	19.29
Ne	W	400	-0.4375e+1	0.2224e+2	-0.8198e+0	0.2476e+1	19.29
Ne	W	500	0.5467e+1	0.1492e+2	-0.6575e+0	0.1916e+1	19.29
Ne	W	700	-0.5159e+1	0.2920e+2	-0.7933e+0	0.2377e+1	19.29
Ne	W	1000	0.9023e+1	0.2037e+2	-0.6511e+0	0.1836e+1	19.29
Ar	W	10	-0.1034e+2	0.1272e+2	-0.1913e+1	0.4455e+1	19.29
Ar	W	20	-0.1242e+2	0.1562e+2	-0.2398e+1	0.5140e+1	19.29
Ar	W	30	-0.8466e+1	0.1233e+2	-0.1438e+1	0.3656e+1	19.29
Ar	W	35	-0.2909e+1	0.6995e+1	-0.1528e+1	0.3465e+1	19.29
Ar	W	40	-0.2888e+1	0.7236e+1	-0.1476e+1	0.3379e+1	19.29
Ar	W	45	-0.6159e+1	0.1072e+2	-0.1616e+1	0.3755e+1	19.29
Ar	W	50	-0.1098e+2	0.1571e+2	-0.1688e+1	0.4009e+1	19.29
Ar	W	55	-0.1012e+2	0.1501e+2	-0.1433e+1	0.3681e+1	19.29
Ar	W	60	-0.8248e+1	0.1337e+2	-0.1455e+1	0.3580e+1	19.29
Ar	W	70	-0.1080e+1	0.6516e+1	-0.1682e+1	0.3508e+1	19.29
Ar	W	80	-0.1326e+2	0.1906e+2	-0.1464e+1	0.3709e+1	19.29
Ar	W	100	-0.9232e+1	0.1559e+2	-0.1609e+1	0.3746e+1	19.29
Ar	W	140	-0.1006e+2	0.1750e+2	-0.1265e+1	0.3254e+1	19.29
Ar	W	200	-0.7248e+1	0.1600e+2	-0.1155e+1	0.2965e+1	19.29
Ar	W	300	-0.1782e+2	0.2848e+2	-0.1004e+1	0.2942e+1	19.29
Ar	W	500	-0.2417e+1	0.1621e+2	-0.8098e+0	0.2203e+1	19.29
Ar	W	700	-0.1405e+1	0.1768e+2	-0.8433e+0	0.2195e+1	19.29
Ar	W	1000	-0.1959e+2	0.3973e+2	-0.6042e+0	0.2137e+1	19.29
Ar	W	1005	0.1559e+2	0.4287e+1	-0.1030e+1	0.1243e+1	19.29
Ar	W	1050	-0.4275e+1	0.2482e+2	-0.6249e+0	0.1905e+1	19.29
Ar	W	30000	0.1249e+3	0.3178e+2	-0.1281e+1	0.1139e+1	19.29

Table 27: Constants for the angular dependence of the mean penetration depth at several energies and ion-target combinations.

ion	solid	energy (eV)	c1	c2	c3	c4	ρ (g/cm^3)
Xe	W	9500	0.1684e+2	0.2772e+2	-0.6004e+0	0.9982e+0	19.29
Xe	W	30000	0.5280e+2	0.2267e+2	-0.1417e+1	0.1343e+1	19.29
W	W	10	0.5537e+0	-0.1651e+0	0.2409e+1	-0.1637e+1	19.29
W	W	12	0.2318e+1	-0.5559e+1	0.6517e-1	0.2633e+0	19.29
W	W	15	-0.1391e+0	-0.1737e+1	0.3781e+0	-0.8900e+0	19.29
W	W	20	0.8790e+0	-0.4376e+0	0.2320e+1	-0.1910e+1	19.29
W	W	25	0.9814e+0	-0.5836e+0	0.2230e+1	-0.1951e+1	19.29
W	W	27	0.1058e+1	-0.6677e+0	0.2134e+1	-0.1764e+1	19.29
W	W	30	0.1107e+1	-0.7068e+0	0.2140e+1	-0.1780e+1	19.29
W	W	35	0.1210e+1	-0.8758e+0	0.1862e+1	-0.1564e+1	19.29
W	W	40	0.1301e+1	-0.9433e+0	0.2071e+1	-0.1746e+1	19.29
W	W	50	0.1466e+1	-0.1141e+1	0.1875e+1	-0.1609e+1	19.29
W	W	60	0.1636e+1	-0.1225e+1	0.2149e+1	-0.1839e+1	19.29
W	W	70	0.1777e+1	-0.1402e+1	0.1989e+1	-0.1745e+1	19.29
W	W	80	0.1921e+1	-0.1506e+1	0.1991e+1	-0.1753e+1	19.29
W	W	100	0.2076e+1	-0.1767e+1	0.1802e+1	-0.1742e+1	19.29
W	W	120	0.2151e+1	0.2214e+1	-0.1458e+1	0.1518e+1	19.29
W	W	140	0.2317e+1	-0.2636e+1	0.1242e+1	-0.1341e+1	19.29
W	W	200	0.1963e+1	0.3977e+1	-0.1058e+1	0.1446e+1	19.29
W	W	300	-0.1184e+1	0.8635e+1	-0.7863e+0	0.1569e+1	19.29
W	W	350	-0.1551e+2	0.2357e+2	-0.7086e+0	0.2028e+1	19.29
W	W	400	-0.1936e+2	0.2794e+2	-0.7074e+0	0.2097e+1	19.29
W	W	500	-0.3004e+2	0.3978e+2	-0.6386e+0	0.2144e+1	19.29
W	W	800	-0.2108e+2	0.3317e+2	-0.6542e+0	0.1966e+1	19.29
W	W	1000	-0.1179e+2	0.2475e+2	-0.7683e+0	0.1937e+1	19.29
W	W	2500	-0.1238e+2	0.3453e+2	-0.5324e+0	0.1469e+1	19.29
H	Au	1000	0.1325e+2	0.1519e+3	-0.2660e+0	0.1598e+1	19.31
H	Au	1333	0.1995e+2	0.1710e+3	-0.3824e+0	0.1806e+1	19.31
H	Au	3000	0.2649e+2	0.2865e+3	-0.5593e+0	0.2008e+1	19.31
H	Au	4000	0.8049e+2	0.3756e+3	-0.1909e+0	0.1034e+1	19.31
H	Au	5000	-0.2211e+2	0.4525e+3	-0.8295e+0	0.2456e+1	19.31
H	Au	10000	0.7555e+2	0.8633e+3	-0.2158e+0	0.9602e+0	19.31
D	Au	150	0.5357e+1	0.5460e+2	-0.3004e+0	0.2008e+1	19.31
D	Au	200	0.1555e+1	0.7039e+2	-0.1636e+0	0.1723e+1	19.31
D	Au	250	0.5873e+1	0.7325e+2	-0.3619e+0	0.2010e+1	19.31
D	Au	300	0.9324e+1	0.8172e+2	-0.1859e+0	0.1594e+1	19.31
D	Au	500	-0.6170e+1	0.1229e+3	-0.3484e+0	0.2059e+1	19.31
D	Au	750	0.2160e+2	0.1335e+3	-0.2118e+0	0.1539e+1	19.31
D	Au	1000	0.1359e+2	0.1560e+3	-0.6517e+0	0.2678e+1	19.31
D	Au	1333	0.1906e+2	0.1920e+3	-0.3684e+0	0.1919e+1	19.31
D	Au	2500	0.2445e+2	0.2799e+3	-0.1133e+1	0.3152e+1	19.31
D	Au	3000	0.2534e+2	0.3319e+3	-0.5602e+0	0.2245e+1	19.31
D	Au	5000	0.1620e+2	0.4770e+3	-0.8958e+0	0.2693e+1	19.31
D	Au	8300	0.2942e+2	0.6972e+3	-0.5604e+0	0.2003e+1	19.31
D	Au	10000	0.2301e+2	0.8177e+3	-0.5604e+0	0.2027e+1	19.31

Table 28: Constants for the angular dependence of the mean penetration depth at several energies and ion-target combinations.

ion	solid	energy (eV)	c1	c2	c3	c4	ρ (g/cm^3)
^{4}He	Au	5000	0.2497e+2	0.2793e+3	-0.3170e+0	0.1602e+1	19.31
Ne	Au	6000	0.1537e+2	0.8356e+2	-0.3246e+0	0.1273e+1	19.31
Ne	Au	14000	-0.2602e+2	0.1926e+3	-0.4103e+0	0.1604e+1	19.31
Na	Au	30000	0.7649e+1	0.2716e+3	-0.3862e+0	0.1292e+1	19.31
K	Au	30000	0.1266e+3	0.2398e+2	-0.2032e+1	0.1878e+1	19.31
Ar	Au	1050	0.1848e+2	0.3229e+1	-0.1433e+1	0.1380e+1	19.31
Ar	Au	3000	0.5261e+1	0.3488e+2	-0.5235e+0	0.1518e+1	19.31
Ar	Au	6000	0.5846e+1	0.5590e+2	-0.4477e+0	0.1380e+1	19.31
Ar	Au	10000	0.6182e+2	0.1560e+2	-0.1125e+1	0.1196e+1	19.31
Ar	Au	30000	0.1313e+3	0.2888e+2	-0.1482e+1	0.1380e+1	19.31
Xe	Au	10000	0.2928e+2	0.1424e+2	-0.1082e+1	0.1133e+1	19.31
Kr	Hg	762	-0.8420e+2	0.1070e+3	-0.5283e+0	0.2388e+1	13.55
H	U	2000	-0.2503e+1	0.2825e+3	-0.7124e+0	0.2537e+1	19.04
Kr	U	17900	-0.1189e+3	0.2152e+3	-0.4401e+0	0.1751e+1	19.04